ALTERNATE FOUNDATION SILL PLATE AND HOLD-DOWN ELEMENTS FOR LIGHT-FRAME SHEAR WALLS

By

RICHARD HENRY UTZMAN

A thesis submitted in partial fulfillment of
the requirements for the degree of

MASTER OF SCIENCE IN CIVIL ENGINEERING

WASHINGTON STATE UNIVERSITY
Department of Civil and Environmental Engineering

AUGUST 2009

To the Faculty of Washington State University:

The members of the Committee appointed to examine the thesis of RICHARD HENRY UTZMAN find it satisfactory and recommend that it be accepted.

Donald A. Bender, Ph.D., Chair

J. Daniel Dolan, Ph.D.

David Pollock, Ph.D.

ACKNOWLEDGMENT

There are many people who I need to thank for their assistance and support through this project.

- Committee members; Dr. Donald Bender, Dr. Daniel Dolan and Dr. David Pollock, for all of their guidance and engineering insight.
- The DeVlieg Foundation for providing the funding to perform this project.
- The Office of Naval Research (under grant N00014-06-1-0847) for providing partial funding.
- Washington State University Composite Materials & Engineering Center faculty and staff, especially Bob Duncan and Scott Lewis for their laboratory and technical assistance.
- My family for the support and encouragement to go back to school and accomplish this program.

ALTERNATE FOUNDATION SILL PLATE AND HOLD-DOWN ELEMENTS FOR LIGHT-FRAME SHEAR WALLS

Abstract

by Richard Henry Utzman, M.S.
Washington State University
August 2009

Chair: Donald A. Bender

Hold-down hardware in engineered, light-frame shear wall construction is used to resist uplift forces from the tension chord member. This shear wall hold-down hardware can be expensive, time consuming to install and difficult to install incorrectly on many shear walls. Shear wall hardware can be susceptible to galvanic corrosion caused by the current preservative chemicals used to treat PPT lumber. This study tested an alternative system using a triangular gusset made out of light gauge steel along with a wood plastic composite (WPC) sill plate. This light gauge steel gusset and WPC sill plate have been found to have shear strength values 1-1/2 times greater than conventional IBC 2006 braced walls. WPCs tend to absorb less moisture than solid wood; therefore, WPCs have a better resistance to insects, fungal attack and are more dimensionally stable.

Another objective of this study was to develop and demonstrate laboratory processing procedures for melt bonding pairs of WPC boards. It was found that the melt-bond process utilizing infrared heat lamps produced glue-line shear strength properties similar to the bulk composite properties.

A third objective of the study was to understand the withdrawal resistance of nails used with WPCs, particularly 0.113 in. by 2-3/8 in. smooth and ring-shank nails. These nails are typical for sheathing applications in light-frame construction and usually are driven by a pneumatic nail gun. To determine if pneumatic nail guns are a feasible way to drive nails into WPCs, two sizes of framing nails with a diameter of 0.131 in. and 0.162 in. were studied. The air pressure was increased until the nails were consistently driven. Spacing and edge distance requirements of the nails were also determined for use with WPCs. It was found through experiments the minimum edge distances and spacing requirements from the NDS and SDPWS do not apply to dowel type fasteners in WPCs.

TABLE OF CONTENTS

APPENDIX

LIST OF FIGURES

LIST OF TABLES

CHAPTER 1

Melt-Bond Lamination of WPC Boards

ABSTRACT

During the past few years new interest in wood plastic composites, WPCs, has been fueled by the success of several WPC decking products. Since WPCs absorb less moisture and at a slower rate than solid wood, they have a better resistance to insects, fungal attack and are more dimensionally stable when exposed to moisture. These interests go beyond decking into structural applications in the light-frame construction market. Although WPCs can be extruded in nearly any profile geometry, there is a need to develop the methodology for melt-bonding multiple WPC members together to add versatility without incurring the expense of cutting new dies for each application. The objective of this study was to develop and demonstrate laboratory processing procedures for melt bonding pairs of 1x6x8 ft. WPC boards. Since the majority of WPCs are made with polyethylene resin, HDPE boards were used. The boards were heated under infrared heat lamps until the surface layer melted and then they were pressed together. After the boards cooled, specimens were sampled to test the glue-line shear strength. It was found that the melt-bond process utilizing infrared heat lamps produced glue-line shear strength properties similar to the bulk composite properties.

INTRODUCTION

The International Building Code (IBC 2006), Section 2304.3.1, requires that studs shall have full bearing on an actual 1-1/2 in (3.8 cm) thick or thicker plate or sill. A die for a nominal 2 by 6 was not available for this research; therefore, it was not possible to extrude a solid wood plastic composite (WPC) board to use as a sill plate at the Washington State University Composite Materials & Engineering Center (CMEC). Due to the high cost of manufacturing an extrusion die, it was determined that two 1 in. by 5-1/2 in. (2.5 cm by 14 cm) WPC boards, which could be extruded at CMEC, would be melt-bonded together to make a board thick enough to use for a shear wall sill plate.

BACKGROUND INFORMATION

Wood plastic composites are comprised of wood flour or particles and a thermoplastic polymer, along with other minor ingredients (e.g. lubricants, UV stabilizers). The typical wood particle size ranges from 10 to 80 mesh. Some common wood species used in WPCs include pine, oak and maple. Thermoplastic polymers such as polyethylene, polypropylene and polyvinyl chloride (PVC) can be repeatedly melted. There are many diverse commercial uses for thermoplastic products such as milk jugs, grocery bags and siding for houses.

Commercial interest has been fueled by the success of WPC products in decking applications. Greater awareness and understanding of wood resources, more recycling sources of plastic along with equipment manufacturer developments and opportunities to enter new markets are all factors that are increasing demand in the WPC markets. The forest products industries are changing their view of WPCs as a way to increase wood durability and reduce maintenance for the consumer.

Since WPCs absorb less moisture and at a slower rate than solid wood, they have a better resistance to insects, fungal attack and are more dimensionally stable when exposed to moisture. Unfilled plastic absorbs little, if any, moisture. However, most plastics do expand when heated, therefore, the addition of wood decreases thermal expansion. Because wood has a limited thermal stability, only thermoplastics that melt or can be processed at temperatures below 392°F (200°C) are commonly used in WPCs. In WPC the wood component is hydrophilic (can transiently bond with water through hydrogen bonding) and the plastic component is hydrophobic (it repels moisture). Therefore, a compatibilizer is often used to improve the interfacial bond of the two different phases.

The majority of WPCs are made with polyethylene. The source of polyethylene used in building materials comes from both recycled and new sources. In the manufacturing of thermoplastic composites, the raw materials are mixed in an initial process called compounding. During compounding, fillers and additives are dispersed in the molten polymer. The material that is compounding is, either immediately shaped into an end product or pressed into pellets for future processing. There are several manufacturing options for the molten WPC material. The molten material could be forced through a die (profile extrusion), cold mold (injection molding), calendars (calendaring) or just into molds (thermoforming and compression molding) (Caulfield, Clemons, Jacobson 2005). When the compounding and product manufacturing steps are combined, it is called in-line processing such, as in profile extrusion. In-line processing is where molten composite material is forced through a die to make a continuous desired shape or profile. During the extrusion process many operating parameters can influence the product qualities, such as extruder screw speed, temperature profile in the extruder barrel, die, and with the cooling rate (Chang 2006). The majority of WPCs are produced by a profile extrusion.

For WPCs the greatest industry growth is in building products that have minimal structural requirements, including decking, railings, moldings, fencing, landscaping timbers, roofing and industrial flooring. The voluntary phase-out of chromated copper arsenate (CCA) was a contributing factor in WPCs gaining market share over pressure preservative treated lumber (PPT).

Research by Englund and Wolcott (2005) determined that it was technically feasible to melt bond wood plastic composite (WPC) boards together by utilizing an infrared heating apparatus. Gardner (2001) determined that melt-bonding WPC boards manufactured from polyethylene was a possible adhesion method. Other attempts to reinforce WPC by using an infrared heater to melt reinforcement sheets onto the surface of deck boards have also been proven successful (Jiang et. al. 2007). Previous attempts to laminate (melt-bond) large-scale lamina (greater than 2 ft.) were limited by the size of the heat source. Englund and Wolcott were successful in melt-bonding 30 in. (76.2 cm) WPC boards, where the interfacial shear stress values were similar or greater than the bulk composite properties.

OBJECTIVES

The objectives of this study were to develop and demonstrate laboratory processing procedures for melt bonding pairs of 1x6x8 ft. WPC boards. Bond quality was measured by block shear tests of the unbonded boards and then comparing with the shear strength developed at the melt bond interface.

PROCEDURE

One wood plastic composite material (WPC) material formulation was considered for this study with the following ingredients:

55%	*Pine flour*
41%	*polyethylene*
4%	*Struktol™ TWP 104*

The size of the Pine flour for this formulation was a US sieve #60 which is equivalent to 0.0099 in. (0.251 mm) particle size. The flour was dried to 2% or less moisture content before dry blending.

High density polyethylene (HDPE) was used for this study which had a density of 59.5 lb./ft.^{3} (953.1 kg/m^3). This polyethylene had a vicat softening point temperature of 253.4˚F (123˚C). The vicat softening point is taken as the temperature at which the specimen is penetrated to a depth of 0.04 in. (1 mm) by a flat-ended needle having a 0.0016 sq. in. (1 sq. mm) circular or square cross-section as described in ASTM D 1525.

Struktol™ TWP 104 is a blend of lubricants designed specifically for wood fiber/flour filled polyolefins. It is used to improve the process ability and surface quality of the WPC material.

Ingredients were dry blended in 360 lbs. (163 kg) batches using a drum mixer and extruded using a Cincinnati-Milacron TC86 3-7/16 in. (86mm) conical intermeshing twin-screw extruder with crammer feed. The temperature profile that was used for the extrusion is shown in Table 1-1.

During the WPC extrusion process, the extruder screw rotation rates were adjusted until acceptable surface properties were obtained. The final screw and feed speeds were 12 and 9 RPM, respectively. The dimension of the extruded WPC die was 1-

3/16 in. by 5-1/2 in. (3 cm by 14 cm). Immediately after exiting the die, the WPC was cooled in a Conair water spray bath. Using a Conair flying cut off saw, the boards were rough cut into approximately 102 in. (2.6 m) lengths.

Since the International Building Code (IBC 2006) requires an actual 1-1/2 in. (3.8 cm) thick or thicker plate or sill, the extruded WPC board was melt bonded into a two-ply solid section having the final dimension of 2-7/8 in. by 5-1/2 in. (7.3 cm by 14 cm). This process of melt bonding the WPC boards consisted of placing two extruded 1-3/16 in. by 5-1/2 in. (3 cm by 14 cm) WPC boards side by side under three Fostoria FHK-1324-3A 13.5 kW infrared heat lamps Figure 1-1. The heat lamps were modified by removing the top ends of the heat shield on two of the lamps (lamps 1 and 3) and removing the top and bottom ends of the heat shield on the remaining lamp (lamp 2). The heat lamps were then mounted in series onto two 10 ft. (3 m) sections of slotted metal framing channel (uni-strut). This assembly was then elevated 104 in. (2.64 m) above the floor and secured with four legs consisting of slotted metal framing channel. The WPC boards were placed on a scissor table and raised to a distance of 16-1/2 in. (50 cm) from the heater elements.

It was observed that the three heaters had different temperature outputs. This difference in temperature was primarily due to the heater element ages and amounts of prior use. One end of the WPC boards had to be elevated 3 in. (7.6 cm) to maintain a more uniform temperature along the length of the boards Figure 1-2. The surface temperature of the WPC was monitored using a (Fluke model 53II) thermometer with a Type-J thermocouple. In order to obtain an accurate temperature reading with the thermocouple, a small piece of aluminum foil was placed over the thermocouple to shield it from the infrared heater elements.

After approximately 10 minutes, the outer layer of the WPC boards reached an average temperature of 284°F (140°C) along the length. One of the WPC boards was then rolled over on top of the other, which was already placed in an alignment jig. A jig was needed to keep the edges of the WPC boards aligned and to prevent them from sliding when the hydraulic press was activated. This assembly was placed into a computer controlled 4 ft. by 8 ft. (1.2 m by 2.4 m) hydraulic press. The press was controlled by a PressMan protocol and closed to a final displacement of 3.348 in. (8.5 cm), which was the combined thickness of the two WPC boards and the alignment jig minus 0.152 in. (3.86 mm) for the molten WPC to squeeze out of the sides. The PressMan consol recorded an average pressure of about 120 psi. (827 kPa), which was held for 10 minutes. After the WPC boards exited the hydraulic press, they were allowed to cool overnight. The cooled WPC boards then had the squeeze out bead shown in Figure 1-3 removed with a table saw.

One WPC board assembly was sampled at random and cut into 2 in. x 2 in. (51 mm x 51 mm) glue line shear blocks and tested following the ASTM D 1037-06a (2008) Glue-Line Shear (Block Type) standard. Three glue-line shear blocks were sampled every 16 in. (40.6 cm) along the length of the board as shown in Figure 1-4.

RESULTS AND DISCUSSION

Glue-line shear block test results are presented in Table1-2. The average glue-line shear strength of the WPC was determined from testing eighteen specimens in accordance with ASTM D 1037-06a (2008) to be 977 psi. (6737 kPa). This was compared to the interfacial shear stress values of the bulk shear block test. As can be seen in Figure 1-5 the values are similar or greater than the bulk composite properties. One other thing worth noting is the fact that 83% of the glue-line shear blocks tested had a 90% or greater WPC bulk failure, as shown in Figures 1-5 and 1-6.

SUMMARY AND CONCLUSION

The cost of extrusion dies can be significant. One way to gain more versatility and value in WPC processing is to develop a full-scale melt-bonding technique. The objective of this study was to explore the technical feasibility of melt bonding two wood plastic composite (WPC) boards together by utilizing an infrared heating apparatus.

The three Fostoria FHK-1324-3A 13.5 kW infrared heat lamps were modified so they could be mounted in series to perform as one long heat lamp. This heater assembly was supported 16-1/2 in. (50 cm) above the surface of the WPC boards to be heated. Due to a slight difference in heater element temperatures, one end of the boards had to be elevated 3 in. (7.6 cm) closer to the heat lamps in order to equalize the surface temperature of the boards.

In order to monitor the surface temperature of the boards, a Type-J thermocouple with a heat shield to reflect the heat from the heaters was used. Once the WPC boards reached an average temperature of 284˚F (140˚C) along the length of the boards, one board was rolled on top of the other. It took approximately 10 minutes for the WPC boards to reach this temperature under the heat lamps.

The stacked WPC board assembly was pressed to a final displacement of 0.152 in. (3.86 mm) less the overall thickness of both WPC boards plus the alignment jig. This assembly was held in the press for 10 minutes at an average pressure of 120 psi. (827 kPa).

Upon exiting the press, the WPC boards were carefully removed from the alignment jig and allowed to cool over night on a flat surface before machining. Machining consisted of trimming the excess material with a table saw.

Random specimens were sampled for glue-line block shear tests. It was found that the glue-line shear strength properties were similar or greater than the bulk composite properties. The melt-bond lamination had an average glue-line shear strength of 977 psi. (6736 kPa) compared to the WPC bulk shear strength of 949 psi. (6543 kPa).

This research used just one method to laminate WPC board together utilizing an infrared heating apparatus, however further study should be done using other heat sources. Heat sources which could heat the surface of the WPC quicker may produce better surface bonds by not allowing the heat to slowly penetrate deep into the material.

LITERATURE CITED

Englund, K. and M.P. Wolcott. 2005. Lamination of Wood Plastic Composites by Utilizing an Infrared Heating Apparatus. *In*: Commercialization of Navy Wood Composites: Final Report, Washington State University, Pullman, WA, pp. 1-8.

Caulfield, D.F., C. Clemons, and R.E. Jacobson. 2005. Wood Thermoplastic Composites. *In*: Handbook of Wood Chemistry and Wood Composites, CRC Press, Washington, D.C., pp. 365-378

Chang, A. 2006. Literature Review On Properties and Market Opportunities of Wood-Plastic and Wood-Cement Composites. Product Development Program, University of BC, Vancouver, BC, pp. 1-16

Gardner, D.J. 2001. Assembly of WPCS: Engineered Wood Composites For Naval Waterfront Facilities. *In*: Materials Production: Task 3A-Assembly of WPCs, University of Maine, Orono, ME.

Jiang, L., M.P. Wolcott, J. Zhang, and K. Englund. 2007. Flexural Properties of Surface Reinforced Wood/Plastic Deck Boards. Polymer Engineering and Science, Wiley InterScience, pp. 281-288

LIST OF FIGURES

Figure 1-1 Fostoria FHK-1324-3A 13.5 kW infrared heat lamp

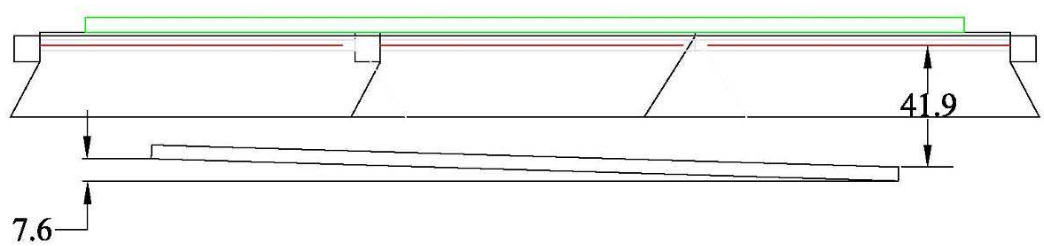

Figure 1-2 WPC under heater elements

Figure 1-3 WPC with Squeeze-out

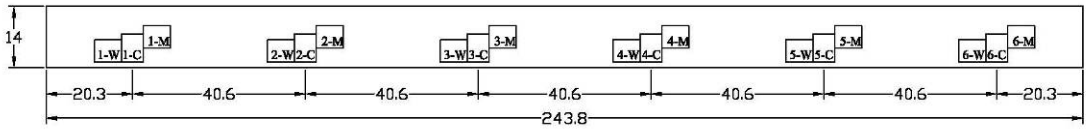

Figure 1-4 Layout of shear block samples

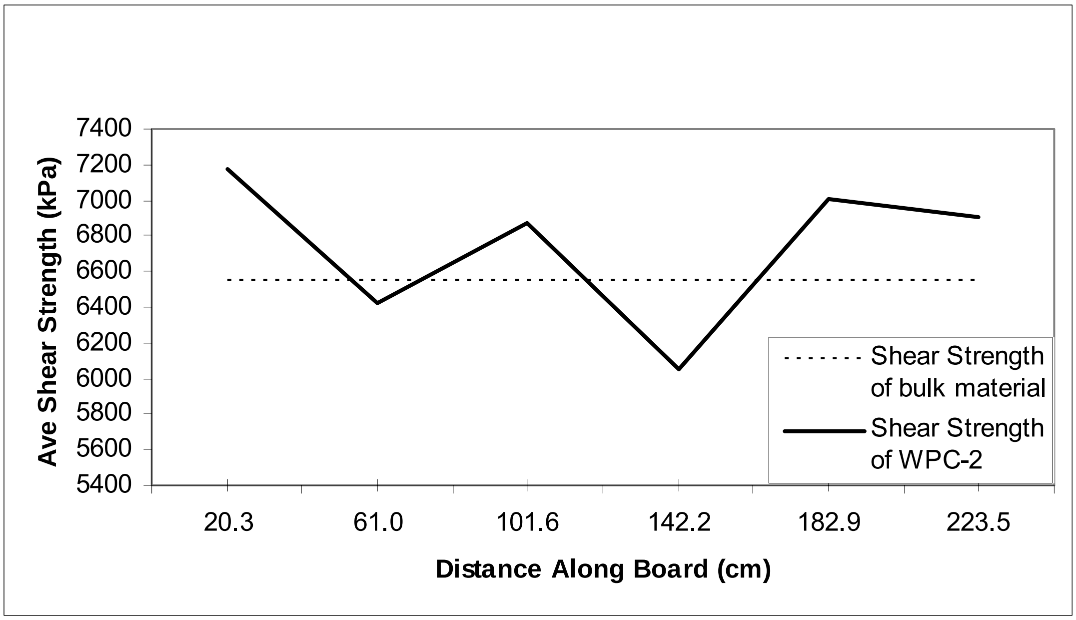

Figure 1-5 Average Shear Strength Along Board

Figure 1-6 Glue-line shear block failure

LIST OF TABLES

Table 1-1 Extruder temperature profile

Zone	Temperature ˚C	(˚F)
Barrel Zone 1	171	(340)
Barrel Zone 2	171	(340)
Barrel Zone 3	171	(340)
Barrel Zone 4	171	(340)
Screw	171	(340)
Die Zone 1	177	(350)
Die Zone 2	177	(350)
Die Zone 3	177	(350)

Table 1-2 Interfacial shear results

Sample	Glue Line Failure (%)	Max Shear kPa	(psi)
1-C2	100	7405	(1074)
2-C2	100	6929	(1005)
3-C2	85	6605	(958)
4-C2	66	6314	(916)
5-C2	100	7484	(1086)
6-C2	100	7500	(1088)
1-W2	100	7127	(1034)
2-W2	100	5195	(754)
3-W2	95	7171	(1040)
4-W2	50	4954	(719)
5-W2	100	6733	(977)
6-W2	100	6641	(963)
1-M2	100	6977	(1012)
2-M2	100	7138	(1035)
3-M2	100	6843	(993)
4-M2	100	6886	(999)
5-M2	100	6800	(986)
6-M2	90	6566	(952)
Avg.		6737	(977)
COV		0.10	

CHAPTER 2

Nail Withdrawal Resistance and Spacing Requirements in WPC Materials

ABSTRACT

The use of wood plastic composites (WPC) is expanding from decking and is being proposed for new structural applications such as sill plates. Therefore, there is a need to understand the nail withdrawal resistance used with WPCs, particularly 8d (0.113 in. by 2-3/8 in.) smooth and ring-shank nails. These nails are typical for sheathing applications in light-frame construction and usually driven by a pneumatic nail gun. To determine if pneumatic nail guns are a feasible way to drive nails, two sizes of framing nails with diameters of 0.131 in. and 0.162 in. were driven into WPC boards. The air pressure was increased until the nails were consistently driven. Spacing and edge distance requirements also need to be determined for use with WPCs. Through experimentation, the minimum edge distances and spacing requirements for nailing into WPC were determined and were found to be different from those published in the NDS and SDPWS for dimension lumber.

INTRODUCTION

Wood plastic composites (WPC) are gaining market share in a variety of structural applications such as residential and industrial decking, railing, sheet piles, and foundation elements (e.g. Bender et al., 2007; Ross et al., 2009). There is a critical need to develop design information on connection systems for WPCs. Dowel-type fasteners (e.g. bolts) have been studied for lateral load transfer for cases of solid and hollow section WPCs (Balma and Bender, 1999; Parsons and Bender, 2004). There is interest in using WPCs for sill plates in light-frame wood walls. Preliminary research (Ross, 2008) found that nails used to attach sheathing to WPC sill plates initially yielded in localized crushing of the OSB sheathing, nail bending, and finally in nail withdrawal from the WPC. Research is needed to characterize the withdrawal resistance of smooth and deformed shank nails in WPC materials.

OBJECTIVES

One objective of this research was to characterize the withdrawal resistance of ring-shank and smooth-shank 8d (0.113 in. by 2-3/8 in.) nails typically used as sheathing nails in light-frame construction embedded in a wood-plastic composite (WPC). The most common resin used in current WPC materials is polyethylene and this type of WPC formulation was chosen for study. A nail with an annularly threaded shank is commonly called a ring-shank nail. This type of nail has multiple ring-like threads which are rolled around the shank perpendicular to the nail axis. It is well known that for solid wood, ring shank nails provide increased withdrawal resistance over smooth shank nails, but this has not been studied for WPCs.

The second objective of this study was to determine the technical feasibility of using a pneumatic nail gun to drive nails into a WPC. Of particular interest was whether or not the WPC would withstand the sudden force or impact of the nail or would it crack or shatter. A procedure needs to be developed for the pneumatic gun settings such as proper air pressure settings and placement of the nails within the board.

Since WPC formulations using HDPE polymer are not being widely used in structural applications, beyond decking, little is known about how close to the edges of the WPC that nails can be placed without causing problems with splitting and edge blow-out. Therefore, a third objective was to develop the minimum edge, end and spacing requirements needed for fasteners with diameters less than ¼ in.

BACKGROUND INFORMATION

There have been many studies that compared the withdrawal performance of threaded nails to smooth-shank nails in wood members (e.g. Wills et al., 1996, Skulteti et al., 1997, and Rammer et al., 2001). The NDS (AF&PA, 2005) published the empirical equation for the smooth nail withdrawal resistance capacity (ASD) in wood based on tests:

$$W = K_W \cdot G^{5/2} \cdot D$$

where

- W = nail or spike withdrawal design value per inch of penetration in main member, lbs
- K_W = empirical constant which accounts for safety, experience and duration of load (K_W = 9.515 for SI units and 1380 for English units)
- G = specific gravity of main member based on ovendry weight and volume, where $0.31 < G < 0.73$
- D = shank diameter of the nail or spike, in., where $0.099 < D < 0.375$

Through this equation, it can be seen that the withdrawal capacity is directly related to the specific gravity of the wood and the diameter of the nail. As a nail is driven into wood or WPC, the material is forced outward. This, in turn, will cause the nail to wedge itself into the material and develop frictional resistance.

The annular threads on ring shank nails provide superior withdrawal resistance under normal and high moisture conditions in wood. Typically ring shank nails have withdrawal capacities up to twice as those of similar size smooth shank nails (Skulteti et al., 1997; Rammer et al., 2001).

PROCEDURES

Nail Withdrawal in HDPE WPC

Ring-shank and smooth-shank 8d nails of nominal size 0.113 in. by 2-3/8 in. were purchased from local suppliers with specifications listed in Table 2-1. Groups of 15 nails were tested for both nail types. All nails were cleaned with mineral spirits to remove any surface film before testing as per ASTM D 1761-06 (2008). Smooth shank nail diameters averaged 0.111 in. Ring shank nails had an average shank diameter of 0.100 in. and an average thread-crest diameter of 0.110 in. Due to the close spacing and shallow annullar threads, it was not practical to accurately measure the thread-root diameter of the ring shank nails.

Four different types of WPC boards were sampled. Two of the boards were manufactured at the Washington State University Composite Materials & Engineering Center, HDPE-41 and HDPE-32 and two others were commercially manufactured by Trex™ and Rino™ and purchased locally. The formulation for the boards manufactured at WSU was as follows; HDPE-41 consisted of:

55% pine flour
41% polyethylene
4% Struktol™ TWP 104

The HDPE-32 consisted of:

58% pine flour
32% polyethylene
7% Talc
2% Zinc Stearate
1% Ethylene Bis-Steramine by volume

The formulation for Trex™ as published in the Material Safety Data Sheet located on the

Trex™ website, was approximately as follows:

50-60% wood fiber
40-50% polyethylene
0-1% Carbon Black

The formulation for Rino™ as published in the Material Safety Data Sheet located on the Rino™ website,:

50-65% wood flour
30-50% polyethylene
1-4% color
0-8% Strukto 0409 N by volume.

The WPC boards were cut into three-inch long pieces. Withdrawal testing was conducted in accordance with ASTM Standard D 1761-06 (2008). Random samples of each WPC board were taken and specific gravity tests were performed following ASTM D 2395-07ae1, Method A (2008).

Nail withdrawal testing was conducted in accordance with ASTM D 1761-06 (2008). All nails were driven by hand to a depth of 1-7/8 in., or approximately 80% of their length, into the narrow face of the boards. The test samples were divided into eight groups of forty-five nails as follows:

Group 1 – HDPE-41 Ring-shank
Group 2 – HDPE-41 Smooth-shank
Group 3 – HDPE-32 Ring-shank
Group 4 – HDPE-32 Smooth-shank
Group 5 – TREX ™ Ring-shank
Group 6 – TREX ™ Smooth-shank
Group 7 – RINO ™ Ring-shank
Group 8 – RINO ™ Smooth-shank

Nail withdrawal tests were then performed using a 2-kip universal electromechanical test machine (Instron model 2200) and data collection software (LabVIEW Version 8) with a data collection rate of 2 Hz. Nails were tested in sets of fifteen nails for each group at time intervals of: within one hour, one week and three months. All tests were continued until the measured resistance reached 80% of post-peak load.

Pneumatically Driven Nails

It was necessary to find out if nails could be pneumatically driven into WPC boards with satisfactory results. A typical pneumatic framing nail gun is supplied by 90 to 110 psi. of air pressure depending on the size and specific application for the nail. Two sizes of framing nails with a diameter of 0.131 in. and 0.162 in. were driven into WPC boards starting at 85 psi. air pressure and increased in 5 psi. increments up to a maximum air pressure of 120 psi. These nail sizes were chosen to reflect typical size nails for connecting WPC and solid-sawn lumber framing, for structural applications such as light-frame shear walls with WPC sill plates. It was determined, by iterative testing, that the most consistent results were achieved at an air pressure rating for driving 0.131 in. x 3-1/4 in. framing nails into the WPC material was 95 psi. For the larger 0.162 in. x 3-1/2 in. nail it did not matter what the air pressure was, because the nail gun could not drive the nails more than half way into the WPC board without bending and jamming in the barrel of the tool.

Nail Spacing Requirements in HDPE WPC

The mechanical and physical properties of the WPC are different from lumber properties. Proper placement of nails in framing lumber is reasonably well understood and is documented in the NDS (2005), but WPC's can be more brittle and have a tendency to crack or shatter if the fastener is driven too close to the edge or end of the member. The NDS 2005 Section 11.5.1 Geometry Factor, C_{Δ} for a typical 8d, supra, page 19, sheathing nail is;

$C_{\Delta} = 1.0$, when $D < ¼”$

where D is the diameter of the nail.

Using Table C11.1.5.6 in the NDS 2005, it was determined that the minimum edge distance for the sill plate loaded perpendicular to grain is 2.5D, where D is the diameter of the nail. Similarly, the minimum published end distance is 15D. Table C11.1.5.6 was used to determine the spacing requirements for fasteners in a row and between rows. To determine the minimum spacing for nails in a row for the sill plate, the Special Design Provisions for Wind and Seismic (SDPWS) 2008, 4.4.1.1 states that nails in any single row shall not be spaced closer than 3-in. on center. The SDPWS 2008 Figure 4G Panel Attachment requires ½-in. spacing between rows of fasteners.

Minimum edge distances and spacing requirements from the NDS and SDPWS apply to dowel type fasteners in wood, but not WPCs. Therefore, similar values had to be developed for WPCs. The WPC to be used for sill plate material was cut in 2-ft. long specimens. Each of the NDS and SDPWS requirements was marked on the specimens and, using a pneumatic tool, 8d, supra, page 19, smooth shank nails with an average diameter of 0.111 in. and ring shank nails which had an average shank diameter of 0.100 were driven into the WPC boards. The spacing was increased in increments of 1/8” until there was no visual sign of the WPC board cracking. It should be noted, however, this portion of the study was not intended to investigate if lateral load applied to the nails would influenced cracking in the WPC. It was determined through this iterative testing that the minimum spacing and distance requirements for the WPC board formulations that were studied should be as follows:

Edge distance	*5/8"*
End distance	*1-1/2"*
Spacing between nails in a row	*2"*
Spacing between rows	*5/8"*

These dimensions work out to be approximately equal to 5D for edge distance, 15.5D for end distance and 5D for the spacing between rows, where D is the diameter of the nail. It should be noted that none of the WPC boards were processed with stranding plates. WPC's processed with a stranding plate would tend to be an orthotropic material, that is, material with a "grain" manufactured into the product. Stranding plates would likely influence the end distance and spacing between nails in a row, and further testing to verify this would be required.

RESULTS AND DISCUSSION

Withdrawal Values. The average withdrawal strengths and coefficients of variation (COV) for all groups of nails are presented in Table 2-2. The average withdrawal strengths for the ring-shank nails were approximately twice the value of the withdrawal strength of the same diameter smooth-shank nail. Similar results were found in other studies with nails driven into solid wood (Skulteti et al., 1997; Rammer et al., 2001).

Research conducted on the withdrawal strength of similar diameter deformed-shank nails in Spruce-Pine Fir and Douglas Fir, reported values of 190.2 lb./in. and 337.2 lb./in. respectively (Rammer et al. 2001). Ring shank nail in three formulations of WPC;

HDPE-41, HDPE-32 and Trex have similar average withdrawal values, within 10% of Douglas Fir. The average ring shank nail withdrawal value for the Rino material was about 29% less than Douglas Fir. When compared to withdrawal values in Spruce-Pine-Fir, the three WPC formulations HDPE-41, HDPE-32 and Trex were about 60% larger for similar diameter ring shank nails.

If calculating the reference withdrawal design value for HDPE-41 using the NDS Equation 11.2-3, using G_{WPC} = 1.11 and D = 0.113 in., then W_{WPC} = 202.4 lb./in.. This value is larger than the withdrawal strength values determined in this study for smooth shank nails in HDPE WPCs. Therefore the NDS reference withdrawal design Equation 11.2-3 should be recalibrated for WPCs. This value is considerably higher than a withdrawal design value using a factor of safety of 5, which for HDPE-41 equals 124.4 lb./in.. This is a difference of 63%.

Load-Displacement Curves. A typical load versus displacement plot for both ring-shank and smooth-shank nails is shown in Figure 2-1. The initial stiffness of the smooth shank nail is slightly higher than that of the ring-shank nail, likely due to the larger diameter. The ring-shank nail generally reached two times the withdrawal load compared to the smooth-shank nail. Just as with wood, the mechanism by which the smooth-shank nail resists withdrawal in WPC is with friction. With the ring-shank nail, the mechanism is the tearing of wood and plastic between the annular threads on the nails. Once the ultimate withdrawal load is reached, there is only a small frictional force between the WPC in the rings on the nails and the surrounding WPC to resist the load.

It can be shown in Figure 2-2 for each of the different types of WPC's, the nail withdrawal resistance decreases over time. It can also be seen that the withdrawal resistance for the ring-shank nails decreases on average 28% over the period of thirty days, where as, the smooth-shank nails decreases on average 17% over the same thirty-day period. This is due to stress relaxation of the WPC material. Brandt and Fridley (2003) developed load duration adjustment factors from bending tests of WPCs made from a range of polymer formulations. Using their suggested load duration factors (for allowable stress design) for polyethylene WPCs, a reduction of 46% would be expected when comparing the strengths from one hour to three months, and could conservatively be applied to nail withdrawal design. Another factor that could significantly reduce nail withdrawal resistance in WPCs would be the effect due to temperature. Sufficient heat would soften the composite, which, in turn, would reduce withdrawal resistance of the fastener (Schildmeyer 2009).

SUMMARY AND CONCLUSIONS

The main purpose of this study was to characterize the withdrawal strengths of ring-shank and smooth-shank nails in wood plastic composites. Two types of nails were studied: 8d, supra, page 19, ring-shank nails and smooth-shank nails, both with similar dimensions of 0.113 in. diameter and 2-3/8 in. long, which are typical nail sizes for attaching sheathing to framing members in light frame construction.

Ring-shank nails developed, on average, approximately two times the withdrawal strength compared to the smooth-shank nails in wood plastic composites. Other studies found similar results for the same size and types of nails in driven into wood (Skulteti et al., 1997; Rammer et al., 2001).

Since this withdrawal study only considered one size of nail for a particular use, more research is needed for other nail sizes and formulations of WPC materials. It would be useful to have withdrawal values for larger nails so WPC materials could be used for more applications in light-frame construction. Future research on withdrawal resistance should also include screws which are commonly used in deck construction.

It was also determined during this study that the minimum spacing and distance requirements for this particular WPC board formulation should be as follows:

Edge distance	*5/8"*
End distance	*1-1/2"*
Spacing between nails in a row	*2"*
Spacing between rows	*5/8"*

These dimensions are equal to 5D for edge distance, 15.5D for end distance and 5D for the spacing between rows where D is the diameter of the nail.

Due to the fact that mechanical and physical properties of WPC formulations using HDPE polymer are different from lumber properties and much more dense, it was confirmed to be feasible to use a pneumatic nail gun to adequately drive 0.131 in. x 3-1/4 in. smooth shank framing nails into this material. Although for larger diameter nails, such as 0.162 in. x 3-1/2 in., it was found to be impossible to use a pneumatic nail gun to drive the nails into HDPE WPC boards. It was also determined that the recommended pneumatic nail gun air pressure rating to uniformly drive 0.131 in. x 3-1/4 in. smooth shank framing nails into WPC was 95 psi.. The WPC held up to the sudden force of the nail and did not crack or shatter when the above minimum spacing requirements were followed.

LITERATURE CITED

American Forest and Paper Association. 2005. ANSI/NF&PA NDS-2005. Nat. Design Specification for Wood Construction. Washington, D.C.: AF&P

American Society for Testing and Materials. 2008. Standard test methods for mechanical fasteners in wood. ASTM D 1761-06. ASTM, Philadelphia, Pa..

American Society for Testing and Materials. 2008. Standard Test Methods for Specific Gravity of Wood and Wood-Based Materials. ASTM D 2395-07ae1. ASTM, Philadelphia, Pa.

Balma, D.A. and D.A. Bender. 1999. Evaluation of bolted connections in wood plastic composites. ASAE Technical Paper No. 994177, American Society of Agricultural Engineers, St. Joseph, MI.

Bender, D.A., M.P. Wolcott and J.D. Dolan. 2007. Wood plastic composites – structural design and applications. Structure magazine (March):43-46.

Brandt, C.W. and K.J. Fridley. 2003. Load-duration behavior of wood-plastic composites. Journal of Materials in Civil Engineering 15(6):524-536.

Parsons, W.R. and D.A. Bender. 2004. Energy-based design of dowel connections in wood-plastic composites hollow sections. ASCE Journal of Structural Engineering 130(4):681-689.

Rammer, D.R., S. G. Winistorfer, D. A. Bender. 2001. Withdrawal Strength of Threaded Nails. Journal of Structural Engineering 127(4):442-449

Ross, Loren Allen. (2008). "Performance of Wood Plastic Composite Foundation Elements in Post-Frame and Light-Frame Shear Walls." MS Thesis, Washington State University, Pullman, WA.

Ross, L.A., D.A. Bender and D.M. Carradine. 2009. Performance of post-frame shear walls with a wood-plastic composite skirtboard subjected to monotonic racking loads. Transactions of the ASABE 52(2):583-589.

Schildmeyer, A.J., M.P. Wolcott and D.A. Bender. 2009. Investigation of the temperature-dependent mechanical behavior of a polypropylene-pine composite. ASCE Journal of Materials in Civil Engineering (in press).

Skulteti, M.J., D. A. Bender, S. G. Winistorfer, D. G. Pollock. 1997. Withdrawal Strength of Ring-Shank Nails Embedded In Southern Pine Lumber. American Society of Agricultural Engineers 40(2):451-456.

Wills, B.L., S. G. Winistorfer, D. A. Bender, D. G. Pollock. 1996. Threaded-Nail Fasteners Research and Standardization Needs. American Society of Agricultural Engineers 39(2):661-668

LIST OF FIGURES

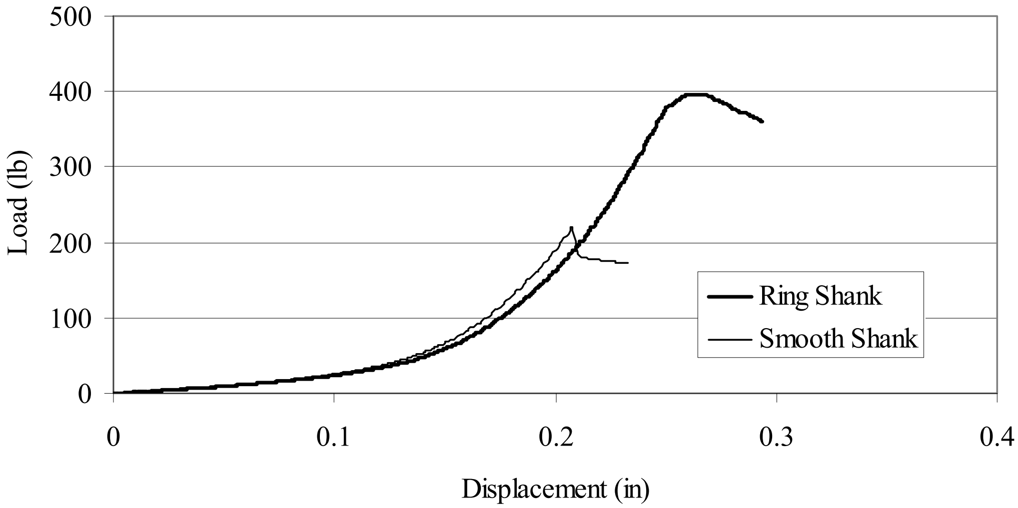

Figure 2-1 Typical load vs. displacement

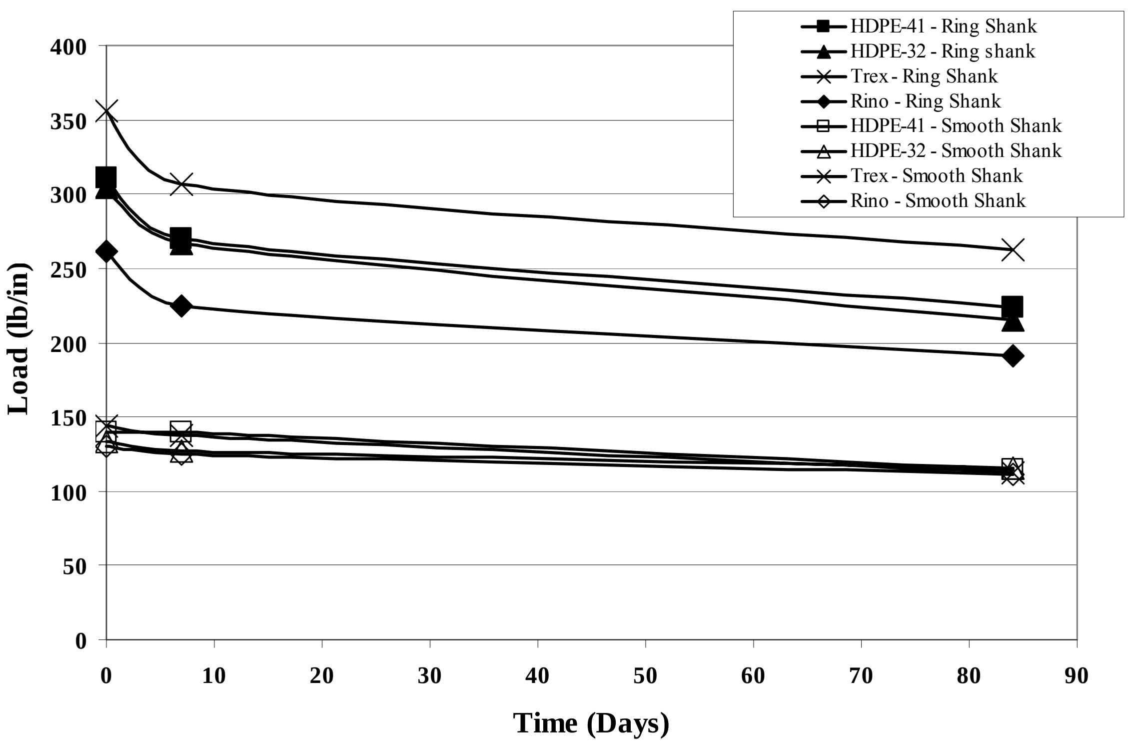

Figure 2-2 – Maximum load vs. time

LIST OF TABLES

Table 2-1 - Nail specifications

	Manufacturer	Diameter	Length
8d smooth-shank	Halsteel	0.113 in.	2-3/8 in.
8d ring-shank	Senco	0.113 in.	2-3/8 in.

Table 2-2 - Summary of nail withdrawal test results

Material Group	1 hour		1 week		3 months	
	lb/in.	Coef. of Variation	lb/in.	Coef. of Variation	lb/in.	Coef. of Variation
HDPE-41, smooth-shank	139	0.05	139	0.07	114	0.07
HDPE-32, smooth-shank	133	0.08	127	0.07	115	0.06
Trex, smooth-shank	144	0.02	137	0.04	112	0.05
Rino, smooth-shank	131	0.11	125	0.07	112	0.06
Average	137	0.07	132	0.06	113	0.06
HDPE-41, ring-shank	311	0.11	269	0.09	224	0.12
HDPE-32, ring-shank	304	0.12	267	0.12	215	0.17
Trex, ring-shank	356	0.06	307	0.07	262	0.05
Rino, ring-shank	262	0.11	225	0.08	191	0.10
Average	308	0.10	267	0.09	223	0.11

Sample size for all groups was 15

CHAPTER 3

Investigation of Alternate Sill Plate and Hold-Down Hardware on Light-Frame Shear Wall Performance

ABSTRACT

Hold-down hardware can be expensive and time consuming to install on light-frame shear walls. This hardware may be susceptible to galvanic corrosion caused by preservative chemicals used to treat the lumber. There is a need for alternative shear wall hold-down systems that are easier to install and for alternatives to PPT lumber. This study tested a hold-down system that incorporates a light gauge triangular steel gusset fastened to the lower corners of a shear wall and into a WPC sill plate. The light gauge steel gusset and WPC sill plate were found to have shear strength values 1-1/2 times greater than compared to a conventional IBC 2006 braced wall.

INTRODUCTION

Hold-down hardware in engineered light-frame shear wall construction is used to resist uplift from the tension chord member. Installation of hold-down hardware that employs bolts embedded into the concrete foundation can significantly increase construction costs due to hardware, labor and installation errors in the field. Research is needed to develop other hold-down methods that are simpler to install and inspect.

Another issue in light-frame shear wall construction is the choice of sill plate material. Typically, preservative pressure-treated (PPT) lumber is used, but it has potential problems of galvanic corrosion caused by copper-rich, preservative chemical formulations and cross grain bending/splitting failures during lateral load events. One promising alternative to PPT lumber is wood plastic composites (WPCs). WPCs are gaining significant market share in residential decking applications and have the potential for other structural applications such as foundation sill plates. Previous research had demonstrated the potential for a built up 3-ply WPC sill plate along with a light gauge steel gusset used as a hold-down device (Ross 2008). Further research is needed to investigate a more economical 2-ply WPC sill plate, improved melt-bonding technique for WPC boards, threaded nails with the gusset, and a complete energy dissipation analysis.

OBJECTIVES

The main objective was to investigate an alternate light-frame shear wall hold-down or tie-down system that is easy to install and inspect. This alternate hold-down system used a triangular 24 Ga. galvanized steel gusset fastened to the outside face of the sheathing at the lower corners of the shear wall along with a WPC sill plate as a way to resist uplift of the shear wall by transferring chord loads to the sill plate. The proposed system has the advantages of being simple and inexpensive to install, and easy to inspect.

A secondary objective of this research was to evaluate the substitution of a WPC sill plate for a PPT lumber sill plate in a light-frame shear wall. In addition to possible consumer concerns about preservative chemicals, PPT lumber sill plates have been shown to be susceptible to splitting and cross-grain bending failures in extreme lateral loading events. WPCs offer potential advantages on both of these issues since they can achieve resistance to decay and insects without preservative chemicals and they do not have a grain structure (unless a stranding plate is used during manufacture).

BACKGROUND INFORMATION

There have been numerous tests, observations and on-site field examinations of failed shear wall panels which show three failure modes, with sill plate failure being the most common (Commins 2007). During lateral loading, shear wall panels tend to lift, rotate and twist the sill plate in cross grain bending. One method to solve this problem is given in Sections 2305.3.11 and 2308.12.8 of the International Building Code (IBC) 2006, which calls for large plate washers on the foundation bolts. These large plate washers reduce cross grain bending in the sill plate and transfer the failure point to the nails in the shear wall sheathing. The performance of the shear wall does not change, but the location of failure moves from the center of the sill plate outward to the edge of the sill plate.

The second failure mode is splitting of the studs, often caused by stress concentrations near bolted connections for hold-down hardware (Commins 2007). When the shear wall is subjected to cyclic loading, the end studs are repeatedly put through cycles of compression and tension loading. One solution to this failure mode is to use a continuous rod system from the top plate down to the foundation to resist the tension. Another solution is to use metal straps with nailed or screw connections.

The third failure mode is nail pull-through that connects the wall sheathing to the shear wall panel chords (Commins 2007). As the shear wall rotates, the perimeter nails are overloaded and tear through the wall sheathing.

Using a triangular light gauge steel gusset fastened to the framing and panels in the lower corners of the shear wall, along with a WPC sill plate, may alleviate these three modes of shear wall failure. The use of a WPC can reduce the likelihood of sill plate failure, since it is a nearly isotropic material and does not have cross grain weakness like lumber. Using a steel gusset can help mitigate the problem of end stud splitting, because the gusset will be fastened to the studs through the sheathing with nails, not bolts. Finally, the steel gusset can help solve the problem of the nail pull through by acting as a large washer under the sheathing nail heads.

Shear Wall Theory

Over the past sixty years there have been many studies to determine the performance characteristics of different shear wall components and their influences on the complete shear wall assemblies. During this period a standardized testing procedure had not been established; hence, it was difficult to compare results from different studies. Initial test protocols used monotonic loading functions, but this did not adequately characterize response under seismic loading. Next came protocols that incorporated the reverse cyclic loading over a period of time, or quasi-static loading. Quasi-static refers to tests where the cycling rate is low, about 0.2-0.5 Hz, so as to inhibit the development of inertial forces within the wall and test hardware.

Pseudo-dynamic protocols that increased the rate of cycling above 1.0 Hz were introduced by Dinehart (1999) and Shenton (1998). They showed that Sequential Phase Displacement (SPD) protocol would reach ultimate peak loads which were slightly less than the peak loads of monotonic tests. These ultimate peak loads also occurred with much smaller displacements. Shear walls tested with SPD testing protocols tend to have lower ductility due to the large number of cycles.

Quasi-static or reverse cyclic protocols are mainly used today for the testing of shear wall assemblies. This type of protocol usually consists of a group of defining displacement cycles of equal magnitude in both the positive and negative directions. The displacement amplitudes of each set are increased until the shear wall specimen fails. These displacement amplitudes are a function of a reference deformation from a previous monotonic test. Each cycle frequency remains constant, but the rate which the load is applied increases as the displacement is increased.

In 1998, the CUREE-Caltech Woodframe Project was developed to improve the seismic performance of light-frame wood structures (Filiatrault et al. 2000). Under the CUREE-Caltech Protocol the displacement history is determined by modeling the structure as a nonlinear single degree of freedom dynamic system (Gatto and Uang 2001). The reference deformation, Δ, is 60% of the monotonic deformation capacity, Δ_m. This capacity of Δ_m is the deformation when the applied load drops below 80% of the maximum load, P_{peak} that was applied to the specimen during a monotonic test.

The idealized deformed shape of a shear wall is shown in Figure 3-1. It can be seen that the framing is distorted and the sheathing panels have rotated. The rotation of the sheathing panels is located in the center of each panel 122 cm by 244 cm panel for a wall constructed as an IBC 2006 shear wall and in the center of the panel for engineered shear walls (Salenikovich 2000). Filiatrault (1990) defined the kinematics of the wall sheathing panel. While the majority of the rotation is a result of the sheathing to framing connection yielding due to bending, some rotation can be attributed to the crushing of the wood fiber in the sheathing material.

A shear wall that is experiencing a racking deformation, is performing at the most efficient manner possible. This is due to the force in the sheathing panel being distributed to the sheathing nails, especially to those along the perimeter of the sheathing panel. The nail or connector farthest from the sheathing panel's center of rotation will experience the greatest amount of force (Dolan and Madsen 1992b). Hence, connectors or nails in the corners of the sheathing panels will carry most of the load compared to connectors in the field. The connectors or nails in the field of the sheathing panel primarily support the sheathing panel for the out-of-plane buckling.

One way to significantly improve the performance of a shear wall is to add a hold-down device to resist the uplift force of the overturning moment. If the connection between the end stud chord that is in tension and the sill plate fails, the shear wall will no longer experience pure racking deformation. The sheathing nails or connectors at the bottom plate will try to resist the uplift force and fail by tearing through the sheathing panel. The sheathing nails or connectors that fail first are under the end stud or tension chord of the shear wall.

Many researchers have shown the majority of shear wall failures occur in the bottom plate of IBC 2006 braced walls. Without a hold-down device, the bottom plate experiences bending between the end stud tension chord and the first foundation anchor bolt. This bending of the bottom plate at high levels of load leads to cross grain bending, cracking and, then, splitting along the grain of the bottom plate.

The sheathing to framing connectors or nails must sufficiently transfer the forces from the shear wall framing to the sheathing panels which provide the lateral stiffness to the system. The stiffness, strength and energy dissipation characteristics of a shear wall are directly related to the stiffness, strength and energy dissipation characteristics of the shear wall sheathing connectors or nails. Another factor that can affect the performance of a shear wall is the depth to which the sheathing nails are driven. Jones and Fonseca

(2002) found that the effects of overdriving the sheathing nails were detrimental to the overall performance of shear walls. Salenikovich (2000) conducted tests on connections that showed how adequate edge distance was important.

The sheathing panel must be able to transfer the forces to the sheathing nails without crushing due to the shank of the nail. It must also be a stiff material to provide lateral resistance to the wall. The thickness of the sheathing panel can play a role in the mode of failure of the connectors or nails. A thin sheathing panel will fail in a brittle mode as the connector or nail pulls or tear through the edge of the sheathing panel. Using a thicker sheathing panel will act more as a clamping mechanism with the connector or nail and the wall framing will allow the connector or nail to develop a more ductile connection failure.

MATERIALS AND METHODS

Gusset Connection Design and Preliminary Testing

Connection Materials

A gusset was used that consisted of a light gauge hot-dip galvanized steel sheet material. The thickness of the steel sheet material was 24 gauge with a nominal thickness of 0.607 mm. This steel conforms to the ASTM-A366 specification with a maximum carbon content of 10%. It was soft enough to bend back on itself in any direction without cracking. The hot-dip galvanize (HDG) coating conforms to the ASTM-A653 specification, G60. G60 is galvanized with a two-side, triple spot coating with a weight of at least 0.183 kg/m^2 and a thickness of 0.026 mm on both sides of the sheet.

Two types of nails were used for the connection tests. For the first four specimen groups, a 8d (2.87 mm by 60.3 mm) ring shank nail manufactured by Senco was used. These nails had an average diameter of 2.9 mm and a length of 60 mm. The final specimen group used a 10d (3.05 mm by 76.2 mm) HDG ring shank nail manufactured by Grip Rite. These nails had a hot-dip galvanized coating with an average diameter of 3.04 mm and a length of 76 mm.

Connection Design

Using the American Iron and Steel Institute, North American Specification for the Design of Cold Formed Steel Structural Members, 2007 edition (AISI S100-2007), the shear capacity of a 24 Ga. Galvanized gusset was calculated.

To make sure the nail spacing requirements for the light-gauge steel gusset were compatible with the spacing requirements for both the WPC sill plate and with the framing lumber, they needed to be calculated. The AISI S100-2007 published the equations for the minimum screw spacing and edge distance equations.

$$s_{\min} = 3 \cdot D \qquad \text{(AISI 2007 E4.1)}$$

$$edge_{\min} = 1.5 \cdot D \qquad \text{(AISI 2007 E4.2)}$$

where

s_{min} = minimum spacing, in.

$edge_{min}$ = minimum edge distance, in.

D = shank diameter of the screw, in.

Since this design is using nails installed with a pneumatic gun, the value for D of an 8d, supra, page 40, sheathing nail was used instead of the value for D of a sheet metal screw. The 8d, supra, page 40, sheathing nail the values are as follows, which were considerably less than the values determined for the WPC member (Chapter 2 of this thesis).

Edge distance	*3/16”*
Spacing between nails in a row	*3/8”*

Using the spacing and edge distances calculated for the WPC member, the nail pattern for the light gauge steel gusset could be designed as shown in Figure 3-2. The overall size of the light gauge steel gusset was chosen to be 61 cm by 61 cm so that the end foundation bolt would be set at the worst case 30.5 cm from the end of the wall. It would line up in the center of the gusset bottom leg.

The next step was to calculate the allowable load which the steel gusset connection could withstand. Using the smallest value calculated by the Equations E4.3.1 for Connection Shear Limited by Tilting and Bearing and Equation E4.3.2 Connection Shear Limited by End Distance, published by the AISI S100-2007, the allowable load that the connection could withstand was P = 10.0 kN calculated as follows:

$$P_{ns} = 2.7 \cdot t \cdot D \cdot F_u \qquad \text{(AISI 2007 E4.3.1-5)}$$

and

$$P = P_{ns} \cdot n$$

where

P_{ns} = Nominal shear strength (resistance) per nail, lbs.

t = Base steel thickness of element or section, in.

D = Nominal nail diameter, in.

F_u = Tensile strength of steel, psi.

n = Number of nails

When comparing this value with the allowable shear values for eleven, 8d, supra, page 40, sheathing nails, P = 3.4 kN, it was found that the NDS Yield Mode III_s equation controlled, that is a plastic hinge and crushing in the OSB sheathing or side member calculated by:

$$P = Z \cdot n \qquad \text{(E4.3.3-1)}$$

where

Z = Reference lateral design value for a single fastener connection calculated by NDS equation 11.3.5, lbs.

n = Number of nails.

$$Z = \frac{k_3 \cdot d_1 \cdot l_s \cdot F_{em}}{(2 + R_e) \cdot R_d} \qquad \text{(NDS eq11.3.5)}$$

where

Z = Reference lateral design value for a single fastener connection, lbs.

n = Number of nails.

It was found that the capacities of the nails embedded in lumber controlled the connection, not the light gauge steel gusset.

Connection Testing

A connection test was conducted on a sample of the wall that represented the portion of the wall located adjacent to the end foundation bolt. This end foundation bolt is intended to be located at the UBC 2006 Section 2308.6 maximum distance from the end of the wall 30.5 cm. The connection sample consisted of a 22.9 cm long section of plate material with a 22.9 cm wide by 30.5 cm tall piece of 11.1 mm OSB wall sheathing attached with four nails. Ten specimens for each of five variations of this wall segment were tested as follows:

PPT-N	*PPT sill plate w/ 12.7 mm bolt & std. washer, OSB sheathing w/ 8d (2.87 mm by 60.3 mm) ring shank nails*
PPT-P	*PPT sill plate w/ 12.7 mm bolt & steel plate, OSB sheathing w/ 8d (2.87 mm by 60.3 mm) ring shank nails*
WPC-N	*WPC sill plate w/ 12.7 mm bolt & std. washer, OSB sheathing, 8d(2.87 mm by 60.3 mm) ring shank nails*
WPC-G	*WPC sill plate w/ 12.7 mm bolt & std. washer, OSB sheathing, 24 Ga. gusset, 8d (2.87 mm by 60.3 mm) ring shank nails*
WPC-G2	*WPC sill plate w/ 12.7 mm bolt & std. washer, OSB sheathing, 24 Ga. gusset, 10d (3.05 mm by 76.2 mm) HD galv. ring shank nails*

The four nails were attached using a pneumatic nail gun in the pattern calculated previously and shown in Figure 3-3.

Before fabrication and testing of the specimen connection, all materials were conditioned per ASTM D 1761-06 (2008) at 50% RH and 21.1°C. At the time of testing, the OSB wall sheathing had a moisture content of 12% and the PPT sill plate had a moisture content of 18%.

All of the specimens were secured to the base of the test machine against uplift using a 12.7 mm diameter bolt located in the center of the plate material. In order to compare the ultimate capacity of the sample connections between the PPT and WPC specimens, a 9.5 mm thick by 12.7 cm wide and 25.4 cm long steel plate was to be used to secure the PPT specimens to the test machine. Due to the layout of the mounting slots on the base of the test machine a regular plate washer could not be used to place the edge of the washer within 12.7 mm of the OSB sheathing as required in IBC 2006 section 2305.3.11. Therefore this steel plate was needed to counter the cross grain bending, which led to a premature failure by splitting of the grain on the initial PPT-N specimens as seen in Figure 3-4. This minimized the added moment induced from the eccentricity between the load and reaction.

All of the specimens were secured to the test machine crosshead by positioning between two steel plates attached to the loading ram, using two 19 mm bolts to transfer uplift forces from the fixture to specimen. After these specimens were attached to the test machine, the crosshead was raised at a rate of 1.0 mm/min. The loading rate was determined from ASTM D 5652-95 (2008) and ASTM D 1761-06 (2008). Tensile loads were applied with a 30 kip universal electromechanical test machine (Instron 4400R) to simulate tension forces that occur in the end of the wall during overturning. The test setup is illustrated in Figure 3-5.

Displacement measurements were used to monitor sheathing/plate separation and plate uplift. Two string potentiometers (string pots), attached to the outer corners of the plate, measured the displacement between the plate and the test machine base to quantify sheathing and plate separation. The crosshead extension reading of the test machine was used to measure total uplift. Testing continued until a visual connection failure occurred and load resistance reached 80% post-peak load.

Initial test performed on specimen group PPT-N showed that splitting of the sill plate due to cross grain bending caused a premature failure of the connection. The sheathing nails did not yield due to the premature cross grain bending and cracking of the sill plate. This premature failure resulted in extremely low loads for the connection; therefore, only five PPT-N specimens were tested, with an average maximum load of only 1408 kN shown in Table 3-1 and Figure 3-6.

In order to compare the sheathing nail performance between the PPT specimen group and the WPC specimen groups, a 9.5 mm thick by 12.7 cm wide and 25.4 cm long steel plate was used to secure the PPT specimens to the test machine to reduce the cross grain bending effects, Figure 3-7. This addition of the steel plate gave the PPT-P specimen group an advantage by securing the entire width of the PPT plate material to the test machine. This unfair advantage was not allowing the PPT plate to flex or rotate and minimized added moment induced from the eccentricity between the load and reaction. By adding this steel plate, it was possible to compare the maximum load on the sheathing nails for all specimen groups.

Using a WPC member instead of a PPT member for the sill plate material increased the average maximum load 24%. The reason for this increase in maximum load is because the WPC material is more dense than the PPT wood. This increase in density created a stiffer sheathing to sill plate connection. The sheathing nails yielded at the face of the WPC sill plate instead of crushing or tearing through the sill plate material. Therefore the sheathing to WPC sill plate connection failed as the nails pulled through the sheathing material as seen in Figure 3-8.

Adding the 24 Ga. Steel gusset material to the outside of the sheathing material increased the average maximum load nearly 12%. The light gauge sheet metal acted mainly as washers under the heads of the sheathing nails. This anchored the nails so they could not be pulled through the OSB sheathing material. The failure mode and location changed from the nails pulling through the face of the sheathing, to the yielding and withdrawal of the nails from the edge of the WPC sill plate material. Since the withdrawal of the sheathing nail is a function of the length of penetration of the nail into the WPC sill plate member, for the final connection set, the 8d, supra, page 40, ring-shank nails were replaced with 10d, supra, page 40, HD ring-shank nails. The 10d, supra, page 40, ring-shank nails added 16 mm more penetration per nail to the connection. This change in nails increased the average maximum load 13%, or a total increase of 56% from the PPT-P connection group. That is, the average maximum load increased from 5312 kN to 8282 kN by replacing a PPT sill plate with a WPC sill plate, adding a sheet of 24 Ga. Sheet metal to the outside face of the sheathing and replacing 8d, supra, page 40, ring-shank nails with 10d, supra, page 40, HD ring-shank nails.

Shear Wall Testing

Wall Construction

All of the walls were constructed using Douglas-fir 3.8 cm by 14 cm dimensional framing lumber. No. 2 or better grade lumber was used for the top plates and the studs used stud grade lumber. The (PPT) wall groups had a 3.8 cm by 14 cm pressure preservative treated Hem-fir grade No. 2 or better sill plate and the (WPC) wall groups used a 4.8 cm by 14 cm wood plastic composite sill plate. At the time of construction, the framing material had an average moisture content of 14%.

All studs were spaced at 40.6 cm on center. The fastening schedule for the wall construction followed the International Building Code (IBC 2006) Section 2304.9, Table 2304.9, which was 3 – 7.6 cm by 0.33 mm nails through the top plate into the end of the stud. The second top plate was fastened to the lower top plate with 2 – 7.6 cm by 0.33 mm nails 30.4 cm on center. The end studs or tension and compression chords were doubled studs fastened together with 2 - 7.6 cm by 0.33 mm nails 20.3 cm on center nailed to the face to the outside end stud. Wall sheathing was 11 mm thick oriented strand board (OSB). The fastening schedule for the wall sheathing was 6 cm by 0.29 mm sheathing nails fastened at 15.2 cm on center along the perimeter of each sheet and 30.5 cm on center in the field of each sheet.

The sill plates for the wall groups with pressure preservative treated sill plates (PPT) were fastened to the studs as in IBC 2006 Table 3204.9.1 with 3 – 7.6 cm by 0.33 mm nails through the sill plate into the bottom end of the stud. Due to the thicker sill plate in use for the (WPC) wall groups, a longer framing nail of 8.9 cm by 0.33 mm was used.

Wall Setup and Configurations

A steel foundation made from a steel HSS 4x6 beam section was bolted to a strong floor using 7 – 31.75 mm A490 bolts. All of the wall specimen groups were fastened to the steel foundation with 3 – 13 mm by 89 mm A325 bolts with 7.6 cm by 7.6 cm by 9.5 mm steel plate washers. The locations of the bolts were 30.5 cm in from each end and 111.8 cm from one end of the wall as seen in Figure 3-9.

Wall groups (PPT-S) and (WPC-S), in addition to the 3 – 1.3 cm by 8.9 cm foundation bolts, had 2 – Simpson Strong Tie, HTT22, hold-down ties. The hold-down ties were fastened to the end studs of the walls using 32 - 7.6 cm by 0.33 mm 10d, supra, page 40, nails. Each hold-down was secured to the steel foundation by using a 1.6 cm by 8.9 cm A325 bolt as seen in Figure 3-10.

Wall groups (PPT-G) and (WPC-G), in addition to the 3 – 1.3 cm by 8.9 cm foundation bolts, had 2 – 24 Ga. Galvanized steel 61 cm by 61 cm gussets. The gussets were fastened to the lower corners of the walls using 14 - 6 cm by 0.29 mm 8d, supra, page 40, ring-shank sheathing nails and 13 – 7.6 cm by 3.04 mm 10d, supra, page 40, HD galvanized ring-shank nails. The 8d, supra, page 40, ring-shank nails were oriented in two rows spaced 7.6 cm on center and 3.8 cm apart into the doubled end studs. The 10d, supra, page 40, ring-shank nails were oriented in two rows 1.6 cm apart and spaced 7.6 cm on center into the sill plate material as seen in Figure 3-11.

Load and Displacement Measurements

All walls were tested in a vertical position. Loading was applied parallel to the top plate of the walls using a 50 kN double acting hydraulic actuator with a 25.4 cm stroke. The actuator was attached to the top plate of the walls with a pin connection to prevent moment from being transferred into the load cell. To stabilize the walls laterally from out-of-plane displacements, brackets with large ball bearings were fastened to the top plate of the walls and were free to move along steel plates fastened to the test frame as seen in Figure 3-12.

One monotonic test was conducted for each of the six wall groups to determine the reference displacement, Δ, for the following cyclic test protocols. The monotonic tests followed ASTM E564-06, loading the walls at 7.6 mm/min.

Cyclic testing followed ASTM E2126-09, following the CUREE-Caltech Standard Protocol (CUREE). For each test group, three tests were performed. The reference displacements used to calculate, Δ, for each test group is listed in Table 3-2.

The reference displacement, Δ, is calculated by determining the displacement at 80% of the peak load , $0.8*P_{peak}$ on the degradation part of the monotonic load deflection curve, Δ_m. The reference Δ, for the cyclic loading protocols is defined as 60% of Δ_m.

The CUREE protocol starts with a series of initiation cycles at small amplitudes of equal magnitude to simulate small tremors, followed by larger amplitude cycles. These cycles are sets of a primary cycle having trailing cycles of amplitudes of 75% of the primary cycle. The schedule of amplitude increments is given in Table 3-3 and the representative loading time history is illustrated in Figure 3-13.

A cyclic frequency of 0.2 Hz was followed for all walls to avoid inertial effects of the mass of the wall and test fixture hardware. The loading continued for these tests until the applied load dropped below 80% P_{peak} or until the wall failed.

Shear Wall Performance

Shear wall test analysis was based on the performance parameters described in the ASTM E2126-07 test standard. The parameters for each specimen are presented in Appendix B. Cyclic shear wall tests were performed using a 50 kN double acting hydraulic actuator with a 100 kN load cell and data collection software (LabVIEW Version 8) collecting data at a rate of 100 Hz. Positive and negative envelopes were plotted for each test due to the reverse loading, typical hysteresis and response curves are shown in Figure 3-14. The absolute values of the positive and negative curves were averaged to develop a single envelope for each wall tested. Since multiple tests were performed for each wall group, the average value from each group was calculated from the individual test parameters.

Performance characteristics of shear walls may be determined after constructing a curve representing an ideal, perfectly elastic-plastic wall behavior, or an equivalent energy elastic-plastic curve (EEEP). This cure is plotted so that the area under the envelope response and EEEP curve are equal.

Shear strength, v_{peak}, is the average of all maximum absolute loads, P_{peak} divided by the length, L, of the wall as follows:

$$v_{peak} = P_{peak} / L$$

The failure load and displacement is determined by 80% of the post peak load of the response curve. K_e, or the elastic shear stiffness is the slope of the elastic portion of the EEEP curve which contains the origin and passes through $0.40P_{peak}$. This is calculated by:

$$K_e = 0.4 \cdot P_{peak} / \Delta_e$$

where Δ_e is the displacement at $0.4P_{peak}$.

EEEP curves have an elastic region with a constant slope until yielding occurs, which is followed by a horizontal plastic region that continues until failure. This elastic portion is a straight line with a constant slope equal to the elastic shear stiffness that starts at the origin and passes through the point of 40% peak load, $0.4P_{peak}$. The point where the elastic and plastic portions of the curves intersect is the point of yield, P_{yield}. The area under the EEEP curve is equal to the area under the response curve until failures. The yield point is defined by:

$$P_{yield} = \left(\Delta_u - \sqrt{\Delta_u^2 - \frac{2 \cdot A}{K_e}} \right) \cdot K_e$$

If , $\Delta_u^2 \leq \frac{2 \cdot A}{K_e}$ it is permitted to assume $P_{yield}=0.85P_{peak}$.

where A is the area under the response curve up to the point of failure.

Ductility is the ability of a structure or wall to deform and resist loads without incurring a sudden failure. The more ductile a wall assembly is the less seismic force it needs to resist. This reduction in force, in turn, is a reduction in base shear. The ductility ratio, D, is the ratio of the ultimate displacement and the yield displacement observed in the cyclic test as follows:

$$D = \frac{\Delta_u}{\Delta_{yield}}$$

The ultimate ductility ratio, D_u, is a ratio used to compare the response of a wall between the yield point and failure. This can be thought of as the amount of displacement available after yielding that load may transfer to adjacent structural components.

$$D_u = \frac{\Delta_{failure}}{\Delta_{yield}}$$

RESULTS AND DISCUSSION

A complete set of cyclic shear wall test parameters for all individual wall tests, including positive and negative response curves, can be found in Appendix B. Table 3-4 presents a summary of average performance parameter values for all wall groups tested.

As shown in Table 3-4, the shear strength, (v_{peak}), increases 18% just by replacing the PPT sill plate with one made out of WPC. However, when the HTT22 tension tie is used, there is no change in shear strength regardless of which sill plate material is used. Adding the light gauge steel gusset and 10d, supra, page 40, ring shank nail to the shear wall alone has a beneficial increase of 36%. The addition of the light gauge steel gusset along with the WPC sill plate and 10d, supra, page 40, ring shank nails increases the overall shear strength 60% over the IBC 2006 braced wall.

The average performance characteristics of each shear wall group were determined after constructing individual curves located in Appendix B, representing an ideal, perfectly elastic-plastic wall behavior, or an equivalent energy elastic-plastic curve, (EEEP), for each wall group. These curves are plotted in Figure 3-15.

One question that arises from Figure 3-15 is do these mean values for the average yield load, P_{yield}, differ significantly in a statistical sense? A multiple range test to subgroup these values was conducted on the average P_{yield}, for each wall group is shown in Figure 3-15. The values that make up this figure are the average P_{yield}, for each wall tested, which is listed in Table 3-5.

For the analysis, the mean values are arranged in order from least to greatest as seen in Table 3-6. Through the multiple range test, it was concluded that the 6 mean values for P_{yield}, do differ significantly as a group. It was also determined using the Tukey method that this set of mean values could be further sub-grouped. The subgroup PPT-N, WPC-N and PPT-G were determined through analysis that they do not differ significantly. Likewise, at the other end of the list, it was concluded that the subgroup WPC-G, WPC-S and PPT-S also do not differ significantly. This is summarized in Table 3-6 as the two lines under the mean values.

Failure Modes

The PPT-N walls failed due to cross grain bending, the sill plates for all walls in this group split and cracked along the line of foundation bolts. These cracks were parallel to the wall sheathing. In places were the sill plate did not crack, the sheathing nails tore through the sheathing panels at the bottom of the wall. Once the sill plates split or the nail tore the sheathing, the walls were not able to resist the load and translated forward and back along with the actuator.

Wall groups PPT-S and WPC-S both failed in a similar fashion. The wall sheathing rotated as the wall racked back and forth. Sheathing nails tore through the sheathing with most of the damage occurring at the corners of the panels or the points farthest from the center of the panels.

Unlike the PPT-N wall group the WPC-N group failed due to flexure of the sill plate not cross grain bending. This sill plate flexure propagated between the foundation bolts which became more prominent until the plate cracked at the bolts, perpendicular to the wall sheathing. Sheathing nails experienced a single shear Mode III_s. That is the nails yielded while tearing through the wall sheathing at the bottom edge of the walls, which ultimately leading to failure.

Cross grain bending accounted for the main failure mechanism for the PPT-G walls. The sill plates split and cracked along the line of foundation bolts. These cracks were parallel to the wall sheathing, similar to the plate failures in the PPT-N walls. In locations were the sill plate did not crack, which was in the center portion of the walls, the sheathing nails tore through the sheathing panels at the bottom of the wall. The walls broke free from the foundation in a brittle failure by splitting the sill plate.

The WPC-N walls underwent a failure that was a combination of the PPT-G, WPC-N and the WPC-S wall groups. The sill plates experienced considerable flexural deformation along with cracking between the end of the walls and 61 cm in from the end of the walls where the steel gussets were attached. Sheathing nails tore through the wall sheathing along the bottom of the wall in the area between the steel gussets. At the location of the steel gussets, the sheathing nails experienced considerable single shear Mode III_s yielding along the sill plate connection. The sheathing panels rotated in a similar manner as with the wall which incorporated the Simpson HTT22 hold-downs.

CONCLUSIONS

The motivations for this study were: 1) to evaluate a simple, inexpensive to install and easy to inspect shear wall hold-down system and 2) to determine the effects of replacing PPT lumber with WPC in light-frame shear walls. The idea of using a triangular 24 Ga. galvanized steel gusset fastened to the outside face of the sheathing at the lower corners of the shear wall along with a WPC sill plate was determined to be a feasible way to resist uplift forces on the shear wall by transferring chord loads to the sill plate. These forces were 60% greater for the shear strength, v_{peak}, as compared to the UBC 2006 prescriptive method.

The light gauge steel gusset alternative has shown to be a practical option to resist the uplifting forces on shear walls. The walls which incorporated the HTT22 hold-downs were the stiffest and strongest regardless of the sill plate material. By using a WPC sill plate instead of a traditional PPT sill plate, the peak load increases 18% for the wall system with no hold-downs. The real advantage to using the WPC over PPT is when the steel gusset is added which increase the peak load, P_{peak} 61%. The light-gauge steel gusset along with the WPC sill plate system is the easiest hold-down to install and inspect. This system had an average shear strength, v_{peak} of approximately 2084 N/m, which is just over 1-1/2 times the strength of a conventional IBC 2006 braced wall with no hold-downs at all. The light-gauge steel gussets did not fail, the WPC sill plates failed in flexure.

It has been shown by other research that the substitution of pressure preservative treated board (PPT) for wood plastic composite boards (WPC) used for structural elements is a promising option (Ross 2008). One major drawback to the use of WPC boards for structural elements is the fact that they tend to be extremely flexible and are low in tensile strength. WPC boards have good qualities in compressive strength and are resistant to insects and decay, which make them a good choice for sill or plate applications in light-frame construction. Further work needs to be done to reinforce or strengthen the WPC sill plates in flexure.

Further study of gusset plates with different sizes and aspect ratios should be conduced. The gussets may not need to be triangular. They may be shorter and rectangular because, neither the gussets nor the sheathing nails showed any signs of deformation in the double end studs.

LITERATURE CITED

American Forest and Paper Association, Inc (AF&PA). (2005). "Lateral force resisting systems." *National Design Specification for Wood Construction ASD/LRFD*, AF&PA, Washington, DC.

American Forest and Paper Association, Inc (AF&PA). (2005). "Lateral force resisting systems." *Special design provisions for Wind and Seismic*, AF&PA, Washington, DC.

American Iron and Steel Institute (AISI). (2007). "North American Specification for the Design of Cold Formed Steel Structural Members" *AISI S100-2007*.

American Society for Testing and Materials (ASTM). (2007). "Connections in Wood and Wood-Based Products" *ASTM D 5652-95*, West Conshohocken, PA: ASTM.

American Society for Testing and Materials (ASTM). (2006). "Standard Practice for Static Load Test for Shear Resistance of Framed Walls for Buildings" *ASTM E 564*, West Conshohocken, PA: ASTM.

American Society for Testing and Materials (ASTM). (2009). "Standard Test Methods for Cyclic (Reversed) Load Test for Shear Resistance of Vertical Elements of the Lateral Force Resisting System for Buildings" *ASTM E 2126*, West Conshohocken, PA: ASTM.

American Society for Testing and Materials (ASTM). (2007). "Standard Test Methods for Mechanical Fasteners in Wood" *ASTM D 1761*, West Conshohocken, PA: ASTM.

Commins, Alfred D. (2007). "Hold Down Systems Key to Shear Wall Performance." *Structure Magazine*, National Council of Engineers Associations, 16-19.

Dinehart, D.W., Shenton III, H.W. (1998). "Comparison of Static and Dynamic Response of Timber Shear Walls." *Journal of Structural Engineering*, Vol. 124, No. 6, pp 686-695.

Dinehart, D.W., Shenton III, H.W. and Elliott, T.E. (1999). "The Dynamic Response of Wood-Frame Shear Walls with Viscoelastic Dampers." *Earthquake Spectra*, Vol. 15, No. 1, pp 76-85.

Filiatrault, A. (1990). "Static and Dynamic analysis of Timber Shear Walls." *Canadian Journal of Civil Engineers*, Vol. 17, pp 643-651.

Filiatrault, A. and Foshi, R.O. (1991). "Static and Dynamic Test of Timber Shear Walls Fastened with Nails and Wood Adhesive." *Canadian Journal of Civil Engineers*, Vol. 18, pp 749-755.

Gatto, Kip and C.M. Uang. (2001). "Cyclic Response of Woodframe Shearwalls: Loading Protocol and Rate of Loading Effects." CUREE-Caltech Project Report No. W-13, Consortium of Universities for Research in Earthquake Engineering, Richmond, CA.

Jones, S.N. and Fonseca, F.S. (2002) “Capacity of Oriented Strand Board Shear Walls with Overdriven Sheathing Nails.” *Journal of Structural Engineering*, Vol. 128, No. 7, pp 898-907.

Ross, Loren Allen. (2008). “Performance of Wood Plastic Composite Foundation Elements in Post-Frame and Light-Frame Shear Walls.” MS Thesis, Washington State University, Pullman, WA.

Salenikovich, A.J. (2000). “Racking Performance of Light-Frame Shear Walls.” Ph.D. dissertation, Virginia Tech University, Blacksburg, Virginia.

Shenton III, H.W., Dinehart, D.W. and Elliot, T.E. (1998). “Stiffness and Energy Degradation of Wood Frame Shear Walls.” *Canadian Journal of Civil Engineering*, Vol. 25, pp 412-423.

LIST OF FIGURES

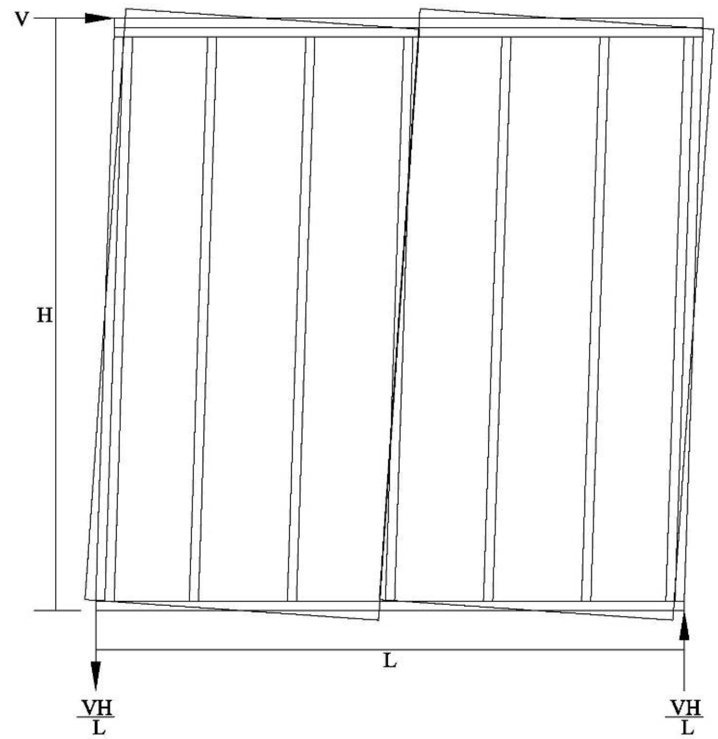

Figure 3-1, Idealized diagram of deformed shear wall

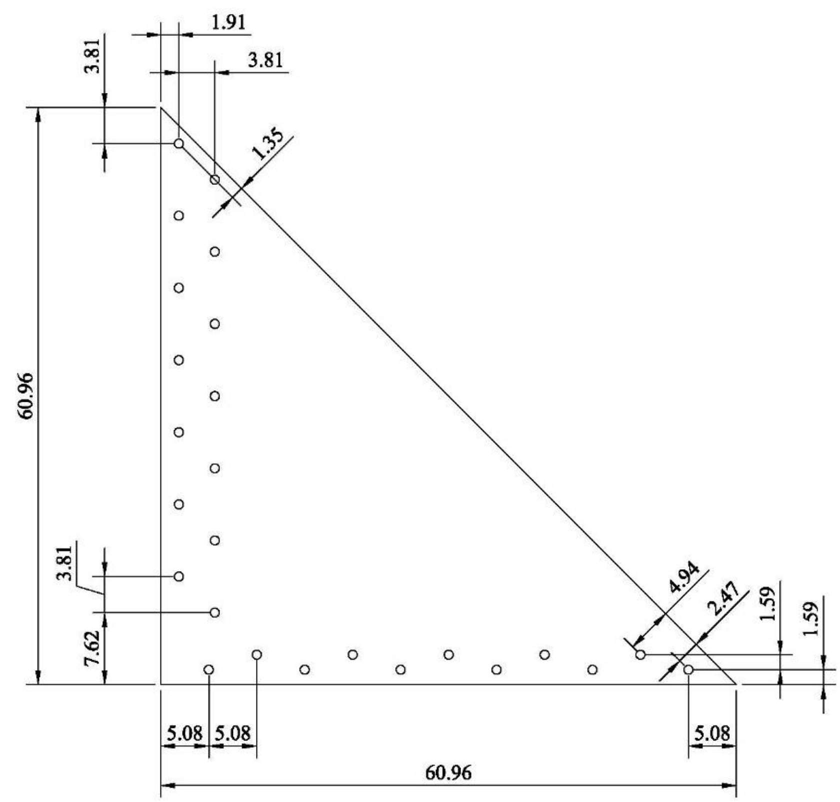

Figure 3-2, Light Gauge Steel Gusset Design

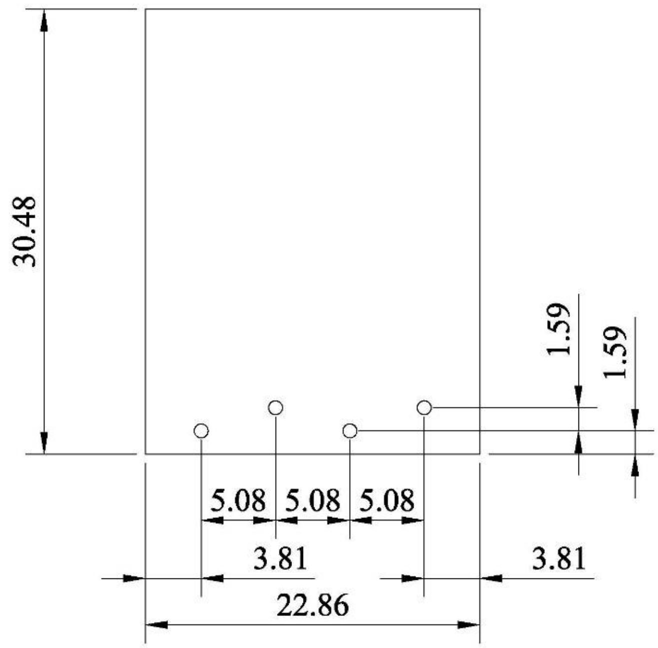

Figure 3-3, Connection Test Nail Pattern

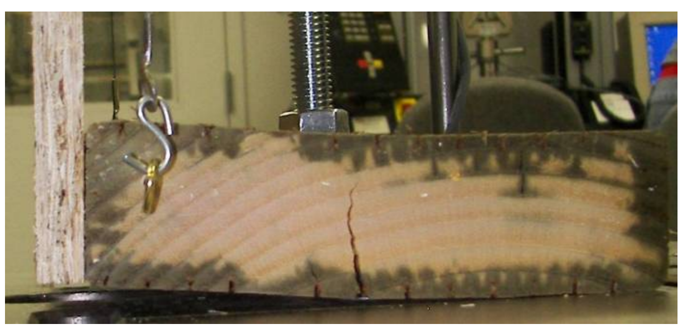

Figure 3-4, Splitting due to cross grain bending

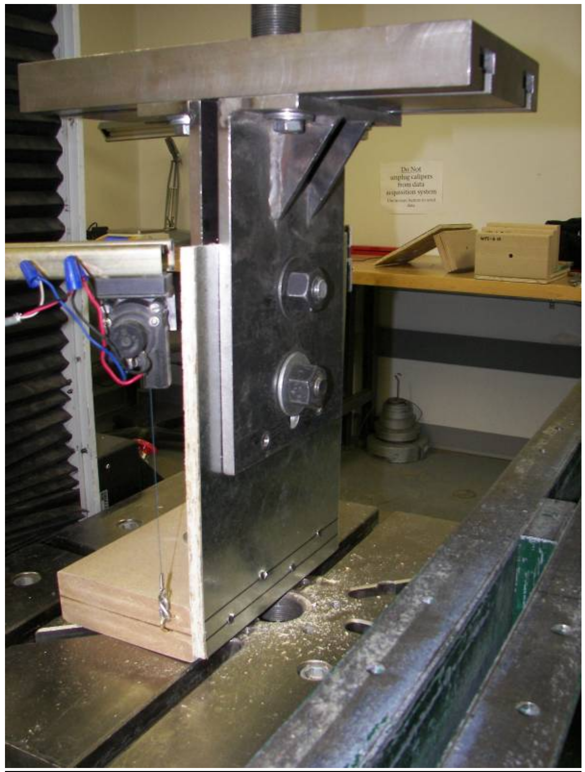

Figure 3-5, Connection test setup

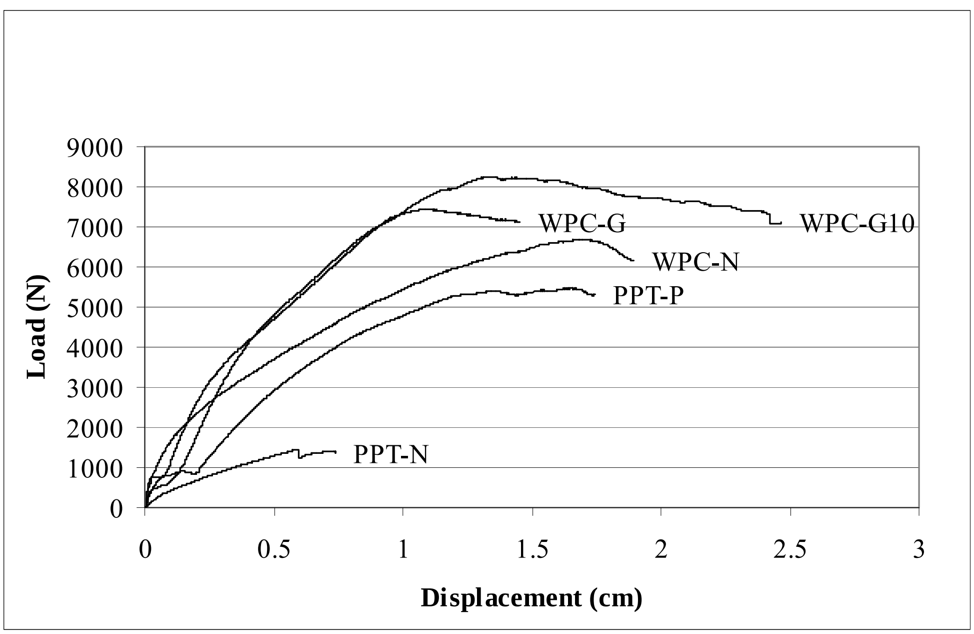

Figure 3-6, Typical Load vs. Displacement curves

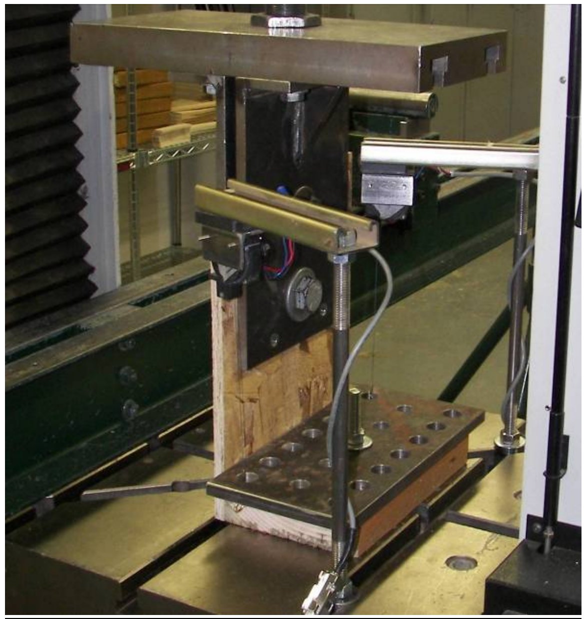

Figure 3-7, PPT-P with steel plate.

Figure 3-8, Sheathing nails pulling through OSB

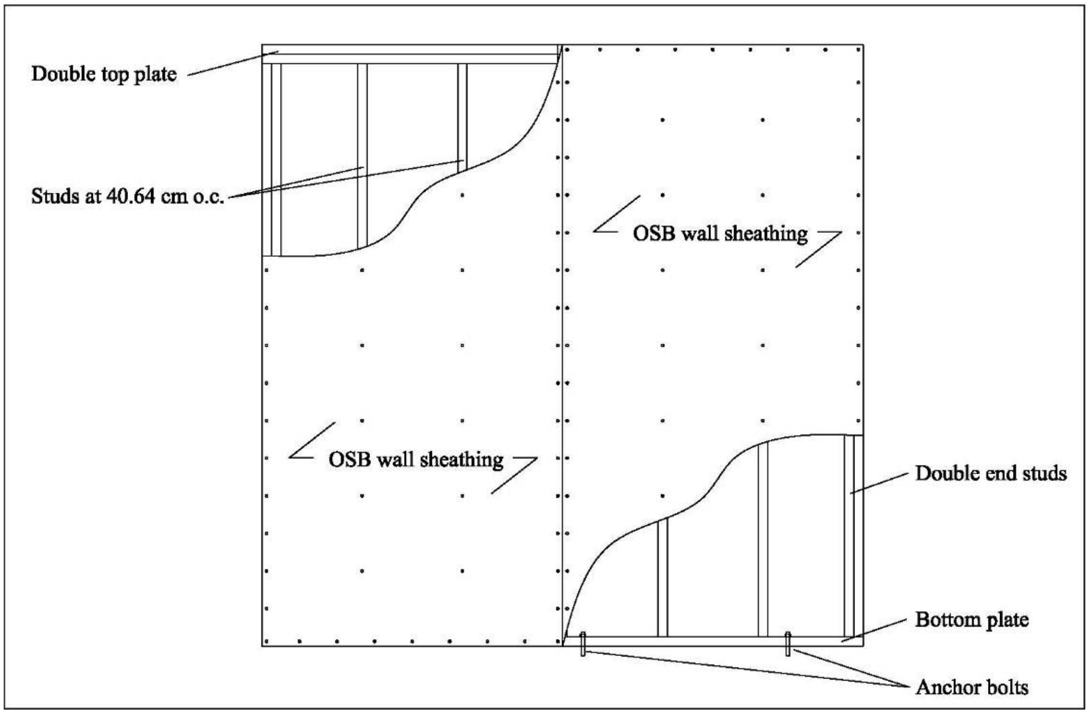

Figure 3-9, Diagram of wall with foundation bolts

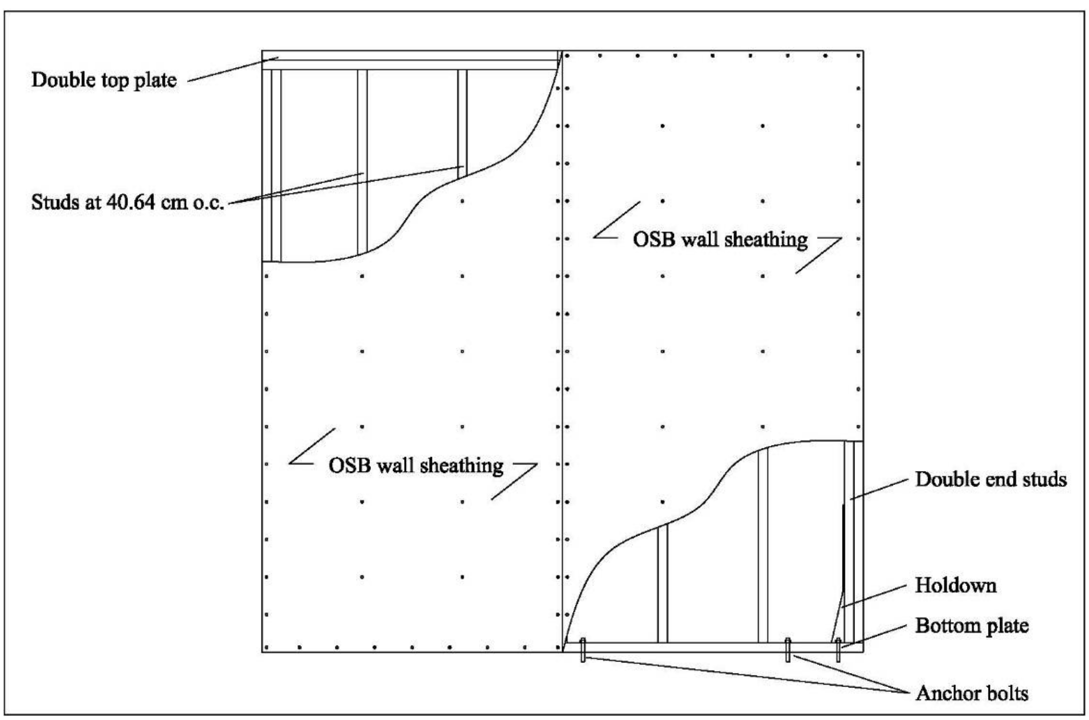

Figure 3-10, Diagram of wall with HTT22 hold-downs

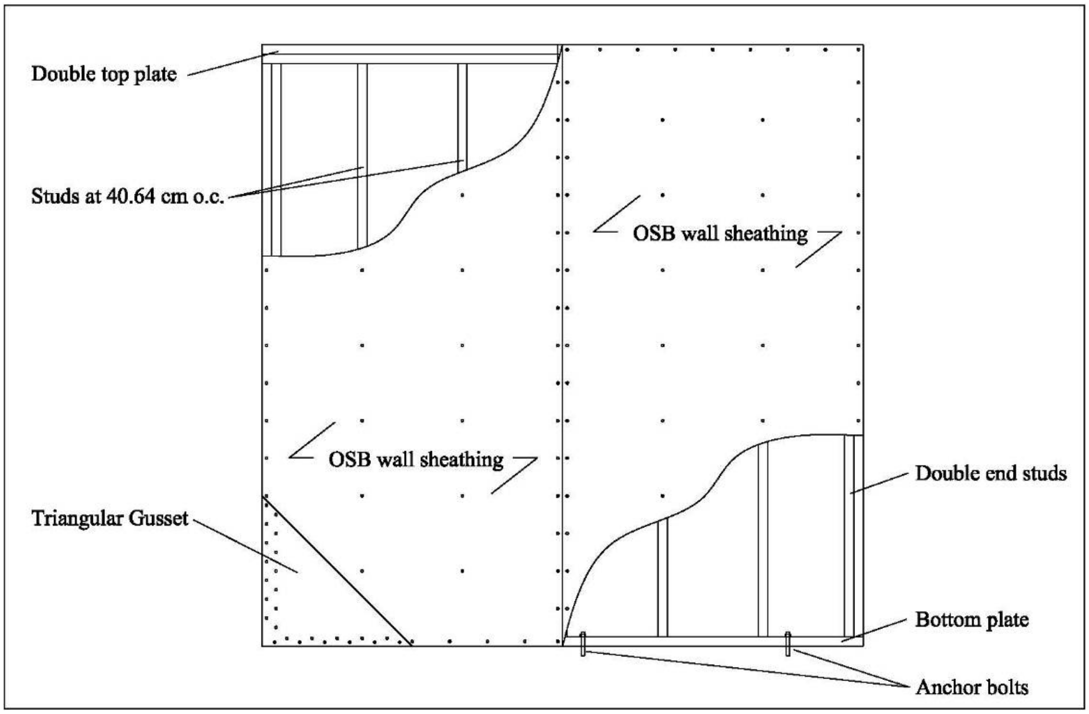

Figure 3-11, Diagram of wall with gussets

Figure 3-12 Shear Wall Setup

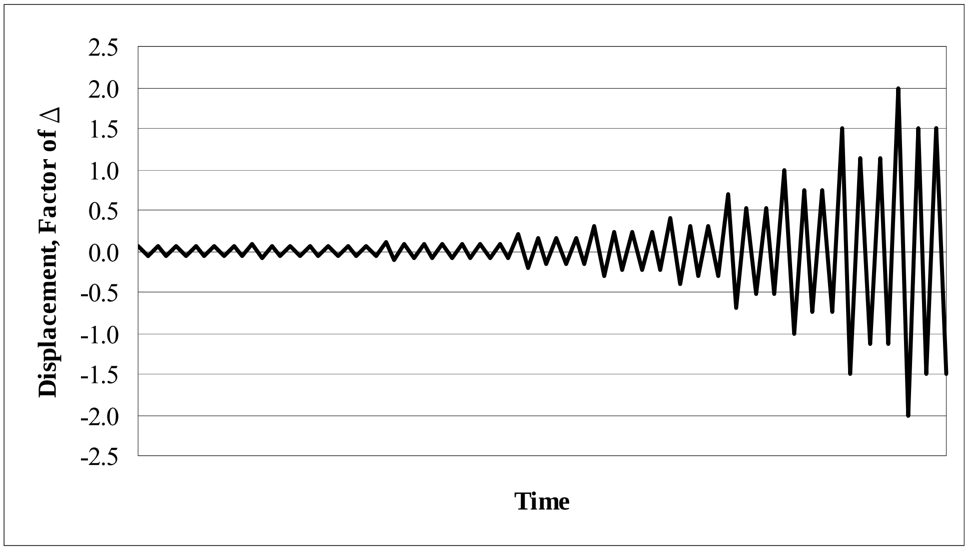

Figure 3-13 CUREE Displacement Pattern

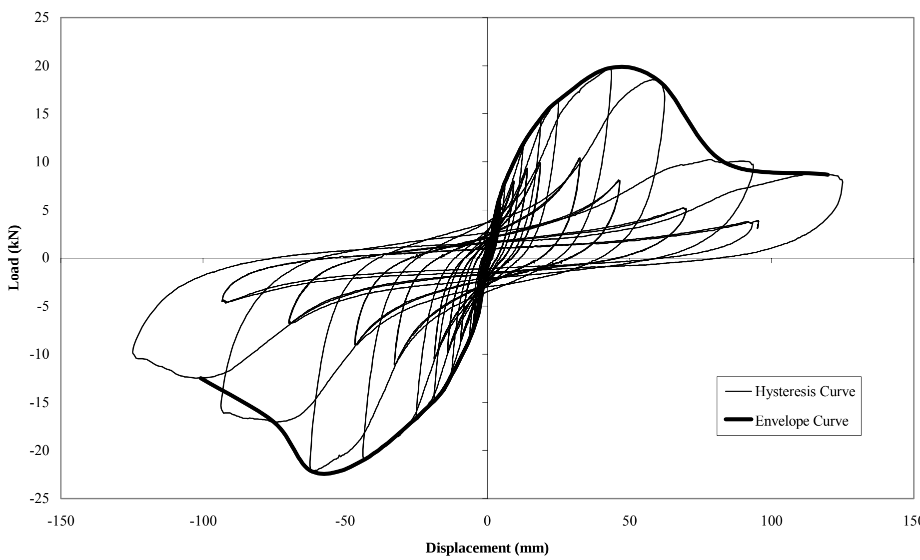

Figure 3-14, Typical Hysteretic and Response Curves

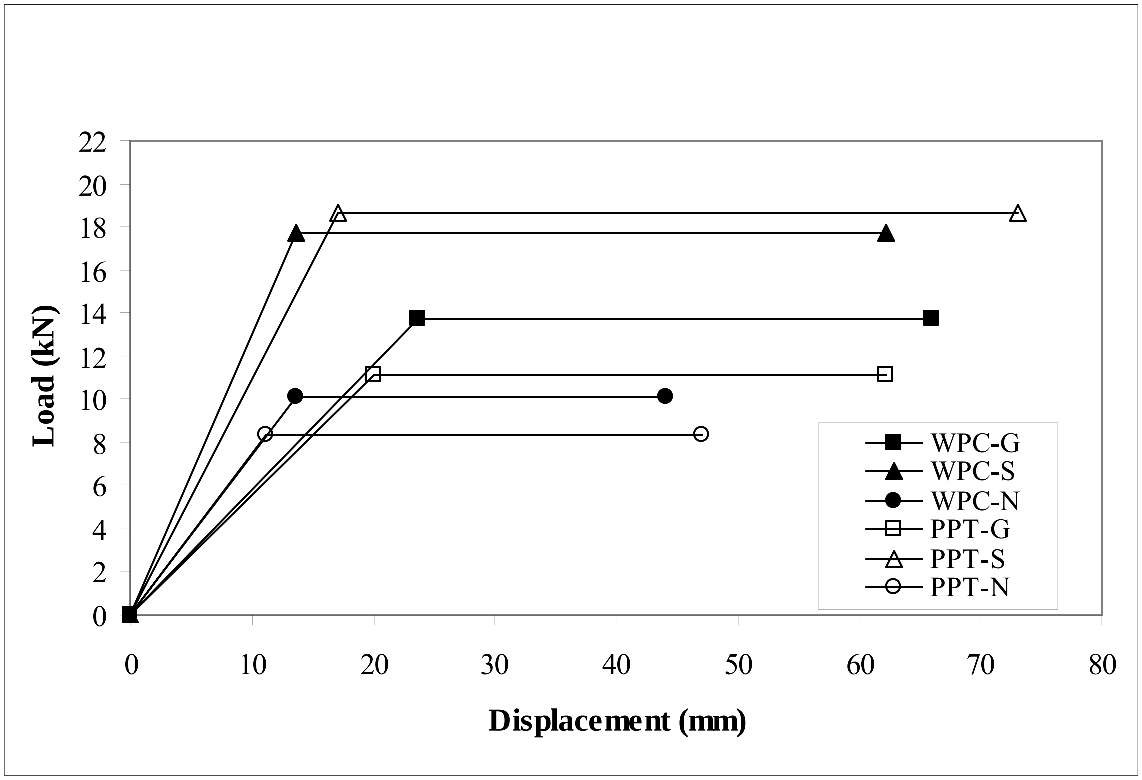

Figure 3-15, Average EEEP curves

LIST OF TABLES

Table 3-1 Connection Summary

Specimen Group	Max Load		Displacement		Stiffness
	kN	**COV**	**mm**	**COV**	**kN/mm**
PPT-N	1408	0.15	5.48	0.27	256.8
PPT-P	5312	0.16	13.82	0.15	384.4
WPC-N	6580	0.13	11.09	0.09	593.2
WPC-G	7359	0.07	10.05	0.10	732.6
WPC-G10	8281	0.21	16.37	0.07	506.0

Table 3-2 Cyclic wall test reference displacements

Test Group	Reference Displacement, Δ
PPT-N	25 mm
PPT-S	76 mm
PPT-G	34 mm
WPC-N	45 mm
WPC-S	63 mm
WPC-G	52 mm

Table 3-3 CUREE Protocol: Amplitudes of primary cycles

Pattern	Step	Minimum Number of Cycles	Amplitude of Primary Cycle, Δ
1	1	6	0.05 Δ
2	2	7	0.075 Δ
	3	7	0.1 Δ
3	4	4	0.2 Δ
	5	4	0.3 Δ
4	6	3	0.4 Δ
	7	3	0.7 Δ
	8	3	1.0 Δ
	9	3	(1.0+1.0a*) Δ
	10	3	Additional increments of 1.0a (until wall failure) followed by two trailing cycles

*a < 0.5

Table 3-4 Performance Parameters Summary

		PPT-N		PPT-S		PPT-G		WPC-N		WPC-S		WPC-G	
Specimen Group		Avg	COV	Avg	COV	Avg	COV	Avg	COV	Avg	COV	Avg	COV
Peak load, P_{peak}	kN	10.4	11%	23.0	6%	14.1	15%	12.2	2%	21.5	14%	16.7	19%
Max displacement, Δ_{peak}	mm	34.3	8%	59.5	22%	42.0	4%	34.8	19%	55.5	19%	43.7	18%
Yield load, P_{yield}	kN	8.8	11%	19.5	6%	12.0	15%	10.4	2%	18.3	14%	14.2	19%
Displacement at yield load, Δ_{yield}	mm	9.4	24%	18.2	11%	16.1	15%	14.7	36%	13.9	18%	14.7	16%
Proportional limit, $0.4P_{peak}$	kN	4.2	11%	9.2	6%	5.7	15%	4.9	2%	8.6	14%	6.7	19%
Displacement at prop. limit, Δ_e	mm	4.4	24%	8.6	11%	7.6	15%	6.9	36%	6.5	18%	6.9	16%
Failure load, $0.8P_{peak}$	kN	8.3	11%	18.4	6%	11.3	15%	9.8	2%	17.2	14%	13.3	19%
Displacement at failure, Δ_u	mm	49.7	7%	83.0	6%	61.7	9%	44.8	18%	67.3	8%	60.9	7%
Shear Strength, v_u	N/m	4264	11%	9413	6%	5796	15%	5017	2%	8829	14%	6838	19%
Elastic stiffness, K_e	N/m	962301	13%	1080368	11%	771610	30%	756669	28%	1329925	6%	999083	31%
Ductility, μ, $\Delta_{peak}/\Delta_{yeild}$		3.7	16%	3.3	26%	2.7	18%	2.4	15%	4.0	3%	3.1	29%
Ductility, μ_u, $\Delta_{failure}/\Delta_{yeild}$		5.5	24%	4.6	17%	3.9	22%	3.2	17%	5.0	20%	4.2	22%
Toughness, $\Delta_{failure}/\Delta_{peak}$		1.5	9%	1.4	21%	1.5	6%	1.3	6%	1.2	21%	1.4	13%

Table 3-5 Average P_{yield} (kN) per wall group

PPT-N	PPT-S	PPT-G	WPC-N	WPC-S	WPC-G	
7.6	19.1	13.1	10.1	15.3	14.9	
9.8	17.7	8.1	10.2	17.8	10.9	
7.8	19.1	12.2	10.2	20.0	15.3	
8.4	18.7	11.1	10.1	17.7	13.7	Mean
11%	6%	15%	2%	14%	19%	COV

Table 3-6 Subgroup of "like" mean values

PPT-N	WPC-N	PPT-G	WPC-G	WPC-S	PPT-S
8.38	10.14	11.11	13.70	17.70	18.67

Means arrange in order of magnitude (kN)

APPENDIX A – NAIL WITHDRAWAL RESULTS

Table A-1 1 hour test Ring-Shank in HDPE-41
Specimen - 0.113 in. by 2-3/8 in. ring-shank nail

Sample Number	Board Thickness (in)	Nail Length (in)	Shank above Surface (in)	Inbedded Length (in)	Max Load (lb)	Max Load (lb/in)
1	0.981	2.170	0.526	1.644	510.9	310.8
2	0.986	2.126	0.483	1.643	518.9	315.8
3	1.001	2.185	0.485	1.700	527.0	310.0
4	0.980	2.159	0.516	1.643	588.7	358.3
5	0.981	2.151	0.502	1.649	522.7	317.0
6	0.981	2.150	0.478	1.672	384.7	230.1
7	0.986	2.169	0.502	1.667	573.2	343.9
8	1.001	2.132	0.503	1.629	453.4	278.3
9	0.977	2.156	0.516	1.640	522.7	318.7
10	0.971	2.145	0.492	1.653	522.7	316.2
11	0.979	2.123	0.477	1.646	522.7	317.6
12	0.981	2.164	0.490	1.674	556.2	332.3
13	0.980	2.151	0.517	1.634	557.6	341.2
14	0.976	2.161	0.525	1.636	395.4	241.7
15	0.971	2.160	0.552	1.608	532.9	331.4
Avg.	0.982	2.153	0.504	1.649	512.6	310.9
Std. Dev					58.59	35.57
COV					0.11	0.11

Table A-2 1 hour test Smooth-Shank in HDPE-41
Specimen - 0.113 in. by 2-3/8 in. smooth-shank nail

Sample Number	Board Thickness (in)	Nail Length (in)	Shank above Surface (in)	Inbedded Length (in)	Max Load (lb)	Max Load (lb/in)
1	0.995	2.139	0.471	1.668	230.7	138.3
2	0.976	2.146	0.492	1.654	226.0	136.6
3	0.971	2.136	0.499	1.637	220.8	134.9
4	0.979	2.164	0.495	1.669	239.9	143.7
5	0.983	2.151	0.506	1.645	227.6	138.4
6	0.982	2.161	0.502	1.659	224.6	135.4
7	0.980	2.152	0.529	1.623	244.8	150.8
8	0.971	2.171	0.522	1.649	235.8	143.0
9	0.979	2.126	0.529	1.597	207.9	130.2
10	1.001	2.126	0.507	1.619	244.8	151.2
11	0.977	2.185	0.506	1.680	244.1	145.3
12	0.978	2.142	0.471	1.672	226.6	135.6
13	0.980	2.157	0.492	1.666	227.6	136.7
14	0.980	2.134	0.529	1.605	197.9	123.3
15	0.981	2.133	0.482	1.651	239.9	145.3
Avg.	0.981	2.148	0.502	1.646	229.3	139.2
Std. Dev					13.44	7.49
COV					0.06	0.05

Table A-3 1 hour test Ring-Shank in HDPE-32

Specimen - 0.113 in. by 2-3/8 in. ring-shank nail

Sample Number	Board Thickness (in)	Nail Length (in)	Shank above Surface (in)	Inbedded Length (in)	Max Load (lb)	Max Load (lb/in)
1	0.980	2.131	0.533	1.598	548.2	343.1
2	0.983	2.149	0.513	1.636	441.6	269.9
3	0.982	2.164	0.519	1.645	483.0	293.6
4	0.980	2.162	0.489	1.673	404.8	242.0
5	0.981	2.133	0.543	1.590	547.9	344.6
6	0.981	2.167	0.517	1.650	518.1	314.0
7	0.980	2.153	0.516	1.637	530.7	324.2
8	0.980	2.165	0.538	1.627	522.1	320.9
9	0.980	2.164	0.480	1.684	523.2	310.7
10	0.980	2.118	0.526	1.592	370.7	232.9
11	0.984	2.172	0.497	1.675	489.9	292.5
12	0.981	2.146	0.480	1.666	573.2	344.1
13	0.980	2.165	0.523	1.642	453.4	276.1
14	0.980	2.146	0.534	1.612	522.7	324.4
15	0.981	2.136	0.546	1.590	527.0	331.4
Avg.	0.981	2.151	0.517	1.634	497.1	304.3
Std. Dev					56.79	35.73
COV					0.11	0.12

Table A-4 1 hour test Smooth-Shank in HDPE-32

Specimen - 0.113 in. by 2-3/8 in. smooth-shank nail

Sample Number	Board Thickness (in)	Nail Length (in)	Shank above Surface (in)	Inbedded Length (in)	Max Load (lb)	Max Load (lb/in)
1	0.995	2.165	0.489	1.676	234.3	139.8
2	0.976	2.135	0.507	1.628	206.6	126.9
3	0.971	2.166	0.506	1.660	207.6	125.1
4	0.979	2.169	0.538	1.631	194.6	119.3
5	0.984	2.149	0.488	1.661	244.8	147.4
6	0.981	2.143	0.529	1.614	244.1	151.2
7	0.980	2.172	0.522	1.650	223.2	135.3
8	0.981	2.146	0.529	1.617	220.1	136.1
9	0.986	2.165	0.482	1.683	230.7	137.1
10	1.001	2.129	0.535	1.594	186.0	116.7
11	0.977	2.143	0.500	1.644	210.8	128.3
12	0.978	2.160	0.446	1.714	235.8	137.6
13	0.966	2.134	0.507	1.627	187.9	115.5
14	0.980	2.133	0.515	1.619	239.9	148.2
15	0.983	2.420	0.521	1.900	250.3	131.8
Avg.	0.981	2.168	0.507	1.661	221.1	133.1
Std. Dev					21.25	11.19
COV					0.10	0.08

Table A-5 1 hour test Ring-Shank in Trex

Specimen - 0.113 in. by 2-3/8 in. ring-shank nail

Sample Number	Board Thickness (in)	Nail Length (in)	Shank above Surface (in)	Inbedded Length (in)	Max Load (lb)	Max Load (lb/in)
1	1.536	2.135	0.533	1.602	597.6	373.0
2	1.524	2.153	0.520	1.633	601.6	368.4
3	1.528	2.164	0.536	1.628	620.1	380.9
4	1.518	2.115	0.514	1.601	536.9	335.4
5	1.522	2.164	0.511	1.653	574.0	347.2
6	1.513	2.134	0.487	1.647	649.4	394.3
7	1.522	2.167	0.506	1.661	569.7	343.0
8	1.525	2.165	0.507	1.658	623.4	376.0
9	1.521	2.147	0.497	1.650	555.4	336.6
10	1.530	2.172	0.504	1.668	628.5	376.8
11	1.525	2.107	0.494	1.613	508.5	315.3
12	1.526	2.157	0.482	1.675	621.5	371.0
13	1.528	2.167	0.509	1.658	579.9	349.8
14	1.525	2.152	0.487	1.665	565.4	339.6
15	1.522	2.170	0.497	1.673	567.0	338.9
Avg.	1.524	2.151	0.506	1.646	586.6	356.4
Std. Dev					38.36	22.19
COV					0.07	0.06

Table A-6 1 hour test Smooth-Shank in Trex

Specimen - 0.113 in. by 2-3/8 in. smooth-shank nail

Sample Number	Board Thickness (in)	Nail Length (in)	Shank above Surface (in)	Inbedded Length (in)	Max Load (lb)	Max Load (lb/in)
1	1.525	2.156	0.480	1.676	243.5	145.3
2	1.522	2.152	0.506	1.646	237.0	144.0
3	1.525	2.171	0.508	1.663	232.2	139.6
4	1.521	2.126	0.475	1.651	239.4	145.0
5	1.540	2.138	0.509	1.629	241.2	148.1
6	1.530	2.147	0.499	1.648	235.6	143.0
7	1.519	2.137	0.508	1.629	235.3	144.4
8	1.528	2.154	0.505	1.649	224.2	136.0
9	1.524	2.139	0.502	1.637	234.2	143.1
10	1.528	2.146	0.510	1.636	241.2	147.5
11	1.518	2.136	0.491	1.646	236.7	143.8
12	1.516	2.127	0.521	1.606	237.4	147.8
13	1.516	2.142	0.489	1.653	239.1	144.6
14	1.519	2.157	0.481	1.676	242.1	144.5
15	1.529	2.157	0.499	1.659	239.7	144.5
Avg.	1.524	2.145	0.499	1.647	237.3	144.1
Std. Dev					4.78	3.08
COV					0.02	0.02

Table A-7 1 hour test Ring-Shank in Rino

Specimen - 0.113 in. by 2-3/8 in. ring-shank nail

Sample Number	Board Thickness (in)	Nail Length (in)	Shank above Surface (in)	Inbedded Length (in)	Max Load (lb)	Max Load (lb/in)
1	0.961	2.131	0.493	1.638	407.2	248.6
2	0.962	2.165	0.505	1.660	445.6	268.4
3	0.940	2.174	0.513	1.661	389.0	234.2
4	0.939	2.161	0.515	1.646	402.4	244.5
5	0.936	2.161	0.482	1.679	369.3	220.0
6	0.960	2.148	0.519	1.629	459.1	281.8
7	0.970	2.163	0.505	1.658	370.7	223.6
8	0.965	2.134	0.507	1.627	422.8	259.9
9	0.939	2.177	0.498	1.679	481.6	286.8
10	0.937	2.186	0.501	1.685	522.1	309.9
11	0.964	2.185	0.500	1.685	439.5	260.8
12	0.967	2.161	0.494	1.667	505.8	303.4
13	0.970	2.169	0.498	1.671	387.9	232.1
14	0.966	2.132	0.502	1.630	470.1	288.4
15	0.963	2.148	0.511	1.637	434.6	265.5
Avg.	0.956	2.160	0.503	1.657	433.8	261.9
Std. Dev					47.41	28.24
COV					0.11	0.11

Table A-8 1 hour test Smooth-Shank in Rino

Specimen - 0.113 in. by 2-3/8 in. smooth-shank nail

Sample Number	Board Thickness (in)	Nail Length (in)	Shank above Surface (in)	Inbedded Length (in)	Max Load (lb)	Max Load (lb/in)
1	0.945	2.145	0.493	1.652	227.0	137.5
2	0.986	2.157	0.475	1.683	210.7	125.2
3	0.942	2.174	0.506	1.669	218.7	131.1
4	0.944	2.145	0.522	1.624	233.4	143.8
5	0.946	2.157	0.514	1.643	214.4	130.5
6	0.940	2.142	0.496	1.646	245.3	149.0
7	0.956	2.160	0.489	1.672	187.2	112.0
8	0.956	2.174	0.500	1.674	192.6	115.1
9	0.962	2.152	0.494	1.658	210.9	127.2
10	0.967	2.132	0.478	1.654	240.1	145.2
11	0.964	2.160	0.482	1.678	164.5	98.1
12	0.949	2.150	0.493	1.657	224.2	135.3
13	0.972	2.150	0.489	1.661	231.3	139.3
14	0.964	2.146	0.486	1.660	215.5	129.8
15	0.934	2.147	0.501	1.646	232.4	141.2
Avg.	0.955	2.153	0.494	1.658	216.5	130.7
Std. Dev					21.58	13.81
COV					0.10	0.11

Table A-9 1 week test Ring-Shank in HDPE-41
Specimen - 0.113 in. by 2-3/8 in. ring-shank nail

Sample Number	Board Thickness (in)	Nail Length (in)	Shank above Surface (in)	Inbedded Length (in)	Max Load (lb)	Max Load (lb/in)
1	0.975	2.148	0.488	1.660	388.7	234.2
2	0.983	2.167	0.484	1.683	485.1	288.2
3	0.982	2.174	0.476	1.699	480.8	283.1
4	0.982	2.124	0.482	1.642	438.9	267.3
5	0.980	2.158	0.502	1.657	449.9	271.6
6	0.982	2.140	0.486	1.655	468.2	283.0
7	0.984	2.114	0.498	1.617	387.4	239.7
8	0.985	2.163	0.491	1.673	492.6	294.5
9	0.972	2.128	0.462	1.666	507.4	304.6
10	0.978	2.149	0.478	1.672	425.0	254.3
11	0.980	2.171	0.492	1.679	535.8	319.1
12	0.976	2.172	0.478	1.695	437.0	257.9
13	0.977	2.117	0.492	1.625	390.6	240.4
14	0.983	2.152	0.476	1.677	423.1	252.4
15	0.978	2.154	0.472	1.682	423.9	252.0
Avg.	0.980	2.149	0.484	1.665	449.0	269.5
Std. Dev					45.11	25.35
COV					0.10	0.09

Table A-10 1 week test Smooth-Shank in HDPE-41
Specimen - 0.113 in. by 2-3/8 in. smooth-shank nail

Sample Number	Board Thickness (in)	Nail Length (in)	Shank above Surface (in)	Inbedded Length (in)	Max Load (lb)	Max Load (lb/in)
1	0.979	2.152	0.480	1.672	241.5	144.4
2	0.979	2.138	0.496	1.642	247.5	150.7
3	0.979	2.161	0.485	1.676	218.5	130.4
4	0.986	2.148	0.498	1.651	228.6	138.5
5	0.983	2.148	0.491	1.658	210.9	127.2
6	0.984	2.143	0.518	1.625	238.4	146.7
7	0.980	2.152	0.496	1.656	222.4	134.3
8	0.973	2.131	0.484	1.647	194.8	118.3
9	0.978	2.117	0.575	1.542	222.9	144.6
10	0.980	2.141	0.477	1.664	222.8	133.9
11	0.982	2.166	0.462	1.704	226.1	132.7
12	0.981	2.152	0.478	1.675	263.1	157.1
13	0.987	2.137	0.492	1.645	233.4	141.9
14	0.980	2.148	0.476	1.673	246.4	147.3
15	0.976	2.175	0.472	1.703	236.6	138.9
Avg.	0.980	2.147	0.492	1.655	230.3	139.1
Std. Dev					16.56	9.97
COV					0.07	0.07

Table A-11 1 week test Ring-Shank in HDPE-32
Specimen - 0.113 in. by 2-3/8 in. ring-shank nail

Sample Number	Board Thickness (in)	Nail Length (in)	Shank above Surface (in)	Inbedded Length (in)	Max Load (lb)	Max Load (lb/in)
1	0.978	2.168	0.533	1.635	492.3	301.1
2	0.980	2.131	0.499	1.632	412.6	252.8
3	0.978	2.157	0.517	1.640	484.3	295.3
4	0.982	2.133	0.495	1.638	451.8	275.8
5	0.983	2.161	0.506	1.655	356.0	215.1
6	0.979	2.168	0.502	1.666	444.0	266.5
7	0.981	2.172	0.535	1.637	464.4	283.7
8	0.981	2.165	0.597	1.568	455.3	290.4
9	0.985	2.148	0.520	1.628	376.8	231.4
10	0.982	2.166	0.547	1.619	506.6	312.9
11	0.982	2.153	0.523	1.630	463.1	284.1
12	0.981	2.157	0.534	1.623	337.0	207.6
13	0.970	2.167	0.546	1.621	406.4	250.7
14	0.981	2.148	0.541	1.607	377.7	235.0
15	0.979	2.164	0.529	1.635	483.8	295.9
Avg.	0.980	2.157	0.528	1.629	434.1	266.6
Std. Dev					53.10	32.81
COV					0.12	0.12

Table A-12 1 week test Smooth-Shank in HDPE-32
Specimen - 0.113 in. by 2-3/8 in. smooth-shank nail

Sample Number	Board Thickness (in)	Nail Length (in)	Shank above Surface (in)	Inbedded Length (in)	Max Load (lb)	Max Load (lb/in)
1	0.975	2.150	0.488	1.662	230.5	138.7
2	0.969	2.147	0.484	1.663	205.2	123.4
3	0.965	2.138	0.476	1.663	233.7	140.6
4	0.977	2.149	0.488	1.661	211.1	127.1
5	0.966	2.142	0.499	1.644	204.6	124.5
6	0.974	2.128	0.482	1.646	238.1	144.7
7	0.967	2.131	0.502	1.629	188.7	115.8
8	0.982	2.142	0.486	1.657	222.1	134.1
9	0.979	2.156	0.498	1.659	210.6	127.0
10	0.976	2.166	0.506	1.660	199.6	120.3
11	0.961	2.145	0.465	1.680	211.8	126.1
12	0.982	2.167	0.509	1.658	202.1	121.9
13	0.979	2.136	0.500	1.637	194.8	119.0
14	0.963	2.144	0.471	1.674	201.4	120.3
15	0.968	2.123	0.471	1.652	208.4	126.2
Avg.	0.972	2.144	0.488	1.656	210.8	127.3
Std. Dev					14.38	8.48
COV					0.07	0.07

Table A-13 1 week test Ring-Shank in Trex

Specimen - 0.113 in. by 2-3/8 in. ring-shank nail

Sample Number	Board Thickness (in)	Nail Length (in)	Shank above Surface (in)	Inbedded Length (in)	Max Load (lb)	Max Load (lb/in)
1	1.522	2.137	0.488	1.649	534.5	324.1
2	1.520	2.147	0.484	1.663	533.7	320.9
3	1.518	2.113	0.476	1.638	509.8	311.3
4	1.522	2.166	0.488	1.678	548.7	327.0
5	1.513	2.124	0.498	1.627	524.0	322.2
6	1.522	2.160	0.501	1.660	506.8	305.4
7	1.522	2.154	0.476	1.678	479.2	285.6
8	1.522	2.151	0.485	1.666	554.6	332.9
9	1.520	2.129	0.498	1.632	503.4	308.6
10	1.517	2.173	0.491	1.683	541.5	321.8
11	1.524	2.120	0.506	1.614	485.6	300.9
12	1.536	2.162	0.465	1.698	417.4	245.9
13	1.528	2.112	0.509	1.603	469.3	292.8
14	1.525	2.153	0.476	1.678	497.2	296.4
15	1.522	2.176	0.472	1.704	516.2	302.9
Avg.	1.522	2.145	0.487	1.658	508.1	306.6
Std. Dev					35.67	21.70

Table A-14 1 week test Smooth-Shank in Trex

Specimen - 0.113 in. by 2-3/8 in. smooth-shank nail

Sample Number	Board Thickness (in)	Nail Length (in)	Shank above Surface (in)	Inbedded Length (in)	Max Load (lb)	Max Load (lb/in)
1	1.536	2.175	0.521	1.654	219.7	132.8
2	1.524	2.173	0.491	1.683	220.5	131.1
3	1.517	2.132	0.474	1.658	228.0	137.5
4	1.516	2.138	0.509	1.629	225.7	138.6
5	1.522	2.155	0.488	1.667	225.2	135.1
6	1.515	2.141	0.498	1.644	220.7	134.3
7	1.523	2.157	0.501	1.657	229.0	138.2
8	1.530	2.135	0.476	1.659	225.4	135.9
9	1.525	2.145	0.484	1.662	222.9	134.2
10	1.526	2.133	0.497	1.636	233.9	143.0
11	1.525	2.150	0.473	1.677	210.7	125.6
12	1.525	2.149	0.476	1.674	229.9	137.4
13	1.516	2.149	0.519	1.630	235.6	144.5
14	1.514	2.126	0.484	1.643	235.2	143.2
15	1.522	2.140	0.496	1.644	237.9	144.7
Avg.	1.522	2.146	0.492	1.654	226.7	137.1
Std. Dev					7.29	5.32
COV					0.03	0.04

Table A15 1 week test Ring-Shank in Rino

Specimen - 0.113 in. by 2-3/8 in. ring-shank nail

Sample Number	Board Thickness (in)	Nail Length (in)	Shank above Surface (in)	Inbedded Length (in)	Max Load (lb)	Max Load (lb/in)
1	0.964	2.162	0.527	1.635	434.6	265.8
2	0.937	2.113	0.519	1.594	390.1	244.7
3	0.941	2.123	0.534	1.589	364.9	229.6
4	0.973	2.159	0.528	1.631	339.9	208.4
5	0.935	2.120	0.500	1.620	361.9	223.4
6	0.935	2.167	0.528	1.639	355.0	216.6
7	0.964	2.175	0.509	1.666	357.3	214.5
8	0.971	2.162	0.512	1.650	331.2	200.7
9	0.973	2.160	0.501	1.659	391.4	235.9
10	0.939	2.159	0.500	1.659	348.0	209.8
11	0.964	2.143	0.533	1.610	331.8	206.1
12	0.941	2.170	0.505	1.665	383.4	230.3
13	0.942	2.118	0.502	1.616	352.3	218.0
14	0.963	2.173	0.527	1.646	346.6	210.6
15	0.942	2.170	0.528	1.642	416.4	253.6
Avg.	0.952	2.152	0.517	1.635	367.0	224.5
Std. Dev					30.38	18.77
COV					0.08	0.08

Table A-16 1 week test Smooth-Shank in Rino

Specimen - 0.113 in. by 2-3/8 in. smooth-shank nail

Sample Number	Board Thickness (in)	Nail Length (in)	Shank above Surface (in)	Inbedded Length (in)	Max Load (lb)	Max Load (lb/in)
1	0.971	2.144	0.501	1.643	222.4	135.4
2	0.962	2.155	0.489	1.666	210.4	126.3
3	0.950	2.144	0.519	1.625	181.6	111.8
4	0.939	2.157	0.497	1.660	215.2	129.6
5	0.944	2.154	0.480	1.674	197.2	117.8
6	0.968	2.158	0.481	1.678	199.9	119.2
7	0.947	2.151	0.487	1.664	192.6	115.7
8	0.947	2.161	0.465	1.696	216.6	127.7
9	0.968	2.180	0.467	1.714	214.4	125.1
10	0.944	2.137	0.471	1.666	226.7	136.1
11	0.939	2.146	0.492	1.655	205.3	124.1
12	0.950	2.140	0.499	1.641	233.1	142.1
13	0.962	2.144	0.479	1.665	211.9	127.3
14	0.971	2.136	0.497	1.639	185.8	113.4
15	0.947	2.162	0.484	1.678	203.6	121.3
Avg.	0.954	2.151	0.487	1.664	207.8	124.9
Std. Dev					14.66	8.67
COV					0.07	0.07

Table A-17 3 month test Ring-Shank in HDPE-41
Specimen - 0.113 in. by 2-3/8 in. ring-shank nail

Sample Number	Board Thickness (in)	Nail Length (in)	Shank above Surface (in)	Inbedded Length (in)	Max Load (lb)	Max Load (lb/in)
1	0.982	2.157	0.488	1.669	345.1	206.8
2	0.980	2.151	0.484	1.667	359.1	215.4
3	0.982	2.145	0.476	1.670	374.3	224.2
4	1.001	2.146	0.488	1.658	424.4	256.0
5	0.980	2.166	0.473	1.693	428.7	253.2
6	0.980	2.100	0.476	1.625	321.5	197.9
7	0.981	2.162	0.519	1.643	432.8	263.4
8	0.981	2.162	0.575	1.587	327.2	206.2
9	1.001	2.110	0.477	1.634	333.2	204.0
10	0.980	2.136	0.462	1.674	396.5	236.9
11	0.981	2.127	0.499	1.629	356.5	218.9
12	0.980	2.129	0.482	1.647	374.4	227.3
13	0.976	2.139	0.519	1.620	429.5	265.1
14	0.976	2.127	0.484	1.644	268.3	163.2
15	0.961	2.105	0.496	1.610	345.3	214.5
Avg.	0.981	2.137	0.493	1.644	367.8	223.5
Std. Dev					47.79	27.86
COV					0.13	0.12

Table A-18 3 month test Smooth-Shank in HDPE-41
Specimen - 0.113 in. by 2-3/8 in. smooth-shank nail

Sample Number	Board Thickness (in)	Nail Length (in)	Shank above Surface (in)	Inbedded Length (in)	Max Load (lb)	Max Load (lb/in)
1	0.978	2.167	0.480	1.687	205.9	122.1
2	0.980	2.148	0.496	1.653	193.6	117.2
3	0.976	2.148	0.485	1.663	193.2	116.2
4	0.977	2.152	0.498	1.655	161.9	97.9
5	0.966	2.133	0.476	1.657	212.9	128.5
6	0.967	2.148	0.484	1.665	203.5	122.3
7	0.982	2.173	0.497	1.676	195.4	116.6
8	0.982	2.152	0.476	1.676	175.4	104.7
9	0.979	2.153	0.484	1.670	194.4	116.4
10	1.001	2.153	0.497	1.656	176.5	106.6
11	0.977	2.145	0.488	1.657	183.5	110.7
12	0.982	2.153	0.509	1.644	184.6	112.3
13	0.986	2.142	0.500	1.643	186.2	113.4
14	1.001	2.162	0.471	1.692	186.2	110.1
15	0.980	2.152	0.471	1.681	194.4	115.6
Avg.	0.981	2.152	0.487	1.665	189.8	114.0
Std. Dev					12.92	7.58
COV					0.07	0.07

Table A-19 3 month test Ring-Shank in HDPE-32
Specimen - 0.113 in. by 2-3/8 in. ring-shank nail

Sample Number	Board Thickness (in)	Nail Length (in)	Shank above Surface (in)	Inbedded Length (in)	Max Load (lb)	Max Load (lb/in)
1	0.972	2.168	0.489	1.679	363.4	216.4
2	0.978	2.102	0.507	1.595	350.9	220.0
3	0.980	2.139	0.506	1.634	347.8	212.9
4	0.979	2.163	0.467	1.697	433.3	255.4
5	0.981	2.152	0.471	1.682	244.6	145.5
6	0.966	2.145	0.492	1.654	394.4	238.5
7	0.974	2.166	0.499	1.667	375.2	225.1
8	0.980	2.150	0.535	1.616	244.6	151.4
9	0.976	2.121	0.500	1.622	414.2	255.4
10	0.975	2.158	0.446	1.712	427.6	249.8
11	0.983	2.152	0.489	1.663	424.7	255.4
12	0.982	2.147	0.519	1.628	307.9	189.1
13	0.981	2.159	0.497	1.662	325.3	195.7
14	0.980	2.154	0.497	1.658	387.1	233.5
15	0.976	2.164	0.471	1.693	301.3	178.0
Avg.	0.977	2.149	0.492	1.657	356.2	214.8
Std. Dev					61.66	36.28
COV					0.17	0.17

Table A-20 3 month test Smooth-Shank in HDPE-32
Specimen - 0.113 in. by 2-3/8 in. smooth-shank nail

Sample Number	Board Thickness (in)	Nail Length (in)	Shank above Surface (in)	Inbedded Length (in)	Max Load (lb)	Max Load (lb/in)
1	0.981	2.194	0.501	1.693	181.7	107.3
2	0.986	2.143	0.489	1.654	187.8	113.5
3	1.001	2.151	0.506	1.646	194.0	117.9
4	0.981	2.177	0.538	1.639	198.0	120.8
5	0.975	2.144	0.446	1.698	186.4	109.8
6	0.983	2.177	0.480	1.697	195.3	115.1
7	0.982	2.140	0.481	1.660	200.5	120.8
8	0.980	2.175	0.487	1.688	210.3	124.6
9	0.976	2.137	0.495	1.642	173.0	105.4
10	0.985	2.156	0.506	1.650	194.9	118.1
11	0.972	2.132	0.502	1.630	193.7	118.8
12	0.978	2.132	0.546	1.586	167.9	105.9
13	0.980	2.143	0.546	1.597	174.8	109.5
14	0.965	2.189	0.541	1.648	192.5	116.8
15	0.977	2.153	0.529	1.624	202.6	124.8
Avg.	0.980	2.156	0.506	1.650	190.2	115.3
Std. Dev					11.73	6.46
COV					0.06	0.06

Table A-21 3 month test Ring-Shank in Trex

Specimen - 0.113 in. by 2-3/8 in. ring-shank nail

Sample Number	Board Thickness (in)	Nail Length (in)	Shank above Surface (in)	Inbedded Length (in)	Max Load (lb)	Max Load (lb/in)
1	1.536	2.132	0.506	1.627	436.8	268.6
2	1.524	2.176	0.538	1.638	487.0	297.3
3	1.517	2.129	0.488	1.642	462.5	281.8
4	1.523	2.148	0.507	1.641	400.5	244.1
5	1.530	2.157	0.506	1.652	416.6	252.3
6	1.525	2.170	0.538	1.632	425.5	260.7
7	1.522	2.124	0.499	1.625	431.4	265.5
8	1.520	2.160	0.517	1.643	432.8	263.4
9	1.517	2.154	0.523	1.631	392.2	240.5
10	1.524	2.117	0.534	1.583	426.3	269.3
11	1.525	2.172	0.546	1.626	425.8	261.9
12	1.521	2.160	0.446	1.714	442.1	257.9
13	1.516	2.131	0.507	1.624	418.0	257.4
14	1.519	2.160	0.488	1.673	427.9	255.8
15	1.529	2.171	0.529	1.642	425.8	259.3
Avg.	1.523	2.151	0.511	1.639	430.1	262.4
Std. Dev					22.68	13.91
COV					0.05	0.05

Table A-22 3 month test Smooth-Shank in Trex

Specimen - 0.113 in. by 2-3/8 in. smooth-shank nail

Sample Number	Board Thickness (in)	Nail Length (in)	Shank above Surface (in)	Inbedded Length (in)	Max Load (lb)	Max Load (lb/in)
1	1.525	2.157	0.488	1.670	194.4	116.4
2	1.522	2.133	0.529	1.605	188.7	117.6
3	1.525	2.156	0.522	1.634	182.7	111.8
4	1.528	2.118	0.529	1.589	185.3	116.6
5	1.518	2.156	0.492	1.665	198.4	119.2
6	1.516	2.142	0.499	1.643	172.8	105.2
7	1.516	2.116	0.479	1.637	181.0	110.6
8	1.516	2.149	0.506	1.644	173.5	105.6
9	1.522	2.154	0.538	1.616	183.4	113.5
10	1.515	2.152	0.488	1.665	177.7	106.8
11	1.522	2.128	0.547	1.581	185.8	117.5
12	1.520	2.143	0.523	1.620	192.4	118.8
13	1.517	2.154	0.499	1.655	183.4	110.8
14	1.525	2.169	0.515	1.655	179.5	108.5
15	1.522	2.165	0.521	1.645	167.9	102.1
Avg.	1.521	2.146	0.511	1.635	183.1	112.1
Std. Dev					8.31	5.55
COV					0.05	0.05

Table A-23 3 month test Ring-Shank in Rino
Specimen - 0.113 in. by 2-3/8 in. ring-shank nail

Sample Number	Board Thickness (in)	Nail Length (in)	Shank above Surface (in)	Inbedded Length (in)	Max Load (lb)	Max Load (lb/in)
1	0.945	2.124	0.521	1.603	305.2	190.4
2	0.986	2.152	0.491	1.662	350.6	211.0
3	0.942	2.136	0.518	1.618	308.2	190.5
4	0.946	2.166	0.478	1.689	280.5	166.1
5	0.940	2.146	0.492	1.654	326.0	197.1
6	0.956	2.165	0.491	1.675	288.6	172.3
7	0.936	2.138	0.474	1.665	322.9	194.0
8	0.960	2.146	0.509	1.637	270.1	165.0
9	0.970	2.121	0.465	1.657	302.5	182.6
10	0.947	2.167	0.509	1.658	335.6	202.4
11	0.964	2.161	0.500	1.662	304.8	183.4
12	0.967	2.135	0.478	1.658	356.0	214.8
13	0.970	2.151	0.492	1.659	359.0	216.4
14	0.966	2.123	0.476	1.648	349.6	212.2
15	0.963	2.167	0.471	1.696	277.4	163.6
Avg.	0.957	2.147	0.491	1.656	315.8	190.8
Std. Dev					29.76	18.44
COV					0.09	0.10

Table A-24 3 month test Smooth-Shank in Rino
Specimen - 0.113 in. by 2-3/8 in. smooth-shank nail

Sample Number	Board Thickness (in)	Nail Length (in)	Shank above Surface (in)	Inbedded Length (in)	Max Load (lb)	Max Load (lb/in)
1	0.971	2.154	0.480	1.674	178.2	106.5
2	0.962	2.165	0.476	1.690	194.0	114.8
3	0.950	2.139	0.519	1.620	175.7	108.5
4	0.939	2.152	0.484	1.669	186.4	111.7
5	0.944	2.143	0.476	1.668	195.7	117.4
6	0.937	2.177	0.519	1.658	192.6	116.2
7	0.964	2.145	0.484	1.662	181.4	109.2
8	0.967	2.191	0.502	1.690	179.9	106.5
9	0.940	2.151	0.486	1.666	193.3	116.1
10	0.939	2.160	0.496	1.665	190.6	114.5
11	0.968	2.165	0.485	1.680	161.4	96.1
12	0.949	2.163	0.498	1.666	177.6	106.6
13	0.972	2.159	0.484	1.675	181.2	108.2
14	0.964	2.166	0.575	1.591	184.3	115.8
15	0.934	2.167	0.496	1.672	208.4	124.7
Avg.	0.953	2.160	0.497	1.663	185.4	111.5
Std. Dev					11.02	6.70
COV					0.06	0.06

APPENDIX B – SHEAR WALL RESULTS

Shear wall specimen PPT-N-1 consisted of a pressure preservative treated sill plate, no hold downs and 3 – 13 mm by 89 mm A325 bolts with 7.6 cm by 7.6 cm by 9.5 mm steel plate washers to fasten the wall to the foundation.

Table B-1 PPT-N-1 EEEP Parameters

		Negative	Positive
Yield Load, P_{yield}	kN	-8.74	6.39
Disp @ Yield Load, Δ_{yield}	mm	-8.99	17.71
Disp @ failure, Δ_u	mm	-53.77	39.85

Table B-2 PPT-N-1 Performance Parameters

Peak load, P_{peak}	kN	-10.28
Displacement at P_{peak}, Δ_{peak}	mm	-35.44
Yield load, P_{yield}	kN	-8.74
Displacement at yield load, Δ_{yield}	mm	-8.99
Proportional limit, $0.4P_{peak}$	kN	-4.11
Displacement at prop. limit, Δ_e	mm	-4.23
Failure load, $0.8P_{peak}$	kN	-8.22
Displacement at failure, Δ_u	mm	-53.77
Shear Strength, v_u	N/m	-4216
Elastic stiffness, K_e	N/m	972196
Ductility, D, $\Delta_{peak}/\Delta_{yeild}$	3.94	
Ductility, D_u, $\Delta_{failure}/\Delta_{yeild}$	5.98	
Toughness, $\Delta_{failure}/\Delta_{peak}$	1.52	

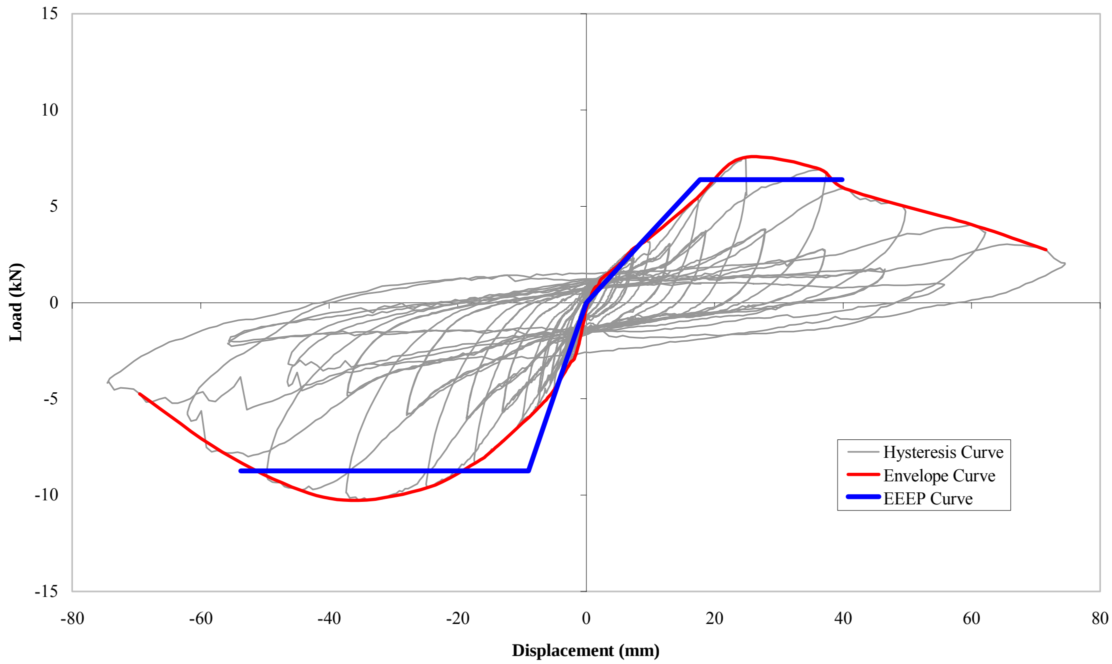

Figure B-1 Load vs. Displacement, Envelope and EEEP Curves – PPT-N-1

Table B-3 PPT-N-1 Data of Primary Cycles

Primary cycle #	Negative		Positive		Average		Average Cycle stiffness
	load	displacement	load	displacement	load	displacement	
	kN	mm	kN	mm	kN	mm	kN/mm
1	-1.032	-0.423	-0.329	-0.019	0.68	0.22	3.08
2	-2.257	-1.256	0.706	1.251	1.48	1.25	1.18
3	-2.929	-1.837	0.896	1.851	1.91	1.84	1.04
4	-3.146	-2.479	1.256	2.442	2.20	2.46	0.89
5	-4.503	-4.939	1.931	4.939	3.22	4.94	0.65
6	-5.447	-7.376	2.796	7.311	4.12	7.34	0.56
7	-7.643	-14.450	3.221	9.372	5.43	11.91	0.46
8	-8.335	-17.292	5.410	17.250	6.87	17.27	0.40
9	-9.601	-24.608	7.517	24.422	8.56	24.51	0.35
10	-10.280	-35.435	6.937	36.421	8.61	35.93	0.24
11	-9.740	-44.425	5.908	40.244	7.82	42.33	0.18
12	-7.751	-56.676	4.045	60.066	5.90	58.37	0.10
13	-4.734	-69.479	2.749	71.535	3.74	70.51	0.05

Shear wall specimen PPT-N-2 consisted of a pressure preservative treated sill plate, no hold downs and 3 – 13 mm by 89 mm A325 bolts with 7.6 cm by 7.6 cm by 9.5 mm steel plate washers to fasten the wall to the foundation.

Table B-4 PPT-N-2 EEEP Parameters

		Negative	Positive
Yield Load, P_{yield}	kN	-9.68	9.83
Disp @ Yield Load, Δ_{yield}	mm	-5.24	11.80
Disp @ failure, Δ_u	mm	-47.95	47.53

Table B-5 PPT-N-2 Performance Parameters

Peak load, P_{peak}	kN	11.56
Displacement at P_{peak}, Δ_{peak}	mm	36.40
Yield load, P_{yield}	kN	9.83
Displacement at yield load, Δ_{yield}	mm	11.80
Proportional limit, $0.4P_{peak}$	kN	4.62
Displacement at prop. limit, Δ_e	mm	5.55
Failure load, $0.8P_{peak}$	kN	9.25
Displacement at failure, Δ_u	mm	47.53
Shear Strength, v_u	N/m	4742
Elastic stiffness, K_e	N/m	832651
Ductility, D, $\Delta_{peak}/\Delta_{yeild}$	3.08	
Ductility, D_u, $\Delta_{failure}/\Delta_{yeild}$	4.03	
Toughness, $\Delta_{failure}/\Delta_{peak}$	1.31	

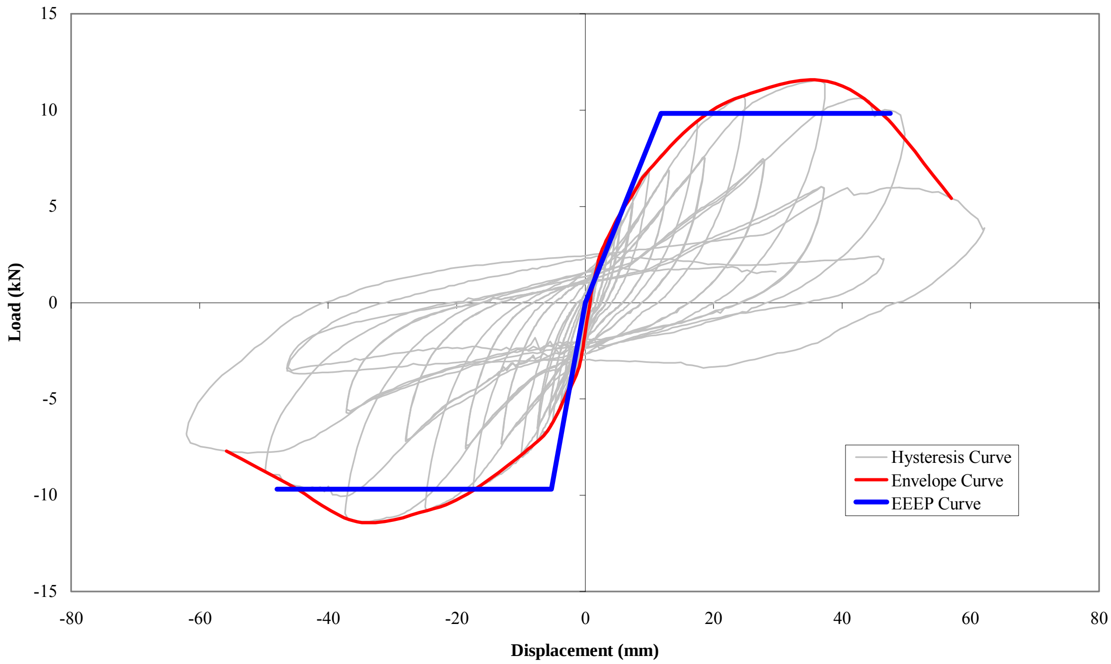

Figure B-2 Load vs. Displacement, Envelope and EEEP Curves – PPT-N-2

Table B-6 PPT-N-2 Data of Primary Cycles

Primary cycle #	Negative		Positive		Average		Average Cycle stiffness
	load	displacement	load	displacement	load	displacement	
	kN	mm	kN	mm	kN	mm	kN/mm
1	-2.847	-0.586	0.974	1.228	1.91	0.91	2.11
2	-3.618	-1.232	1.839	1.879	2.73	1.56	1.75
3	-4.565	-2.479	2.623	2.479	3.59	2.48	1.45
4	-4.378	-2.432	4.320	4.972	4.35	3.70	1.17
5	-6.166	-4.939	5.600	7.418	5.88	6.18	0.95
6	-7.208	-7.372	6.889	9.925	7.05	8.65	0.82
7	-9.730	-17.292	9.373	17.227	9.55	17.26	0.55
8	-10.795	-24.589	10.704	24.403	10.75	24.50	0.44
9	-11.383	-35.412	11.562	36.398	11.47	35.90	0.32
10	-9.404	-46.281	9.916	45.872	9.66	46.08	0.21
11	-7.700	-55.811	5.420	57.029	6.56	56.42	0.12

Shear wall specimen PPT-N-3 consisted of a pressure preservative treated sill plate, no hold downs and 3 – 13 mm by 89 mm A325 bolts with 7.6 cm by 7.6 cm by 9.5 mm steel plate washers to fasten the wall to the foundation.

Table B-7 PPT-N-3 EEEP Parameters

		Negative	Positive
Yield Load, P_{yield}	kN	-7.95	7.69
Disp @ Yield Load, Δ_{yield}	mm	-7.34	15.92
Disp @ failure, Δ_u	mm	-47.91	45.21

Table B-8 PPT-N-3 Performance Parameters

Peak load, P_{peak}	kN	-9.35
Displacement at P_{peak}, Δ_{peak}	mm	-30.97
Yield load, P_{yield}	kN	-7.95
Displacement at yield load, Δ_{yield}	mm	-7.34
Proportional limit, $0.4P_{peak}$	kN	-3.74
Displacement at prop. limit, Δ_e	mm	-3.46
Failure load, $0.8P_{peak}$	kN	-7.48
Displacement at failure, Δ_u	mm	-47.91
Shear Strength, v_u	N/m	-3834
Elastic stiffness, K_e	N/m	1082057
Ductility, D, $\Delta_{peak}/\Delta_{yeild}$	4.22	
Ductility, D_u, $\Delta_{failure}/\Delta_{yeild}$	6.52	
Toughness, $\Delta_{failure}/\Delta_{peak}$	1.55	

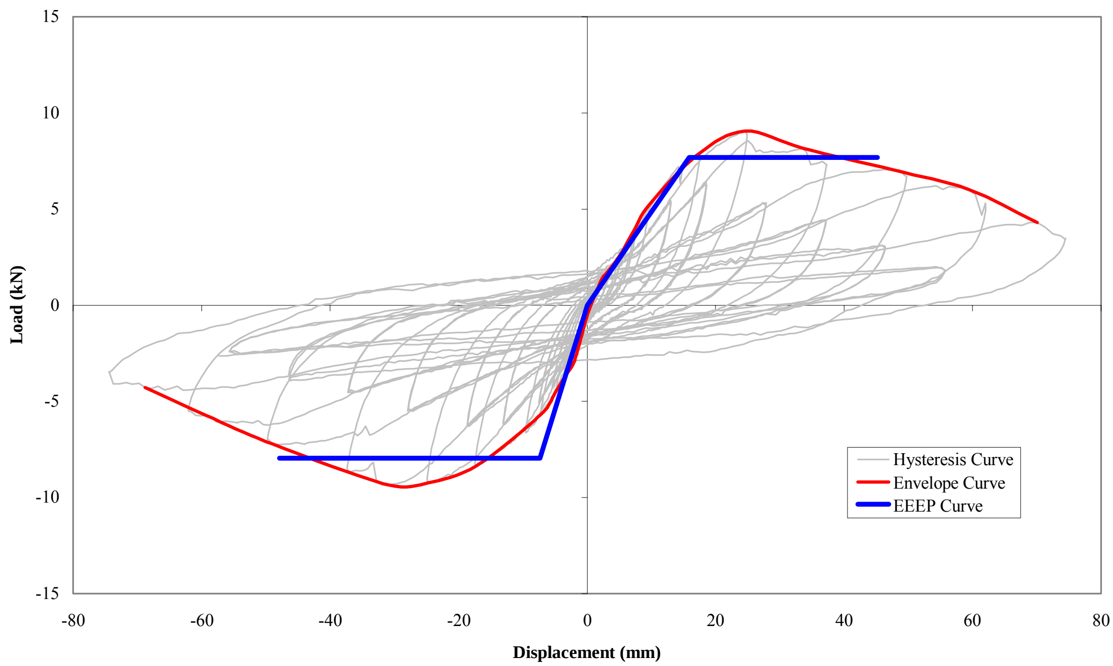

Figure B-3 Load vs. Displacement, Envelope and EEEP Curves – PPT-N-3

Table B-9 PPT-N-3 Data of Primary Cycles

Primary cycle #	Negative		Positive		Average		Average Cycle stiffness
	load	displacement	load	displacement	load	displacement	
	kN	mm	kN	mm	kN	mm	kN/mm
1	-2.067	-1.200	-0.448	0.084	1.26	0.64	1.96
2	-2.634	-1.749	0.984	1.767	1.81	1.76	1.03
3	-3.102	-2.260	1.391	2.391	2.25	2.33	0.97
4	-3.782	-3.536	2.440	4.790	3.11	4.16	0.75
5	-4.463	-4.809	3.842	7.232	4.15	6.02	0.69
6	-5.691	-7.214	5.220	9.692	5.46	8.45	0.65
7	-8.345	-17.148	7.843	17.315	8.09	17.23	0.47
8	-9.245	-24.738	9.051	24.585	9.15	24.66	0.37
9	-9.350	-30.966	8.162	33.561	8.76	32.26	0.27
10	-7.205	-49.062	7.042	47.723	7.12	48.39	0.15
11	-5.732	-59.322	6.020	59.373	5.88	59.35	0.10
12	-4.283	-68.782	4.307	70.047	4.29	69.41	0.06

Shear wall specimen PPT-S-1 consisted of a pressure preservative treated sill plate, two Simpson HTT22 hold downs with 32 - 7.6 cm by 0.33 mm 10d (3.05 mm by 76.2 mm) nails. Each hold-down was secured to the steel foundation by using a 1.6 cm by 8.9 cm A325 bolt and 3 – 13 mm by 89 mm A325 bolts with 7.6 cm by 7.6 cm by 9.5 mm steel plate washers to fasten the wall to the foundation.

Table B-10 PPT-S-1 EEEP Parameters

		Negative	Positive
Yield Load, P_{yield}	kN	-20.60	17.67
Disp @ Yield Load, Δ_{yield}	mm	-17.49	15.73
Disp @ failure, Δ_u	mm	-82.86	70.00

Table B-11 PPT-S-1 Performance Parameters

Peak load, P_{peak}	kN	-24.23
Displacement at P_{peak}, Δ_{peak}	mm	-74.44
Yield load, P_{yield}	kN	-20.60
Displacement at yield load, Δ_{yield}	mm	-17.49
Proportional limit, $0.4P_{peak}$	kN	-9.69
Displacement at prop. limit, Δ_e	mm	-8.23
Failure load, $0.8P_{peak}$	kN	-19.39
Displacement at failure, Δ_u	mm	-82.86
Shear Strength, v_u	N/m	-9939
Elastic stiffness, K_e	N/m	1178099
Ductility, D, $\Delta_{peak}/\Delta_{yeild}$	4.26	
Ductility, D_u, $\Delta_{failure}/\Delta_{yeild}$	4.74	
Toughness, $\Delta_{failure}/\Delta_{peak}$	1.11	

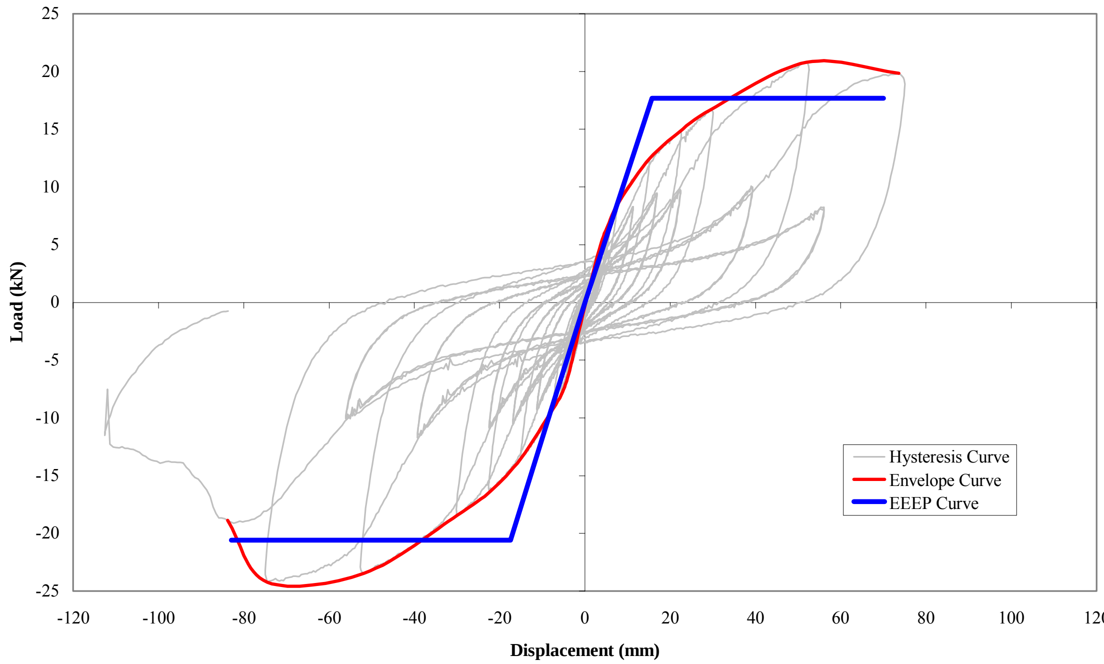

Figure B-4 Load vs. Displacement, Envelope and EEEP Curves – PPT-S-1

Table B-12 PPT-S-1 Data of Primary Cycles

Primary cycle #	Negative		Positive		Average		Average Cycle stiffness
	load	displacement	load	displacement	load	displacement	
	kN	mm	kN	mm	kN	mm	kN/mm
1	-0.312	-0.009	5.138	3.763	2.73	1.89	1.44
2	-6.173	-3.804	6.879	5.660	6.53	4.73	1.38
3	-8.026	-5.581	8.393	7.539	8.21	6.56	1.25
4	-9.248	-7.520	12.092	14.343	10.67	10.93	0.98
5	-13.497	-14.976	14.512	21.324	14.00	18.15	0.77
6	-16.324	-21.961	16.724	29.677	16.52	25.82	0.64
7	-18.438	-29.942	20.793	52.020	19.62	40.98	0.48
8	-23.447	-51.839	19.833	73.577	21.64	62.71	0.35
9	-24.235	-74.442	31.816	-44.272	28.03	59.36	0.47
10	-18.883	-83.739	14.888	83.148	16.89	83.44	0.20

Shear wall specimen PPT-S-2 consisted of a pressure preservative treated sill plate, two Simpson HTT22 hold downs with 32 - 7.6 cm by 0.33 mm 10d (3.05 mm by 76.2 mm) nails. Each hold-down was secured to the steel foundation by using a 1.6 cm by 8.9 cm A325 bolt and 3 – 13 mm by 89 mm A325 bolts with 7.6 cm by 7.6 cm by 9.5 mm steel plate washers to fasten the wall to the foundation.

Table B-13 PPT-S-2 EEEP Parameters

		Negative	Positive
Yield Load, P_{yield}	kN	-18.45	17.05
Disp @ Yield Load, Δ_{yield}	mm	-16.58	14.99
Disp @ failure, Δ_u	mm	-88.40	59.98

Table B-14 PPT-S-2 Performance Parameters

Peak load, P_{peak}	kN	-21.71
Displacement at P_{peak}, Δ_{peak}	mm	-52.12
Yield load, P_{yield}	kN	-18.45
Displacement at yield load, Δ_{yield}	mm	-16.58
Proportional limit, $0.4P_{peak}$	kN	-8.68
Displacement at prop. limit, Δ_e	mm	-7.80
Failure load, $0.8P_{peak}$	kN	-17.37
Displacement at failure, Δ_u	mm	-88.40
Shear Strength, v_u	N/m	-8902
Elastic stiffness, K_e	N/m	1112690
Ductility, D, $\Delta_{peak}/\Delta_{yeild}$	3.14	
Ductility, D_u, $\Delta_{failure}/\Delta_{yeild}$	5.33	
Toughness, $\Delta_{failure}/\Delta_{peak}$	1.70	

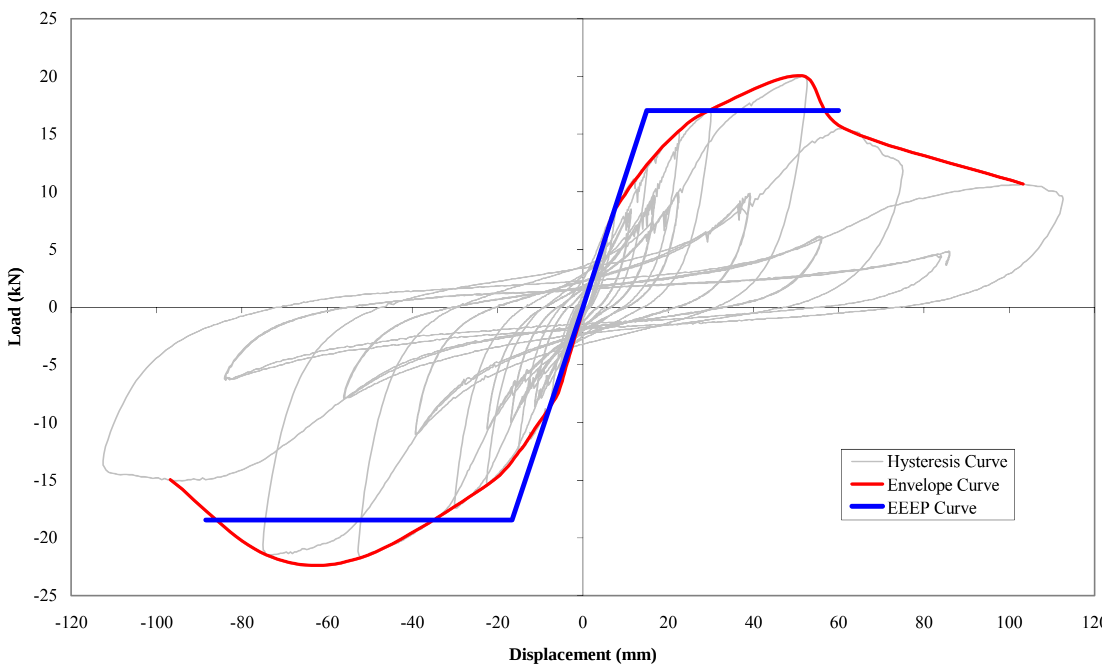

Figure B-5 Load vs. Displacement, Envelope and EEEP Curves – PPT-S-2

Table B-15 PPT-S-2 Data of Primary Cycles

Primary cycle #	Negative		Positive		Average		Average Cycle stiffness
	load	displacement	load	displaceme nt	load	displaceme nt	
	kN	mm	kN	mm	kN	mm	kN/mm
1	-4.968	-3.772	-4.151	-3.097	4.56	3.43	1.33
2	-7.232	-5.642	6.611	5.637	6.92	5.64	1.23
3	-8.478	-7.423	8.389	7.423	8.43	7.42	1.14
4	-10.507	-11.189	12.357	15.022	11.43	13.11	0.87
5	-12.536	-14.953	15.211	22.357	13.87	18.65	0.74
6	-15.357	-22.282	17.057	29.594	16.21	25.94	0.62
7	-21.706	-52.118	20.054	51.453	20.88	51.79	0.40
8	-21.472	-74.237	15.492	61.145	18.48	67.69	0.27
9	-14.946	-96.748	10.653	103.203	12.80	99.98	0.13

Shear wall specimen PPT-S-3 consisted of a pressure preservative treated sill plate, two Simpson HTT22 hold downs with 32 - 7.6 cm by 0.33 mm 10d (3.05 mm by 76.2 mm) nails. Each hold-down was secured to the steel foundation by using a 1.6 cm by 8.9 cm A325 bolt and 3 – 13 mm by 89 mm A325 bolts with 7.6 cm by 7.6 cm by 9.5 mm steel plate washers to fasten the wall to the foundation.

Table B-16 PPT-S-3 EEEP Parameters

		Negative	Positive
Yield Load, P_{yield}	kN	-19.48	18.77
Disp @ Yield Load, Δ_{yield}	mm	-20.50	17.68
Disp @ failure, Δ_u	mm	-77.62	60.01

Table B-17 PPT-S-3 Performance Parameters

Peak load, P_{peak}	kN	-22.91
Displacement at P_{peak}, Δ_{peak}	mm	-51.89
Yield load, P_{yield}	kN	-19.48
Displacement at yield load, Δ_{yield}	mm	-20.50
Proportional limit, $0.4P_{peak}$	kN	-9.17
Displacement at prop. limit, Δ_e	mm	-9.64
Failure load, $0.8P_{peak}$	kN	-18.33
Displacement at failure, Δ_u	mm	-77.62
Shear Strength, v_u	N/m	-9397
Elastic stiffness, K_e	N/m	950315
Ductility, D, $\Delta_{peak}/\Delta_{yeild}$	2.53	
Ductility, D_u, $\Delta_{failure}/\Delta_{yeild}$	3.79	
Toughness, $\Delta_{failure}/\Delta_{peak}$	1.50	

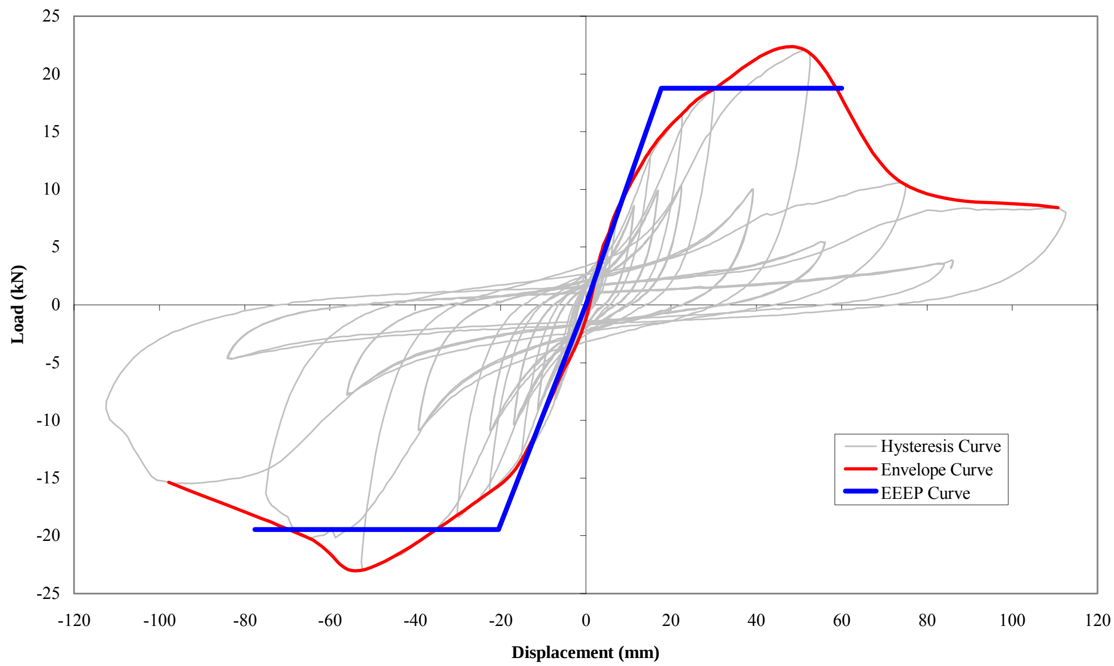

Figure B-6 Load vs. Displacement, Envelope and EEEP Curves – PPT-S-3

Table B-18 PPT-S-3 Data of Primary Cycles

Primary cycle #	Negative		Positive		Average		Average Cycle stiffness
	load	displacement	load	displaceme nt	load	displaceme nt	
	kN	mm	kN	mm	kN	mm	kN/mm
1	-1.290	-0.009	4.463	3.511	2.88	1.76	1.63
2	-4.459	-3.502	6.278	5.437	5.37	4.47	1.20
3	-4.585	-3.651	8.084	7.200	6.33	5.43	1.17
4	-5.763	-5.335	13.388	15.139	9.58	10.24	0.94
5	-13.375	-14.976	16.415	22.278	14.90	18.63	0.80
6	-16.171	-22.357	18.594	29.528	17.38	25.94	0.67
7	-22.914	-51.890	22.080	51.253	22.50	51.57	0.44
8	-20.176	-65.122	10.575	74.075	15.38	69.60	0.22
9	-15.357	-97.794	8.403	110.654	11.88	104.22	0.11

Shear wall specimen PPT-G-1 consisted of a pressure preservative treated sill plate, two 24 Ga. Galvanized steel 61 cm by 61 cm gussets. The gussets were fastened to the lower corners of the walls using 14 - 6 cm by 0.29 mm 8d (2.87 mm by 60.3 mm) ring-shank sheathing nails and 13 – 7.6 cm by 3.04 mm 10d (3.05 mm by 76.2 mm) HD Galvanized ring-shank nails. The 8d (2.87 mm by 60.3 mm) ring-shank nails were oriented in two rows spaced 7.6 cm on center and 3.8 cm apart into the doubled end studs. The 10d (3.05 mm by 76.2 mm) ring-shank nails were oriented in two rows spaced 7.6 cm on center and 1.6 cm apart into the sill plate material for hold downs and 3 – 13 mm by 89 mm A325 bolts with 7.6 cm by 7.6 cm by 9.5 mm steel plate washers to fasten the wall to the foundation.

Table B-19 PPT-G-1 EEEP Parameters

		Negative	Positive
Yield Load, P_{yield}	kN	-13.64	12.52
Disp @ Yield Load, Δ_{yield}	mm	-13.66	17.29
Disp @ failure, Δ_u	mm	-67.20	62.46

Table B-20 PPT-G-1 Performance Parameters

Peak load, P_{peak}	kN	-16.04
Displacement at P_{peak}, Δ_{peak}	mm	-43.56
Yield load, P_{yield}	kN	-13.64
Displacement at yield load, Δ_{yield}	mm	-13.66
Proportional limit, $0.4P_{peak}$	kN	-6.42
Displacement at prop. limit, Δ_e	mm	-6.43
Failure load, $0.8P_{peak}$	kN	-12.83
Displacement at failure, Δ_u	mm	-67.20
Shear Strength, v_u	N/m	-6579
Elastic stiffness, K_e	N/m	998297
Ductility, D, $\Delta_{peak}/\Delta_{yeild}$	3.19	
Ductility, D_u, $\Delta_{failure}/\Delta_{yeild}$	4.92	
Toughness, $\Delta_{failure}/\Delta_{peak}$	1.54	

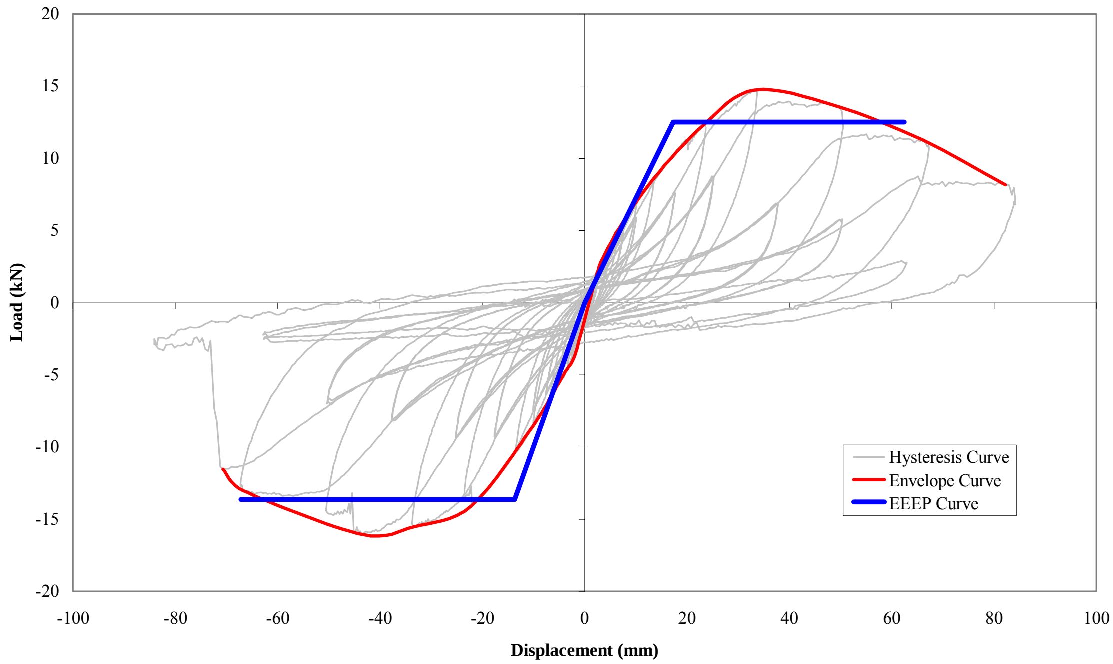

Figure B-7 Load vs. Displacement, Envelope and EEEP Curves – PPT-G-1

Table B-21 PPT-G-1 Data of Primary Cycles

Primary cycle #	Negative		Positive		Average		Average Cycle stiffness
	load	displacement	load	displaceme nt	load	displaceme nt	
	kN	mm	kN	mm	kN	mm	kN/mm
1	-3.363	-1.665	1.052	1.693	2.21	1.68	1.31
2	-4.123	-2.511	2.135	2.516	3.13	2.51	1.24
3	-4.578	-3.367	2.630	2.949	3.60	3.16	1.14
4	-5.574	-5.024	2.973	3.400	4.27	4.21	1.01
5	-6.570	-6.683	5.152	6.693	5.86	6.69	0.88
6	-8.518	-10.009	8.600	13.408	8.56	11.71	0.73
7	-14.053	-22.031	12.309	23.226	13.18	22.63	0.58
8	-15.523	-33.305	14.732	33.240	15.13	33.27	0.45
9	-16.042	-43.555	13.670	48.788	14.86	46.17	0.32
10	-13.025	-66.684	11.294	66.029	12.16	66.36	0.18
11	-11.532	-70.689	8.182	82.214	9.86	76.45	0.13

Shear wall specimen PPT-G-2 consisted of a pressure preservative treated sill plate, two 24 Ga. Galvanized steel 61 cm by 61 cm gussets. The gussets were fastened to the lower corners of the walls using 14 - 6 cm by 0.29 mm 8d (2.87 mm by 60.3 mm) ring-shank sheathing nails and 13 – 7.6 cm by 3.04 mm 10d (3.05 mm by 76.2 mm) HD Galvanized ring-shank nails. The 8d (2.87 mm by 60.3 mm) ring-shank nails were oriented in two rows spaced 7.6 cm on center and 3.8 cm apart into the doubled end studs. The 10d (3.05 mm by 76.2 mm) ring-shank nails were oriented in two rows spaced 7.6 cm on center and 1.6 cm apart into the sill plate material for hold downs and 3 – 13 mm by 89 mm A325 bolts with 7.6 cm by 7.6 cm by 9.5 mm steel plate washers to fasten the wall to the foundation.

Table B-22 PPT-G-2 EEEP Parameters

		Negative	Positive
Yield Load, P_{yield}	kN	-6.02	10.10
Disp @ Yield Load, Δ_{yield}	mm	-26.73	18.62
Disp @ failure, Δ_u	mm	-55.98	62.41

Table B-23 PPT-G-2 Performance Parameters

Peak load, P_{peak}	kN	11.88
Displacement at P_{peak}, Δ_{peak}	mm	41.93
Yield load, P_{yield}	kN	10.10
Displacement at yield load, Δ_{yield}	mm	18.62
Proportional limit, $0.4P_{peak}$	kN	4.75
Displacement at prop. limit, Δ_e	mm	8.76
Failure load, $0.8P_{peak}$	kN	9.50
Displacement at failure, Δ_u	mm	62.41
Shear Strength, v_u	N/m	4871
Elastic stiffness, K_e	N/m	542194
Ductility, D, $\Delta_{peak}/\Delta_{yeild}$	2.25	
Ductility, D_u, $\Delta_{failure}/\Delta_{yeild}$	3.35	
Toughness, $\Delta_{failure}/\Delta_{peak}$	1.49	

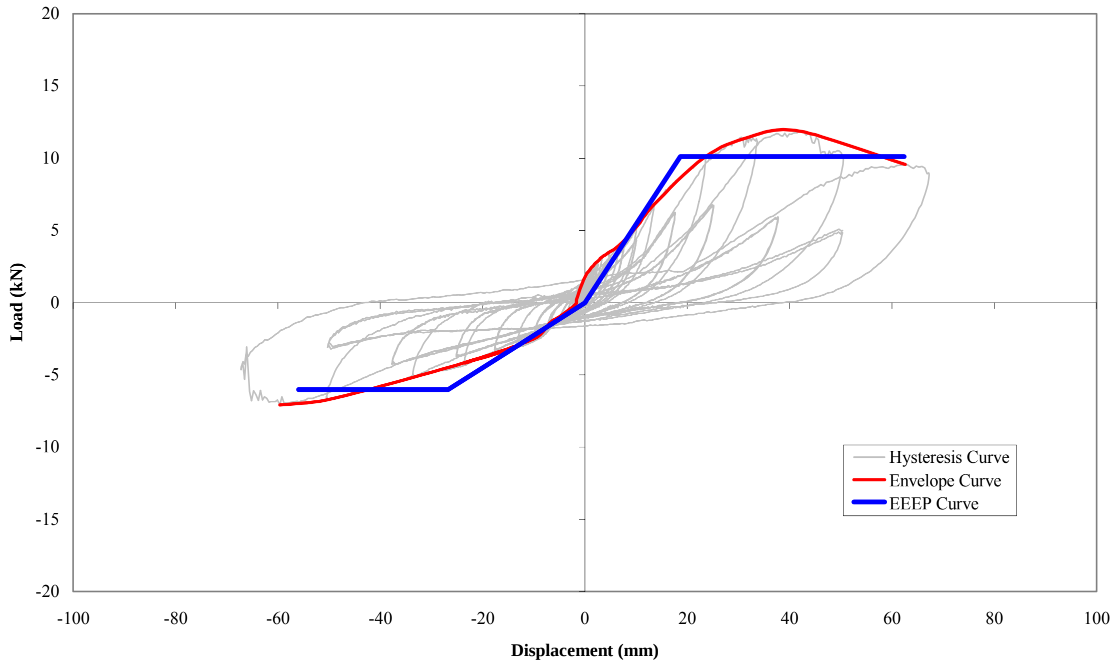

Figure B-8 Load vs. Displacement, Envelope and EEEP Curves – PPT-G-2

Table B-24 PPT-G-2 Data of Primary Cycles

Primary cycle #	Negative		Positive		Average		Average Cycle stiffness
	load	displacement	load	displaceme nt	load	displaceme nt	
	kN	mm	kN	mm	kN	mm	kN/mm
1	0.217	-1.693	1.758	0.005	0.99	0.85	1.16
2	-0.044	-1.665	2.576	1.660	1.31	1.66	0.79
3	-0.543	-3.321	2.874	2.507	1.71	2.91	0.59
4	-1.008	-5.032	3.166	3.302	2.09	4.17	0.50
5	-1.354	-6.753	3.933	6.562	2.64	6.66	0.40
6	-2.508	-9.958	5.226	10.041	3.87	10.00	0.39
7	-4.171	-23.422	6.777	13.469	5.47	18.45	0.30
8	-3.272	-14.920	10.042	23.324	6.66	19.12	0.35
9	-5.108	-33.072	11.467	32.212	8.29	32.64	0.25
10	-6.709	-50.169	11.878	41.932	9.29	46.05	0.20
11	-7.079	-59.638	9.564	62.582	8.32	61.11	0.14
12	-3.200	-49.620	5.087	49.616	4.14	49.62	0.08

Shear wall specimen PPT-G-3 consisted of a pressure preservative treated sill plate, two 24 Ga. Galvanized steel 61 cm by 61 cm gussets. The gussets were fastened to the lower corners of the walls using 14 - 6 cm by 0.29 mm 8d (2.87 mm by 60.3 mm) ring-shank sheathing nails and 13 – 7.6 cm by 3.04 mm 10d (3.05 mm by 76.2 mm) HD Galvanized ring-shank nails. The 8d (2.87 mm by 60.3 mm) ring-shank nails were oriented in two rows spaced 7.6 cm on center and 3.8 cm apart into the doubled end studs. The 10d (3.05 mm by 76.2 mm) ring-shank nails were oriented in two rows spaced 7.6 cm on center and 1.6 cm apart into the sill plate material for hold downs and 3 – 13 mm by 89 mm A325 bolts with 7.6 cm by 7.6 cm by 9.5 mm steel plate washers to fasten the wall to the foundation.

Table B-25 PPT-G-3 EEEP Parameters

		Negative	Positive
Yield Load, P_{yield}	kN	-12.31	12.06
Disp @ Yield Load, Δ_{yield}	mm	-15.90	28.12
Disp @ failure, Δ_u	mm	-55.65	69.31

Table B-26 PPT-G-3 Performance Parameters

Peak load, P_{peak}	kN	-14.48
Displacement at P_{peak}, Δ_{peak}	mm	-40.53
Yield load, P_{yield}	kN	-12.31
Displacement at yield load, Δ_{yield}	mm	-15.90
Proportional limit, $0.4P_{peak}$	kN	-5.79
Displacement at prop. limit, Δ_e	mm	-7.48
Failure load, $0.8P_{peak}$	kN	-11.58
Displacement at failure, Δ_u	mm	-55.65
Shear Strength, v_u	N/m	-5939
Elastic stiffness, K_e	N/m	774340
Ductility, D, $\Delta_{peak}/\Delta_{yeild}$	2.55	
Ductility, D_u, $\Delta_{failure}/\Delta_{yeild}$	3.50	
Toughness, $\Delta_{failure}/\Delta_{peak}$	1.37	

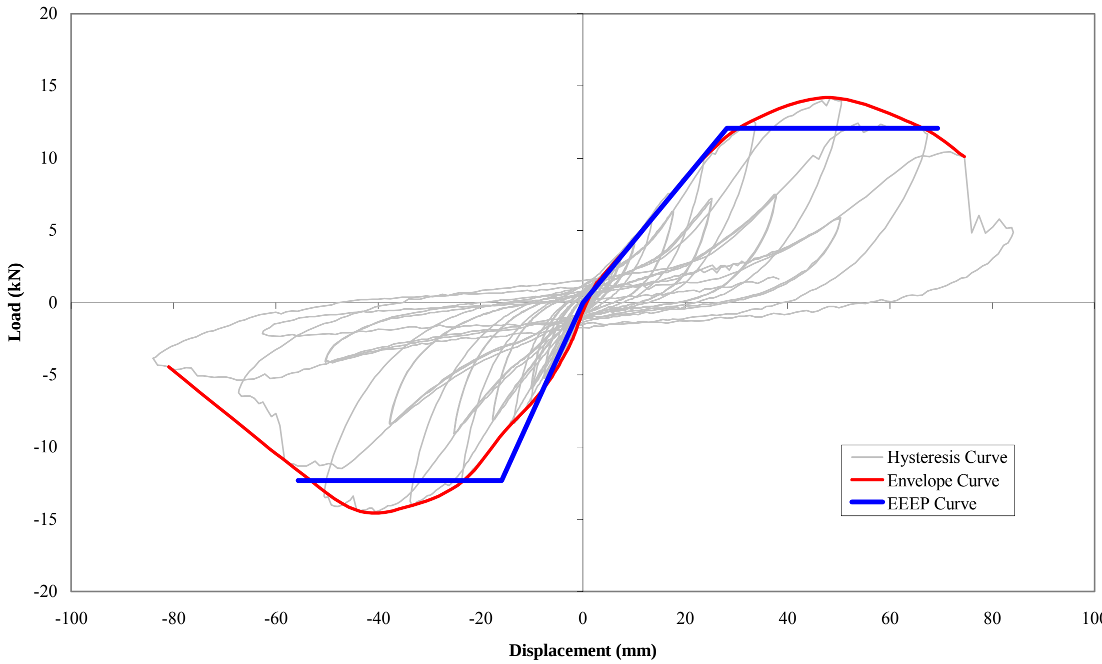

Figure B-9 Load vs. Displacement, Envelope and EEEP Curves – PPT-G-3

Table B-27 PPT-G-3 Data of Primary Cycles

Primary cycle #	Negative		Positive		Average		Average Cycle stiffness
	load	displacement	load	displaceme nt	load	displaceme nt	
	kN	mm	kN	mm	kN	mm	kN/mm
1	-0.876	-0.288	-0.445	-0.005	0.66	0.15	4.51
2	-2.131	-1.553	-0.726	-0.140	1.43	0.85	1.69
3	-2.790	-2.372	1.198	2.386	1.99	2.38	0.84
4	-3.417	-3.242	1.585	3.237	2.50	3.24	0.77
5	-5.355	-6.521	2.929	6.516	4.14	6.52	0.64
6	-7.028	-10.195	4.286	10.097	5.66	10.15	0.56
7	-8.966	-15.422	5.796	13.506	7.38	14.46	0.51
8	-12.360	-23.403	9.988	23.571	11.17	23.49	0.48
9	-14.040	-33.254	12.577	32.970	13.31	33.11	0.40
10	-14.352	-44.221	14.189	48.383	14.27	46.30	0.31
11	-11.152	-57.434	12.183	65.856	11.67	61.65	0.19
12	-4.456	-80.921	10.096	74.526	7.28	77.72	0.09

Shear wall specimen WPC-N-1 consisted of a wood plastic composite sill plate, no hold downs and 3 – 13 mm by 89 mm A325 bolts with 7.6 cm by 7.6 cm by 9.5 mm steel plate washers to fasten the wall to the foundation.

Table B-28 WPC-N-1 EEEP Parameters

		Negative	Positive
Yield Load, P_{yield}	kN	-9.91	10.24
Disp @ Yield Load, Δ_{yield}	mm	-6.81	11.40
Disp @ failure, Δ_u	mm	-43.51	37.60

Table B-29 WPC-N-1 Performance Parameters

Peak load, P_{peak}	kN	12.05
Displacement at P_{peak}, Δ_{peak}	mm	30.92
Yield load, P_{yield}	kN	10.24
Displacement at yield load, Δ_{yield}	mm	11.40
Proportional limit, $0.4P_{peak}$	kN	4.82
Displacement at prop. limit, Δ_e	mm	5.37
Failure load, $0.8P_{peak}$	kN	9.64
Displacement at failure, Δ_u	mm	37.60
Shear Strength, v_u	N/m	4942
Elastic stiffness, K_e	N/m	898321
Ductility, D, $\Delta_{peak}/\Delta_{yeild}$	2.71	
Ductility, D_u, $\Delta_{failure}/\Delta_{yeild}$	3.30	
Toughness, $\Delta_{failure}/\Delta_{peak}$	1.22	

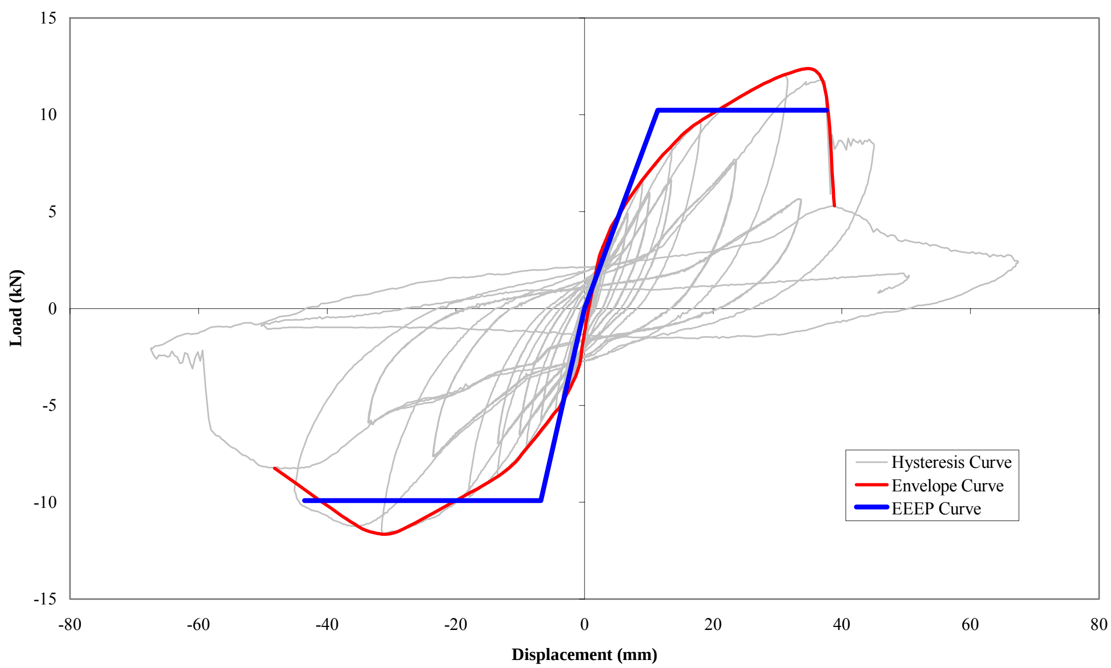

Figure B-10 Load vs. Displacement, Envelope and EEEP Curves – WPC-N-1

Table B-30 WPC-N-1 Data of Primary Cycles

Primary cycle #	Negative		Positive		Average		Average Cycle stiffness
	load	displacement	load	displaceme nt	load	displaceme nt	
	kN	mm	kN	mm	kN	mm	kN/mm
1	-2.868	-0.777	-1.205	0.009	2.04	0.39	5.18
2	-4.083	-2.232	2.522	2.200	3.30	2.22	1.49
3	-5.203	-4.097	3.591	3.367	4.40	3.73	1.18
4	-5.335	-4.502	4.378	4.488	4.86	4.50	1.08
5	-7.229	-9.009	6.614	8.925	6.92	8.97	0.77
6	-8.651	-13.353	8.301	13.357	8.48	13.36	0.63
7	-11.471	-28.659	9.631	17.818	10.55	23.24	0.45
8	-11.664	-31.193	12.051	30.924	11.86	31.06	0.38
9	-11.254	-35.184	11.780	36.961	11.52	36.07	0.32
10	-8.257	-48.160	5.301	38.886	6.78	43.52	0.16

Shear wall specimen WPC-N-2 consisted of a wood plastic composite sill plate, no hold downs and 3 – 13 mm by 89 mm A325 bolts with 7.6 cm by 7.6 cm by 9.5 mm steel plate washers to fasten the wall to the foundation.

Table B-31 WPC-N-2 EEEP Parameters

		Negative	Positive
Yield Load, P_{yield}	kN	-10.34	9.98
Disp @ Yield Load, Δ_{yield}	mm	-11.99	10.28
Disp @ failure, Δ_u	mm	-43.10	40.63

Table B-32 WPC-N-2 Performance Parameters

Peak load, P_{peak}	kN	-12.16
Displacement at P_{peak}, Δ_{peak}	mm	-31.26
Yield load, P_{yield}	kN	-10.34
Displacement at yield load, Δ_{yield}	mm	-11.99
Proportional limit, $0.4P_{peak}$	kN	-4.86
Displacement at prop. limit, Δ_e	mm	-5.64
Failure load, $0.8P_{peak}$	kN	-9.73
Displacement at failure, Δ_u	mm	-43.10
Shear Strength, v_u	N/m	-4987
Elastic stiffness, K_e	N/m	862385
Ductility, D, $\Delta_{peak}/\Delta_{yeild}$	2.61	
Ductility, D_u, $\Delta_{failure}/\Delta_{yeild}$	3.60	
Toughness, $\Delta_{failure}/\Delta_{peak}$	1.38	

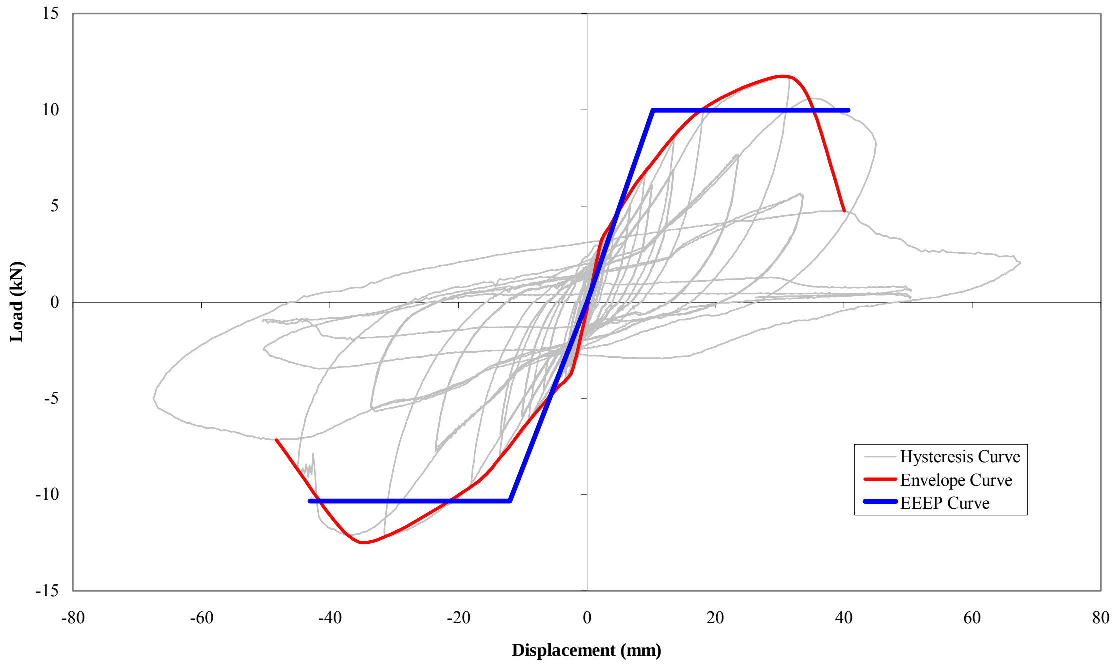

Figure B-11 Load vs. Displacement, Envelope and EEEP Curves – WPC-N-2

Table B-33 WPC-N-2 Data of Primary Cycles

Primary cycle #	Negative		Positive		Average		Average Cycle stiffness
	load	displacement	load	displacement	load	displacement	
	kN	mm	kN	mm	kN	mm	kN/mm
1	-0.370	0.005	-0.322	0.005	0.35	0.00	74.47
2	-3.496	-2.265	3.098	2.195	3.30	2.23	1.48
3	-4.093	-3.349	3.835	3.363	3.96	3.36	1.18
4	-4.412	-4.465	4.466	4.442	4.44	4.45	1.00
5	-6.126	-8.920	4.972	5.353	5.55	7.14	0.78
6	-8.030	-13.390	6.730	8.967	7.38	11.18	0.66
7	-9.533	-17.766	9.998	17.836	9.77	17.80	0.55
8	-12.160	-31.263	11.742	30.194	11.95	30.73	0.39
9	-12.105	-37.244	10.592	34.510	11.35	35.88	0.32
10	-7.157	-48.323	4.731	40.095	5.94	44.21	0.13

Shear wall specimen WPC-N-3 consisted of a wood plastic composite sill plate, no hold downs and 3 – 13 mm by 89 mm A325 bolts with 7.6 cm by 7.6 cm by 9.5 mm steel plate washers to fasten the wall to the foundation.

Table B-34 WPC-N-3 EEEP Parameters

		Negative	Positive
Yield Load, P_{yield}	kN	-10.62	9.72
Disp @ Yield Load, Δ_{yield}	mm	-20.85	21.08
Disp @ failure, Δ_u	mm	-53.80	46.31

Table B-35 WPC-N-3 Performance Parameters

Peak load, P_{peak}	kN	-12.49
Displacement at P_{peak}, Δ_{peak}	mm	-42.27
Yield load, P_{yield}	kN	-10.62
Displacement at yield load, Δ_{yield}	mm	-20.85
Proportional limit, $0.4P_{peak}$	kN	-5.00
Displacement at prop. limit, Δ_e	mm	-9.81
Failure load, $0.8P_{peak}$	kN	-9.99
Displacement at failure, Δ_u	mm	-53.80
Shear Strength, v_u	N/m	-5123
Elastic stiffness, K_e	N/m	509301
Ductility, D, $\Delta_{peak}/\Delta_{yeild}$	2.03	
Ductility, D_u, $\Delta_{failure}/\Delta_{yeild}$	2.58	
Toughness, $\Delta_{failure}/\Delta_{peak}$	1.27	

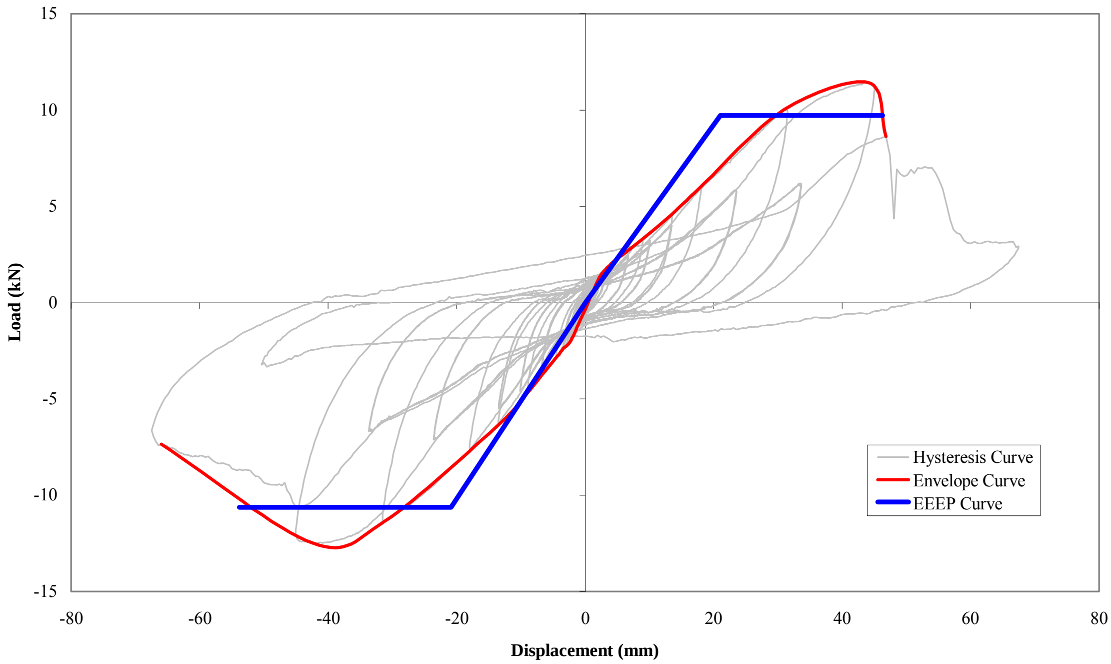

Figure B-12 Load vs. Displacement, Envelope and EEEP Curves – WPC-N-3

Table B-36 WPC-N-3 Data of Primary Cycles

Primary cycle #	Negative		Positive		Average		Average Cycle stiffness
	load	displacement	load	displaceme nt	load	displaceme nt	
	kN	mm	kN	mm	kN	mm	kN/mm
1	-1.989	-2.256	1.307	2.214	1.65	2.23	0.74
2	-2.338	-3.330	1.744	3.246	2.04	3.29	0.62
3	-2.827	-4.446	2.145	4.474	2.49	4.46	0.56
4	-3.747	-6.678	3.292	8.888	3.52	7.78	0.45
5	-4.666	-8.911	4.554	13.381	4.61	11.15	0.41
6	-6.272	-13.283	5.953	17.855	6.11	15.57	0.39
7	-11.366	-31.254	10.022	30.975	10.69	31.11	0.34
8	-12.492	-42.272	11.433	44.118	11.96	43.20	0.28
9	-7.354	-65.973	8.623	46.816	7.99	56.39	0.14

Shear wall specimen WPC-S-1 consisted of a wood plastic composite sill plate, two Simpson HTT22 hold downs with 32 - 7.6 cm by 0.33 mm 10d (3.05 mm by 76.2 mm) nails. Each hold-down was secured to the steel foundation by using a 1.6 cm by 8.9 cm A325 bolt and 3 – 13 mm by 89 mm A325 bolts with 7.6 cm by 7.6 cm by 9.5 mm steel plate washers to fasten the wall to the foundation.

Table B-37 WPC-S-1 EEEP Parameters

		Negative	Positive
Yield Load, P_{yield}	kN	-15.51	15.13
Disp @ Yield Load, Δ_{yield}	mm	-10.94	11.84
Disp @ failure, Δ_u	mm	-65.45	59.70

Table B-38 WPC-S-1 Performance Parameters

Peak load, P_{peak}	kN	-18.25
Displacement at P_{peak}, Δ_{peak}	mm	-43.00
Yield load, P_{yield}	kN	-15.51
Displacement at yield load, Δ_{yield}	mm	-10.94
Proportional limit, $0.4P_{peak}$	kN	-7.30
Displacement at prop. limit, Δ_e	mm	-5.15
Failure load, $0.8P_{peak}$	kN	-14.60
Displacement at failure, Δ_u	mm	-65.45
Shear Strength, v_u	N/m	-7485
Elastic stiffness, K_e	N/m	1417473
Ductility, D, $\Delta_{peak}/\Delta_{yeild}$	3.93	
Ductility, D_u, $\Delta_{failure}/\Delta_{yeild}$	5.98	
Toughness, $\Delta_{failure}/\Delta_{peak}$	1.52	

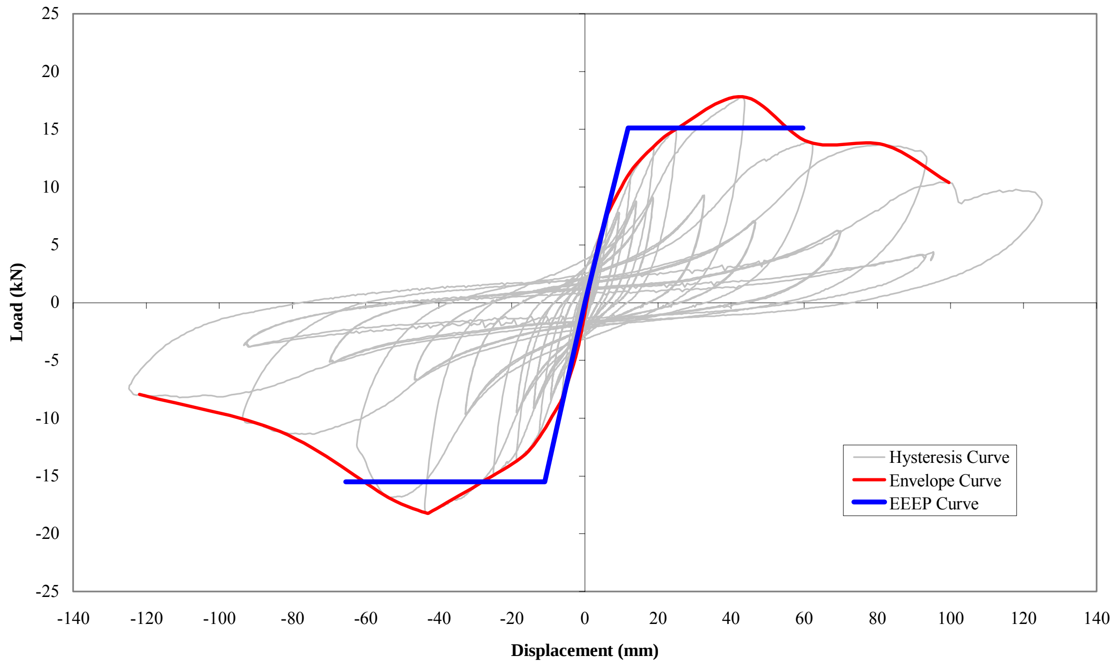

Table B-13 Load vs. Displacement, Envelope and EEEP Curves – WPC-S-1

Table B-39 WPC-S-1 Data of Primary Cycles

Primary cycle #	Negative		Positive		Average		Average Cycle stiffness
	load	displacement	load	displaceme nt	load	displaceme nt	
	kN	mm	kN	mm	kN	mm	kN/mm
1	-3.065	-1.339	-0.910	-0.009	1.99	0.67	2.95
2	-5.335	-3.139	4.320	3.125	4.83	3.13	1.54
3	-8.294	-6.167	6.302	4.660	7.30	5.41	1.35
4	-8.308	-6.218	7.755	6.274	8.03	6.25	1.29
5	-11.613	-12.418	11.311	12.418	11.46	12.42	0.92
6	-13.670	-18.631	13.436	18.562	13.55	18.60	0.73
7	-18.160	-42.514	14.936	24.589	16.55	33.55	0.49
8	-18.251	-43.002	17.803	43.114	18.03	43.06	0.42
9	-16.877	-53.676	13.904	61.280	15.39	57.48	0.27
10	-11.152	-83.293	13.660	81.865	12.41	82.58	0.15
11	-7.938	-121.890	10.378	99.566	9.16	110.73	0.08

Shear wall specimen WPC-S-2 consisted of a wood plastic composite sill plate, two Simpson HTT22 hold downs with 32 - 7.6 cm by 0.33 mm 10d (3.05 mm by 76.2 mm) nails. Each hold-down was secured to the steel foundation by using a 1.6 cm by 8.9 cm A325 bolt and 3 – 13 mm by 89 mm A325 bolts with 7.6 cm by 7.6 cm by 9.5 mm steel plate washers to fasten the wall to the foundation.

Table B-40 WPC-S-2 EEEP Parameters

		Negative	Positive
Yield Load, P_{yield}	kN	-18.86	16.79
Disp @ Yield Load, Δ_{yield}	mm	-14.93	13.25
Disp @ failure, Δ_u	mm	-73.25	67.60

Table B-41 WPC-S-2 Performance Parameters

Peak load, P_{peak}	kN	-22.19
Displacement at P_{peak}, Δ_{peak}	mm	-61.57
Yield load, P_{yield}	kN	-18.86
Displacement at yield load, Δ_{yield}	mm	-14.93
Proportional limit, $0.4P_{peak}$	kN	-8.88
Displacement at prop. limit, Δ_e	mm	-7.02
Failure load, $0.8P_{peak}$	kN	-17.75
Displacement at failure, Δ_u	mm	-73.25
Shear Strength, v_u	N/m	-9099
Elastic stiffness, K_e	N/m	1263589
Ductility, D, $\Delta_{peak}/\Delta_{yeild}$	4.13	
Ductility, D_u, $\Delta_{failure}/\Delta_{yeild}$	4.91	
Toughness, $\Delta_{failure}/\Delta_{peak}$	1.19	

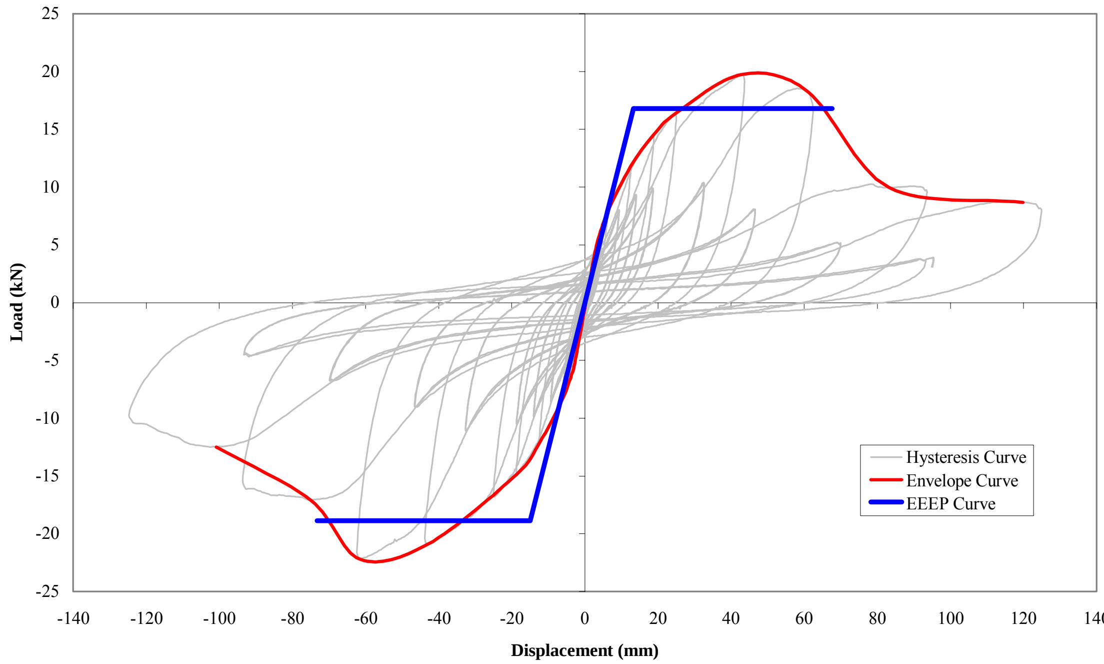

Figure B-14 Load vs. Displacement, Envelope and EEEP Curves – WPC-S-2

Table B-42 WPC-S-2 Data of Primary Cycles

Primary cycle #	Negative		Positive		Average		Average Cycle stiffness
	load	displacement	load	displaceme nt	load	displaceme nt	
	kN	mm	kN	mm	kN	mm	kN/mm
1	-0.468	-0.009	4.880	3.139	2.67	1.57	1.70
2	-5.416	-2.828	6.496	4.642	5.96	3.73	1.59
3	-5.756	-3.135	7.853	6.158	6.80	4.65	1.46
4	-8.382	-6.204	11.803	12.483	10.09	9.34	1.08
5	-12.116	-12.413	14.478	18.683	13.30	15.55	0.86
6	-14.837	-18.590	16.348	24.724	15.59	21.66	0.72
7	-20.902	-42.937	19.755	42.983	20.33	42.96	0.47
8	-22.188	-61.573	18.238	61.075	20.21	61.32	0.33
9	-17.091	-74.986	9.954	83.279	13.52	79.13	0.17
10	-12.496	-100.826	8.674	119.821	10.59	110.32	0.10

Shear wall specimen WPC-S-3 consisted of a wood plastic composite sill plate, two Simpson HTT22 hold downs with 32 - 7.6 cm by 0.33 mm 10d (3.05 mm by 76.2 mm) nails. Each hold-down was secured to the steel foundation by using a 1.6 cm by 8.9 cm A325 bolt and 3 – 13 mm by 89 mm A325 bolts with 7.6 cm by 7.6 cm by 9.5 mm steel plate washers to fasten the wall to the foundation.

Table B-43 WPC-S-3 EEEP Parameters

		Negative	Positive
Yield Load, P_{yield}	kN	-20.53	19.40
Disp @ Yield Load, Δ_{yield}	mm	-15.69	15.23
Disp @ failure, Δ_u	mm	-63.10	65.91

Table B-44 WPC-S-3 Performance Parameters

Peak load, P_{peak}	kN	-24.15
Displacement at P_{peak}, Δ_{peak}	mm	-61.88
Yield load, P_{yield}	kN	-20.53
Displacement at yield load, Δ_{yield}	mm	-15.69
Proportional limit, $0.4P_{peak}$	kN	-9.66
Displacement at prop. limit, Δ_e	mm	-7.38
Failure load, $0.8P_{peak}$	kN	-19.32
Displacement at failure, Δ_u	mm	-63.10
Shear Strength, v_u	N/m	-9904
Elastic stiffness, K_e	N/m	1308713
Ductility, D, $\Delta_{peak}/\Delta_{yeild}$	3.94	
Ductility, D_u, $\Delta_{failure}/\Delta_{yeild}$	4.02	
Toughness, $\Delta_{failure}/\Delta_{peak}$	1.02	

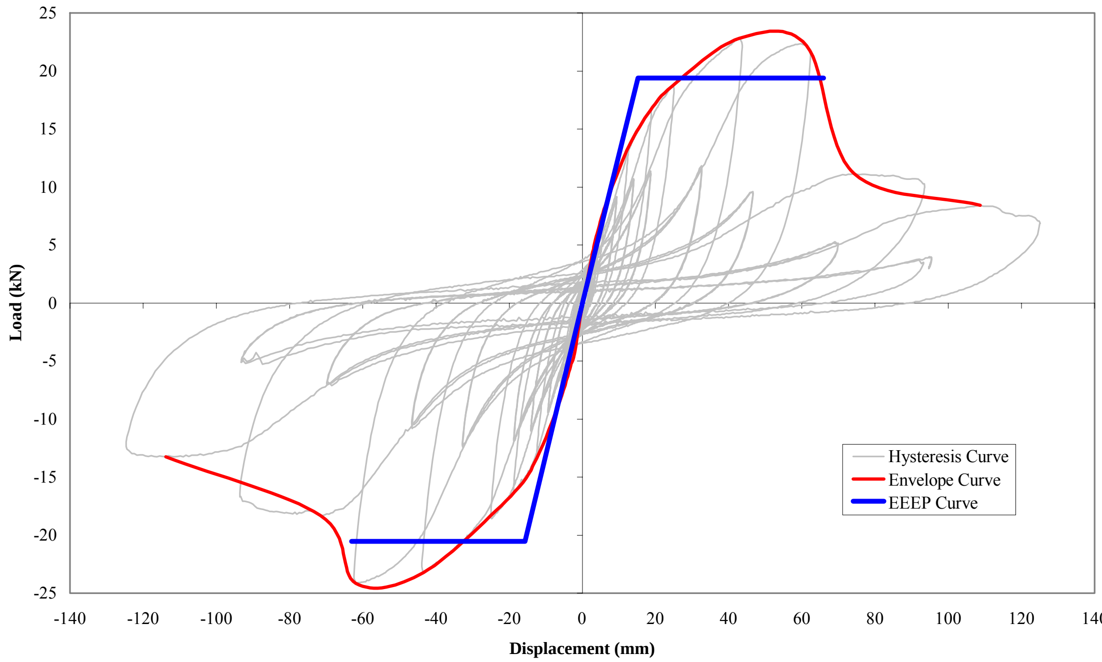

Figure B-15 Load vs. Displacement, Envelope and EEEP Curves – WPC-S-3

Table B-45 WPC-S-3 Data of Primary Cycles

Primary cycle #	Negative		Positive		Average		Average Cycle stiffness
	load	displacement	load	displaceme nt	load	displaceme nt	
	kN	mm	kN	mm	kN	mm	kN/mm
1	-0.333	-0.014	4.860	3.111	2.60	1.56	1.66
2	-4.371	-2.130	6.658	4.669	5.51	3.40	1.62
3	-5.369	-3.121	8.352	6.200	6.86	4.66	1.47
4	-8.457	-6.181	13.405	12.516	10.93	9.35	1.17
5	-13.358	-12.436	16.609	18.636	14.98	15.54	0.96
6	-16.283	-18.557	18.710	24.640	17.50	21.60	0.81
7	-23.227	-43.346	22.819	42.830	23.02	43.09	0.53
8	-24.150	-61.875	22.192	61.280	23.17	61.58	0.38
9	-18.309	-71.572	11.169	74.237	14.74	72.90	0.20
10	-13.269	-113.821	8.420	108.691	10.84	111.26	0.10

Shear wall specimen WPC-G-1 consisted of a wood plastic composite sill plate, two 24 Ga. Galvanized steel 61 cm by 61 cm gussets. The gussets were fastened to the lower corners of the walls using 14 - 6 cm by 0.29 mm 8d (2.87 mm by 60.3 mm) ring-shank sheathing nails and 13 – 7.6 cm by 3.04 mm 10d (3.05 mm by 76.2 mm) HD Galvanized ring-shank nails. The 8d (2.87 mm by 60.3 mm) ring-shank nails were oriented in two rows spaced 7.6 cm on center and 3.8 cm apart into the doubled end studs. The 10d (3.05 mm by 76.2 mm) ring-shank nails were oriented in two rows spaced 7.6 cm on center and 1.6 cm apart into the sill plate material for hold downs and 3 – 13 mm by 89 mm A325 bolts with 7.6 cm by 7.6 cm by 9.5 mm steel plate washers to fasten the wall to the foundation.

Table B-46 WPC-G-1 EEEP Parameters

		Negative	Positive
Yield Load, P_{yield}	kN	-16.11	13.71
Disp @ Yield Load, Δ_{yield}	mm	-14.35	14.78
Disp @ failure, Δ_u	mm	-57.86	66.19

Table B-47 WPC-G-1 Performance Parameters

Peak load, P_{peak}	kN	-18.95
Displacement at P_{peak}, Δ_{peak}	mm	-35.66
Yield load, P_{yield}	kN	-16.11
Displacement at yield load, Δ_{yield}	mm	-14.35
Proportional limit, $0.4P_{peak}$	kN	-7.58
Displacement at prop. limit, Δ_e	mm	-6.75
Failure load, $0.8P_{peak}$	kN	-15.16
Displacement at failure, Δ_u	mm	-57.86
Shear Strength, v_u	N/m	-7770
Elastic stiffness, K_e	N/m	1122065
Ductility, D, $\Delta_{peak}/\Delta_{yeild}$	2.48	
Ductility, D_u, $\Delta_{failure}/\Delta_{yeild}$	4.03	
Toughness, $\Delta_{failure}/\Delta_{peak}$	1.62	

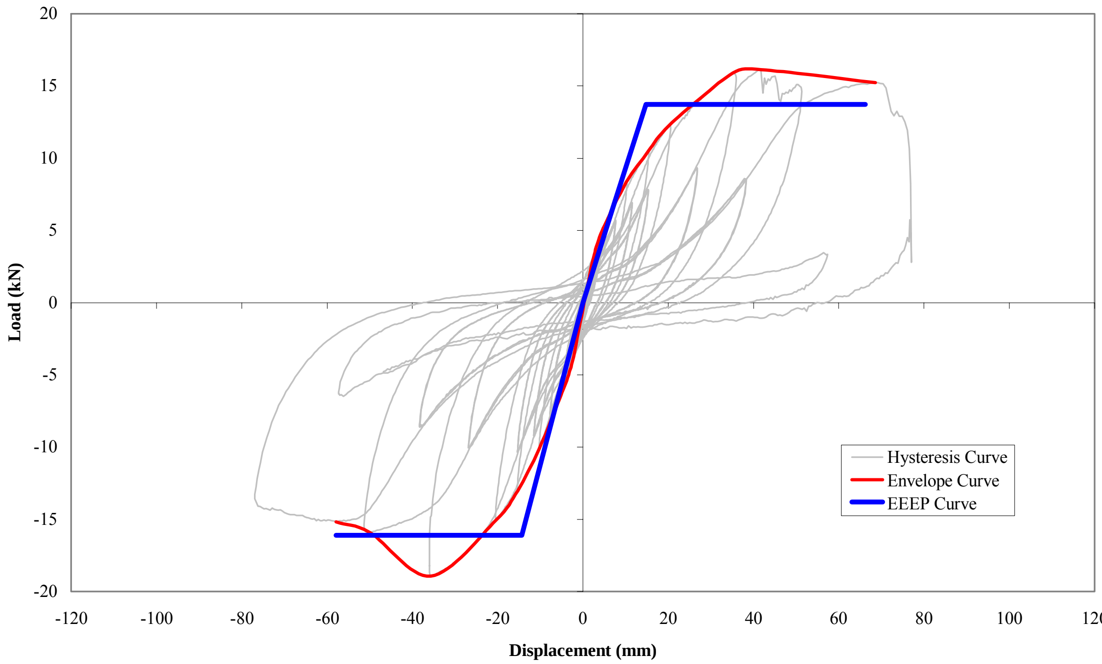

Figure B-16 Load vs. Displacement, Envelope and EEEP Curves – WPC-G-1

Table B-48 WPC-G-1 Data of Primary Cycles

Primary cycle #	Negative		Positive		Average		Average Cycle stiffness
	load	displacement	load	displaceme nt	load	displaceme nt	
	kN	mm	kN	mm	kN	mm	kN/mm
1	-4.089	-2.474	-0.462	-0.005	2.28	1.24	1.84
2	-5.206	-3.632	3.092	2.451	4.15	3.04	1.36
3	-6.238	-4.907	4.344	3.721	5.29	4.31	1.23
4	-10.100	-10.227	5.318	5.014	7.71	7.62	1.01
5	-13.029	-15.241	8.335	10.171	10.68	12.71	0.84
6	-15.061	-20.375	10.487	15.357	12.77	17.87	0.71
7	-18.947	-35.663	12.275	20.217	15.61	27.94	0.56
8	-15.913	-50.030	15.896	35.226	15.90	42.63	0.37
9	-15.167	-57.903	16.134	41.728	15.65	49.82	0.31
10	-4.785	-5.488	15.231	68.573	10.01	37.03	0.27

Shear wall specimen WPC-G-2 consisted of a wood plastic composite sill plate, two 24 Ga. Galvanized steel 61 cm by 61 cm gussets. The gussets were fastened to the lower corners of the walls using 14 - 6 cm by 0.29 mm 8d (2.87 mm by 60.3 mm) ring-shank sheathing nails and 13 – 7.6 cm by 3.04 mm 10d (3.05 mm by 76.2 mm) HD Galvanized ring-shank nails. The 8d (2.87 mm by 60.3 mm) ring-shank nails were oriented in two rows spaced 7.6 cm on center and 3.8 cm apart into the doubled end studs. The 10d (3.05 mm by 76.2 mm) ring-shank nails were oriented in two rows spaced 7.6 cm on center and 1.6 cm apart into the sill plate material for hold downs and 3 – 13 mm by 89 mm A325 bolts with 7.6 cm by 7.6 cm by 9.5 mm steel plate washers to fasten the wall to the foundation.

Table B-49 WPC-G-2 EEEP Parameters

		Negative	Positive
Yield Load, P_{yield}	kN	-10.69	11.10
Disp @ Yield Load, Δ_{yield}	mm	-66.53	17.16
Disp @ failure, Δ_u	mm	-82.43	59.06

Table B-50 WPC-G-2 Performance Parameters

Peak load, P_{peak}	kN	13.06
Displacement at P_{peak}, Δ_{peak}	mm	44.63
Yield load, P_{yield}	kN	11.10
Displacement at yield load, Δ_{yield}	mm	17.16
Proportional limit, $0.4P_{peak}$	kN	5.22
Displacement at prop. limit, Δ_e	mm	8.08
Failure load, $0.8P_{peak}$	kN	10.44
Displacement at failure, Δ_u	mm	59.06
Shear Strength, v_u	N/m	5354
Elastic stiffness, K_e	N/m	646517
Ductility, D, $\Delta_{peak}/\Delta_{yeild}$	2.60	
Ductility, D_u, $\Delta_{failure}/\Delta_{yeild}$	3.44	
Toughness, $\Delta_{failure}/\Delta_{peak}$	1.32	

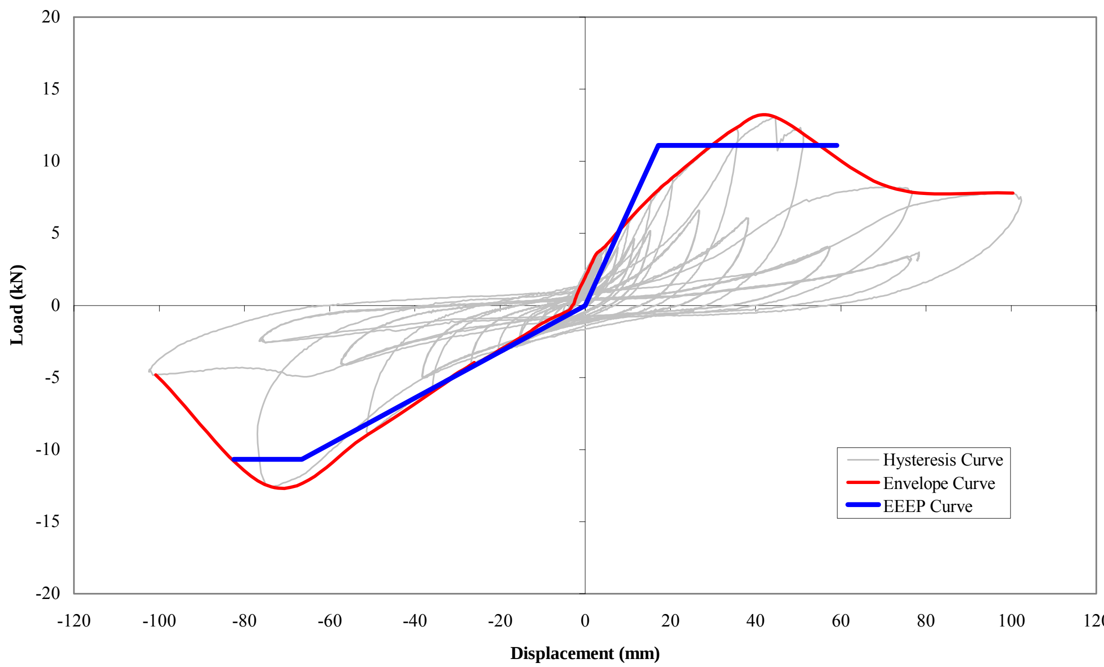

Figure B-17 Load vs. Displacement, Envelope and EEEP Curves – WPC-G-2

Table B-51 WPC-G-2 Data of Primary Cycles

Primary cycle #	Negative		Positive		Average		Average Cycle stiffness
	load	displacement	load	displaceme nt	load	displaceme nt	
	kN	mm	kN	mm	kN	mm	kN/mm
1	0.703	-2.042	1.938	0.000	1.32	1.02	1.29
2	0.180	-2.544	3.557	2.549	1.87	2.55	0.73
3	-0.083	-3.157	3.865	3.763	1.97	3.46	0.57
4	-0.346	-3.772	4.229	5.032	2.29	4.40	0.52
5	-1.252	-10.153	5.895	10.139	3.57	10.15	0.35
6	-2.236	-15.213	7.473	15.325	4.85	15.27	0.32
7	-5.766	-35.542	8.803	20.282	7.28	27.91	0.26
8	-4.066	-26.329	12.278	35.230	8.17	30.78	0.27
9	-8.932	-50.922	13.056	44.634	10.99	47.78	0.23
10	-12.577	-73.637	8.223	71.331	10.40	72.48	0.14
11	-4.812	-100.780	7.789	100.394	6.30	100.59	0.06

Shear wall specimen WPC-G-3 consisted of a wood plastic composite sill plate, two 24 Ga. Galvanized steel 61 cm by 61 cm gussets. The gussets were fastened to the lower corners of the walls using 14 - 6 cm by 0.29 mm 8d (2.87 mm by 60.3 mm) ring-shank sheathing nails and 13 – 7.6 cm by 3.04 mm 10d (3.05 mm by 76.2 mm) HD Galvanized ring-shank nails. The 8d (2.87 mm by 60.3 mm) ring-shank nails were oriented in two rows spaced 7.6 cm on center and 3.8 cm apart into the doubled end studs. The 10d (3.05 mm by 76.2 mm) ring-shank nails were oriented in two rows spaced 7.6 cm on center and 1.6 cm apart into the sill plate material for hold downs and 3 – 13 mm by 89 mm A325 bolts with 7.6 cm by 7.6 cm by 9.5 mm steel plate washers to fasten the wall to the foundation.

Table B-52 WPC-G-3 EEEP Parameters

		Negative	Positive
Yield Load, P_{yield}	kN	-15.32	15.29
Disp @ Yield Load, Δ_{yield}	mm	-12.47	16.57
Disp @ failure, Δ_u	mm	-65.66	64.48

Table B-53 WPC-G-3 Performance Parameters

Peak load, P_{peak}	kN	-18.02
Displacement at P_{peak}, Δ_{peak}	mm	-50.95
Yield load, P_{yield}	kN	-15.32
Displacement at yield load, Δ_{yield}	mm	-12.47
Proportional limit, $0.4P_{peak}$	kN	-7.21
Displacement at prop. limit, Δ_e	mm	-5.87
Failure load, $0.8P_{peak}$	kN	-14.42
Displacement at failure, Δ_u	mm	-65.66
Shear Strength, v_u	N/m	-7390
Elastic stiffness, K_e	N/m	1228667
Ductility, D, $\Delta_{peak}/\Delta_{yeild}$	4.09	
Ductility, D_u, $\Delta_{failure}/\Delta_{yeild}$	5.27	
Toughness, $\Delta_{failure}/\Delta_{peak}$	1.29	

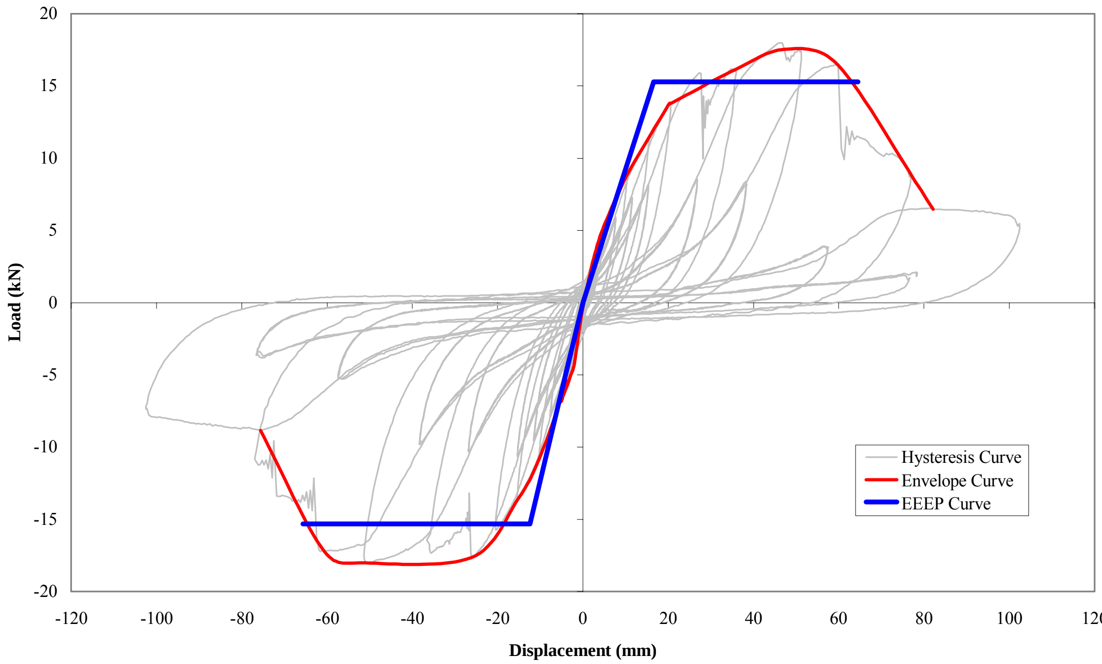

Figure B-18 Load vs. Displacement, Envelope and EEEP Curves – WPC-G-3

Table B-54 WPC-G-3 Data of Primary Cycles

Primary cycle #	Negative		Positive		Average		Average Cycle stiffness
	load	displacement	load	displaceme nt	load	displaceme nt	
	kN	mm	kN	mm	kN	mm	kN/mm
1	-0.285	-0.009	3.092	2.577	1.69	1.29	1.31
2	-4.178	-2.014	4.371	3.767	4.27	2.89	1.48
3	-4.806	-2.581	5.447	5.088	5.13	3.83	1.34
4	-6.866	-5.097	8.780	10.251	7.82	7.67	1.02
5	-5.525	-3.814	11.423	15.427	8.47	9.62	0.88
6	-10.738	-10.171	13.795	20.306	12.27	15.24	0.80
7	-13.605	-15.250	13.772	20.464	13.69	17.86	0.77
8	-17.658	-26.105	16.110	35.575	16.88	30.84	0.55
9	-18.021	-50.946	17.535	47.206	17.78	49.08	0.36
10	-17.237	-60.606	16.453	59.880	16.84	60.24	0.28
11	-8.858	-75.614	6.468	82.139	7.66	78.88	0.10